Department of Chemical Engineering

The University of Alberta
Edmonton, Alberta
Canada T6G 2G6

1-2

THE EFFECT OF STIRRING ON ENHANCED SEPARATION OF PARTICULATES FROM LIQUIDS

by

Dr. Jacob H. Masliyah

REQ. NO. 0-9173

THE EFFECT OF STIRRING ON ENHANCED SEPARATION OF PARTICULATES FROM LIQUIDS

CONTRACT REPORT NO. OSU81-00152

by

Dr. Jacob H. Masliyah

Department of Chemical Engineering
University of Alberta
Edmonton, Alberta

Submitted to:

Department of Energy, Mines and Resources

Contract Number:

DSS-14SU 23440-0-9173

June 1, 1981 - May 31, 1982

TABLE OF CONTENTS

	Page
Summary	1
Conclusions and Recommendations	2
Background	3
Description of Equipment	5
Theoretical Background	10
Experimental Results and Discussion	14
Simulation of a Gravity Separation Vessel	44
Nomenclature	53
Acknowledgement	55
References	56
List of Figures	58
List of Tables	60
Appendix A : Conductivity Cell	61
Appendix B : Pressure Drop Plots	66
Appendix C : Raw Experimental Data	85

SUMMARY

An experimental study was carried out to examine the effect of stirring on the height of a water fluidized bed. A star and a paddle type zero pitch stirrers were employed. Three types of solid particles having a diameter range of $1.9\text{-}1.3\times10^{-4}$ m were used: sand, smooth glass beads and rolled elongated aluminum particles. For the case of sand and glass bead fluidized beds, it was found that a large drop in the bed height occurs when the bed is subjected to stirring rates of up to 150 RPM. For the case of rolled aluminum particles fluidized bed, stirring had no effect on the bed height.

Utilizing the experimental data gathered from the fluidized bed study, the effect of rotary action on hindered settling/floatation of a slurry of sand/bitumen droplets in a gravity separation vessel was theoretically investigated. Results show that there is a slight benefit in the separation efficiency when rotary motion is present in a gravity separation vessel.

CONCLUSIONS AND RECOMMENDATIONS

Within a wide range of operating conditions it is found that stirring action contracts a fluidized bed. Mathematical simulation of a gravity separation vessel where sand/bitumen droplets are separated, indicates that stirring action only slightly enhances separation.

Improved bitumen recovery can be better achieved by devising processes where large bitumen droplets are produced.

BACKGROUND

Gravity separation vessels are used commercially in the Clark Hot Water Method (1930) for processing Athabasca oil sands. In Clark's process the oil sand is first treated with steam and caustic soda in a conditioning drum. The oil sand slurry is then fed to a gravity separation vessel where the bitumen in the form of a dispersion floats to the top of the vessel and forms a froth. This froth is then pumped into upgrading units for further processing. Any bitumen carried out by the tailings stream is considered as a loss. A side stream carrying clay fines, sand and bitumen referred to as the middlings stream, is usually drawn from the middle of the vessel for further processing. A disadvantage of the hot water process is that the high process temperature tends to swell the clay particles and thus impeding the separation process in the gravity vessel. An alternative process for gravity separation of bitumen is to use cold water and a solvent to extract the bitumen. The employment of the solvent circumvents the use of high processing temperature.

Such a process was suggested by Magna International Inc. In addition, it is proposed the use of a different gravity separation vessel. The new separation vessel (MAGNA RTGS) does not have a middlings stream and more importantly a swirling action is introduced to the separation vessel via rotating paddles. It is suggested that such a rotationary action enhances the separation of the sand and bitumen droplets.

In order to isolate the effect of rotary action on the separation of sand and bitumen droplets, the effects of rotary action has to be first studied for a simple system where the physical parameters are better controlled. To this end, the effect of stirring on water fluidized bed will be studied to quantify the relationship between stirring rate and bed height.

Moreover, from measurement of fluidized bed solids concentration variation with water velocity it is possible to evaluate the coefficients of the hindered settling equations when stirring action is present.

Once the coefficients of settling equations are determined for the case where stirring is present, it becomes possible to evaluate the importance of stirring in the separation of sand and bitumen droplets in a gravity separation vessel via the use of a model of the gravity separation vessel already developed by Jacob Masliyah Consulting Ltd.

DESCRIPTION OF EQUIPMENT

A schematic diagram of the experimental set-up is shown in Figure 1. The fluidized bed is made of a lucite tubing, 0.137 m ID and 0.73 m height. The fluidized bed section of the lucite tubing was fitted with 10 pressure taps at 2.5 cm intervals. The pressure taps were connected to a Celesco type pressure tranducer (0.1 psi). The pressure tranducer was calibrated by applying known hydrostatic heads of water. The fludizing fluid is water at 15°C.

A stirrer shaft (0.013 m dia) and 0.93 m in length was attached to a variable speed motor which was in turn attached to a free standing frame. The stirrers were a paddle type and a star impeller type with zero pitch blades. A detailed description of the stirrers is given in Figure 2.

To ensure a good water distribution and uniformity of the fluidized bed, a conical entrance section was attached to the botton of the bed. The conical section was filled with 1 mm glass beads sandwiched between two wire screens. It was found necessary to place a bed of 3 mm diameter lead shot packed for a depth of 5 cm over the fluidized bed inlet screen. The bed of lead shot gave an excellent water distribution.

In the lower section of the fluidized bed, the bed was fitted with two conductivity probes to measure the radial variation of the solids concentration. Details of the probes are given in Appendix A. Three types of solids were used, namely sand, glass beads and rolled aluminum particles. The physical properties of the solids are given in Table 1.

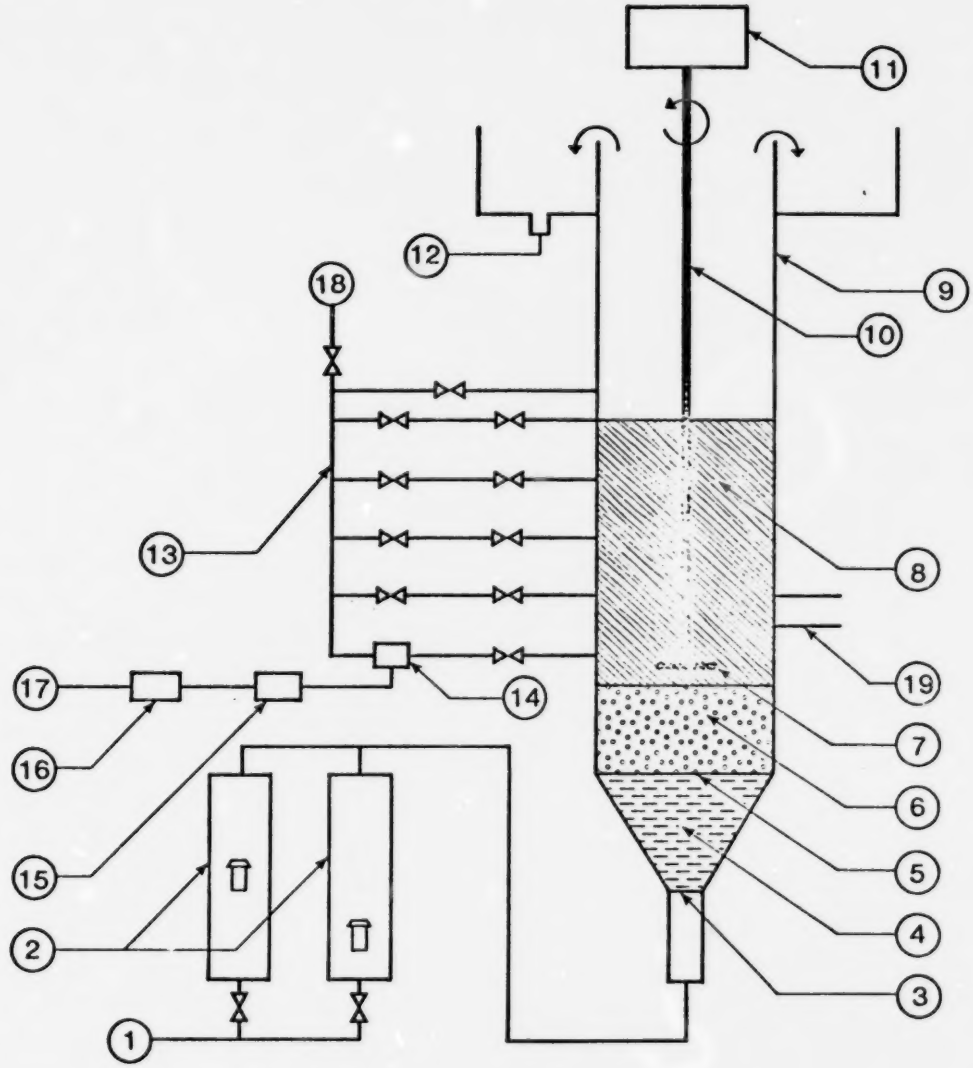

(1) Water from constant lead tank
(2) Rotameters #1 & #2
(3) Fine screen
(4) Conical section
(5) 100 mesh screen
(6) Calming section
(7) Stirrer blade
(8) Fluidized bed
(9) Lucite column
(10) Stirrer shaft
(11) Variable speed motor
(12) Overflow (to drain)
(13) Pressure taps
(14) Pressure transducer
(15) Carrier demodulator
(16) Voltmeter (dc)
(17) Power source
(18) Purge valve
(19) Conductvity probes

Figure 1 Schematic Diagram of Equipment

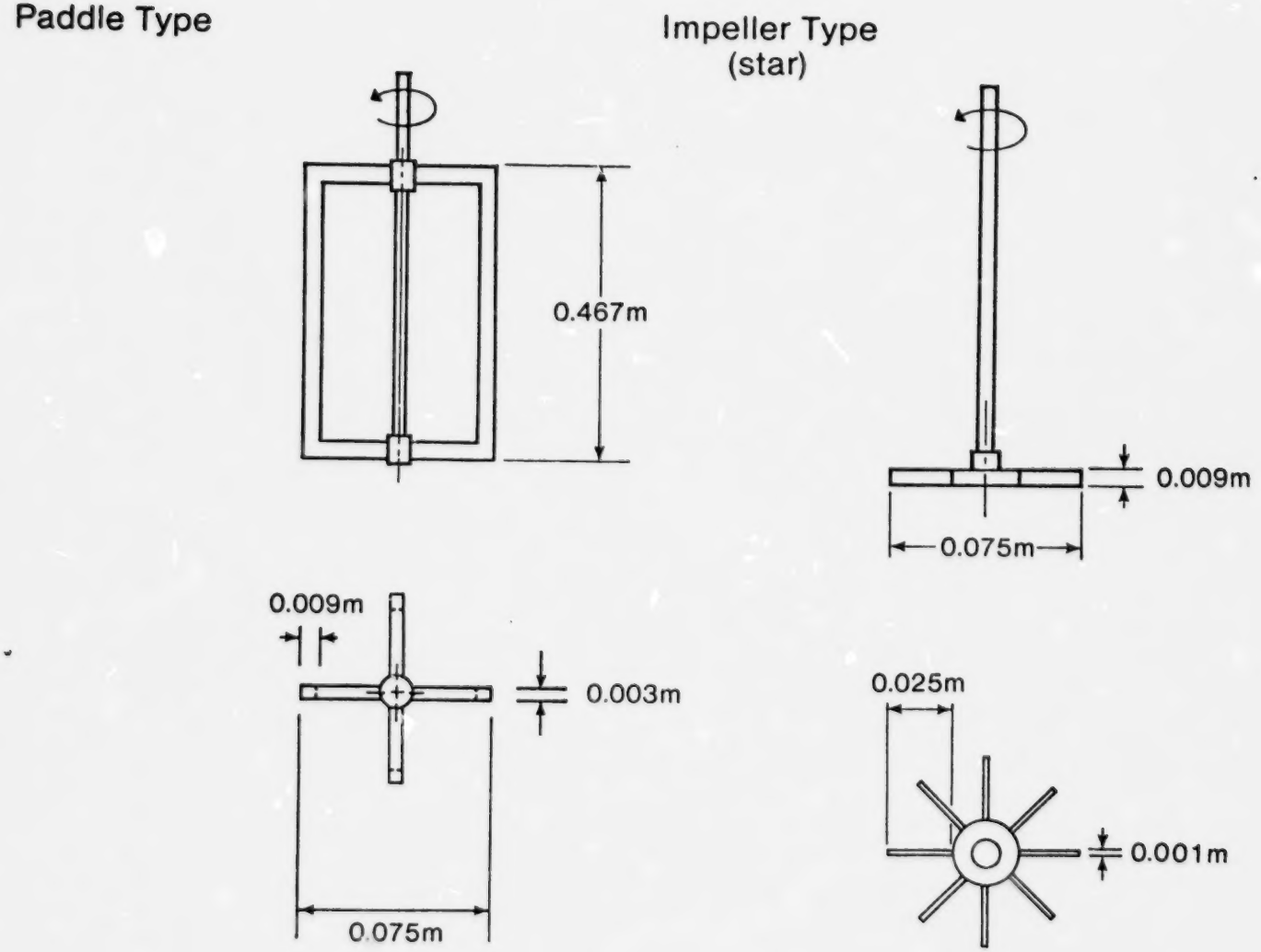

Figure 2 Stirrers description

TABLE 1 : PARTICLE PROPERTIES

PARTICLE	SHAPE	SIEVE ANALYSIS TYLER EQUIV. MESH	SIEVE OPENING M (10^{-4})	DENSITY KG/M**3	HYDRODYNAMIC PARTICLE DIA.,M (10^{-4})
SAND	IRREGULAR	-80+100	-1.77+1.49	2650	1.50
GLASS BEADS	REGULAR	-80+100	-1.77+1.49	2465	1.31
ALUMINUM	IRREGULAR	-65+80	-2.10+1.77	2588	1.90

Photographs of the particles are given in plate 1.

Experimental Procedure

An initial charge of about one kilogram of solids was introduced to the bed. In order to obtain a narrow size of solids from a given sieve cut, the solids were fluidized at a high water rate to elutriate all the fines and in order to narrow the particle size range of the solids.

With a given stirrer in place, the fluidized bed height and the pressure drop at the various bed locations were measured at a preselected water flow rate. These measurements gave the base values at zero RPM at the preselected flow rate. The stirrer was then switched on at a predetermined stirring rate. The new equilibrium bed height and pressure drop along the bed were recorded. The establishment of a new equilibrium takes about 3 minutes. The stirrer was then switched off and the measurements were repeated for a different water flow rate.

Measurements were made for the paddle and impeller type stirrers at different water flow rates and stirring rates. For the impeller, the effect of stirring at two stirrer's blade locations, namely, at 1.0 cm above the base of the bed, to be referred to as base level, BS, and at 8.5 cm above the bed base to be referred to as middle level, MD.

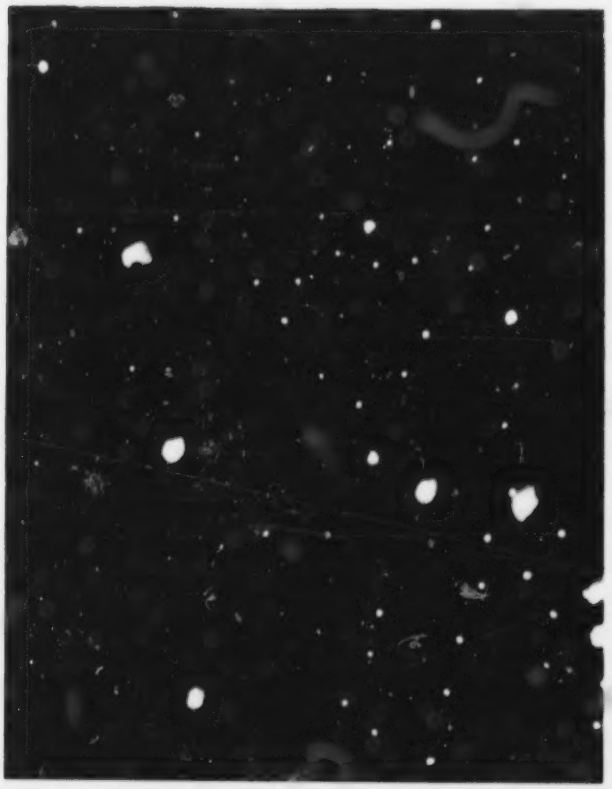

a) SPHERES

b) SAND

c) ROLLED ALUMINUM

THEORETICAL BACKGROUND

Pressure Drop Measurements and Bed Solids Concentration

A force balance on a fluidized bed gives the pressure gradient due to the presence of solids, Juma and Richardson(1979).

$$\frac{\Delta P}{L} = (1 - \alpha_f)\ (\rho_s - \rho_f) g \qquad (1)$$

leading to

$$\alpha_f = 1 - (\frac{\Delta P}{L})\ \frac{1}{(\rho_s - \rho_f) g} \qquad (2)$$

where ΔP is the pressure drop over a bed length L and α_f is the average fluid volumetric concentration (bed porosity) over a bed length of L.

Measurements of pressure drop along the bed provide information regarding the axial variation of the bed porosity.

Slip Velocity Relationships

The slip velocity between solid particles and the fluid can be given by; Rowe and Henwood (1961), Arastoopour et.al (1982) and Wallis (1969).

$$(v_s - v_f)\,|(v_s - v_f)| = \frac{4}{3}\,\frac{(\rho_s - \rho_f)}{\rho_f\ C_D}\ g\ d\ F(\alpha_f) \qquad (3)$$

where v_s and v_f are velocity of the solids and the fluid relative to a stationary observer, respectively. ρ_s and ρ_f are the solids and the fluid density, respectively. The function $F(\alpha_f)$ is a hindered settling correction factor. The drag coefficient is given by

$$C_D = \frac{24}{Re}\ [\ 1 + 0.15\ Re^{0.687}\ ]\ ; \qquad Re < 1000 \qquad (4)$$

and

$$Re = \frac{d\ \rho_f |v_s - v_f| \alpha_f}{\mu_f} \qquad (5)$$

d and μ_f are the particle diameter and fluid viscosity, respectively. Making use of equations (4) and (5), the slip velocity as given by equation (3) becomes

$$v_s - v_f = \frac{g\, d^2 (\rho_s - \rho_f) \alpha_f F(\alpha_f)}{18\, \mu_f [\, 1 + 0.15\, Re^{0.687}\,]} \tag{6}$$

For the case of a uniformly fluidized bed with no recirculation the solids velocity is assumed to be zero and equation (6) becomes

$$V_f = \frac{g\, d^2 (\rho_s - \rho_f) \alpha_f F(\alpha_f)}{18\, \mu_f [\, 1 + 0.15\, Re^{0.687}\,]} \tag{7}$$

where V_f is the fluidization fluid upwards velocity defined as

$$M = V_f\, \alpha_f\, A\, \rho_f$$

where M is mass flow rate of water and A the empty tube area.

For perfectly smooth spherical particles, the function $F(\alpha_f)$ can be given either from experimental correlations or from theoretical consideration. The most accepted form of $F(\alpha_f)$ is that due to Richardson and Zaki (1954) where

$$F(\alpha_f) = \alpha_f^{2.6} \tag{8}$$

The exponent of the α_f in expression (8) is larger than 2.6 when the particles are either non-spherical, rough or very small particles, say, below 100 μ diameter. A general expression for the fluidization fluid velocity can thus be written as

$$V_f = \frac{g\, d^2 (\rho_s - \rho_f)\, \alpha_f^{N-1}}{18\, \mu_f [\, 1 + 0.15\, Re^{0.687}\,]} \tag{9}$$

where N is 4.6 for smooth spherical particles. It should be pointed out here, that the correction term in the square brackets in equations (4) and (9) is for the inertial effects and consequently, the power N can be con-

sidered to be fairly independent of Reynolds number, Richardson and Jeronimo (1979).

Letting $A = V_f(1 + 0.15\ Re^{0.687})$ (10a)

and $C = g\ d^2(\rho_s-\rho_f)/18\ \mu_f$ (10b)

equation (9) becomes

$$\ln A = \ln C + (N-1)\ \ln \alpha_f \tag{11}$$

A plot of $\ln A$ versus $\ln \alpha_f$ gives $N-1$ as its slope. The intercept gives C from which the hydrodynamic particle diameter d can be calculated. Normally, the hydrodynamic value of d is not known a priori and hence Re cannot be precisely evaluated. An iterative approach is followed in the plotting of equation (11).

Although equation (9) is strictly valid for a fluidized bed with no stirring, it is possible to use equation (9) to examine the effect of stirring. To this end a modification to equation (9) can be introduced by replacing the constant "18" by a variable which is a function of the stirring action alone. Equation (9) can then be written as

$$V_f = \frac{g\ d^2(\rho_s-\rho_f)\ \alpha_f^{N-1}}{\beta\ \mu_f[\ 1+0.15\ Re^{0.687}\ ]} \tag{12}$$

Equation (12) can be used to examine the effect of stirring action on the exponent N and the parameter β.

A modification of Richardson and Zaki (1954) hindered settling equation is given by

$$\frac{v_{susp}}{v_\infty} = (1-K\ \alpha_s)^{4.6} \tag{13}$$

where K is a hydrodynamic volume factor. This type of modification has been explored by Fouda and Capes (1977, 1979) and Epstein (1979). This modification assumes the presence of immobile liquid surrounding the particle.

The equivalent form of equation (13) can be cast in a generalized form as

$$\frac{V_f(1-\alpha_s)^2 \left[1+0.15\ Re_{eff}^{0.687} \right]}{(\rho_{eff} - \rho_{susp})} = \left(\frac{g\ d^2\ K^{2/3}}{\gamma\ \mu}\right)(1-K\ \alpha_s)^{4.6} \qquad (14)$$

where

$$\rho_{eff} = [\rho_s + \rho_f(K-1)]/K \qquad (15a)$$

$$\rho_{susp} = \alpha_s(\rho_s-\rho_f) + \rho_f \qquad (15b)$$

and $$Re_{eff} = d\ K^{1/3}\ \rho_f\ v_f\ (1-K\ \alpha_s)/\mu_f \qquad (15c)$$

Equation (14) offers an alternate equation to correlate fluidization data. In the absence of stirring the constant γ approaches 18.

EXPERIMENTAL RESULTS AND DISCUSSION

It was ovserved that for sand and glass beads fluidized bed, a stirring action tends to reduce the effective height of the fluidized bed. Measurements of the bed porosity was made via pressure drop measurements rather than simply using the fluidized bed charge and the visual bed height. This was because a small fraction of the solids charge penetrates the lead shot calming section and because of a slight build-up of solids at the bed walls at high stirring rates, Leva (1960). The effect of stirring rates on the apparent fluidized bed height is shown in Figure 3. As it can be observed, there is a marked influence of stirring on the fluidized bed height.

The variation of the pressure drop with bed height is shown in Figure 4 for various water flow rates. The slope of ΔP vs L gives the average bed fluid volumetric concentration, α_f or the bed porosity. The value of α_f obtained from this type of a plot is subsequently used to determine the effect of stirring. The linearity of ΔP vs L indicates that the bed solid concentration is constant along the bed height. A complete set of the pressure drop variation for all cases considered is given in Appendix B and the raw data are given in Appendix C.

From the pressure drop measurements, the variation of the average bed porosity (fluid volumetric concentration) with water flow rate is shown in Figures 5 to 7 for the sand, glass and aluminum fluidized beds. In all cases, at a given stirring rate, the bed expands with increase of water flow rate. At high water flow rates, the bed porosity decreases monotonically with an increase in the stirring rate. In other words, for a given high water flow rate, the bed height decreases with an increase in the stirring rate. However, it can be observed that for the case of the sand bed with the impeller at MD position and for all the cases of the glass bed, that at <u>low</u> water flow rates, a higher stirring rate tends to expand the bed. This is

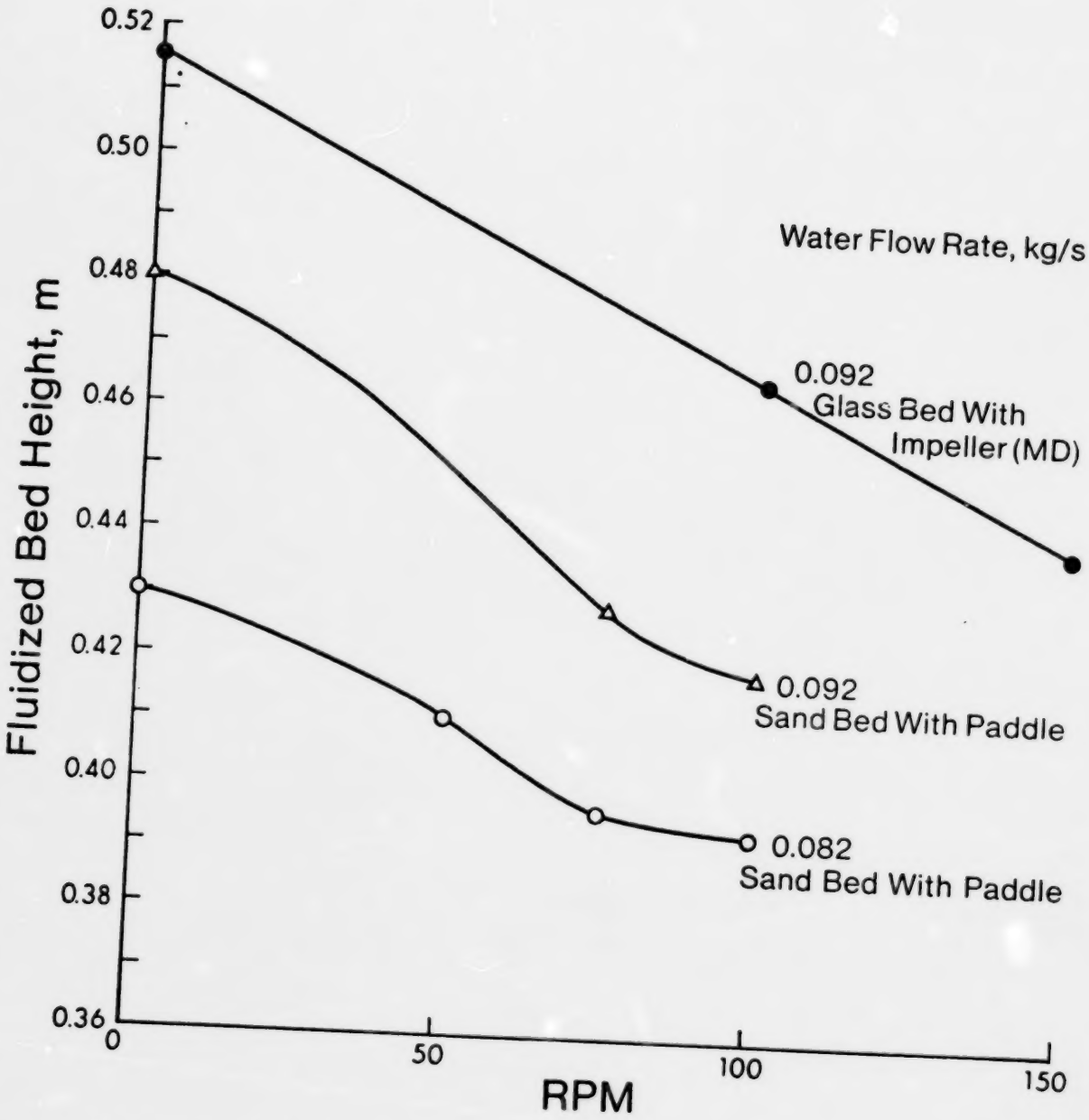

Figure 3 Variation of apparent bed height with rpm

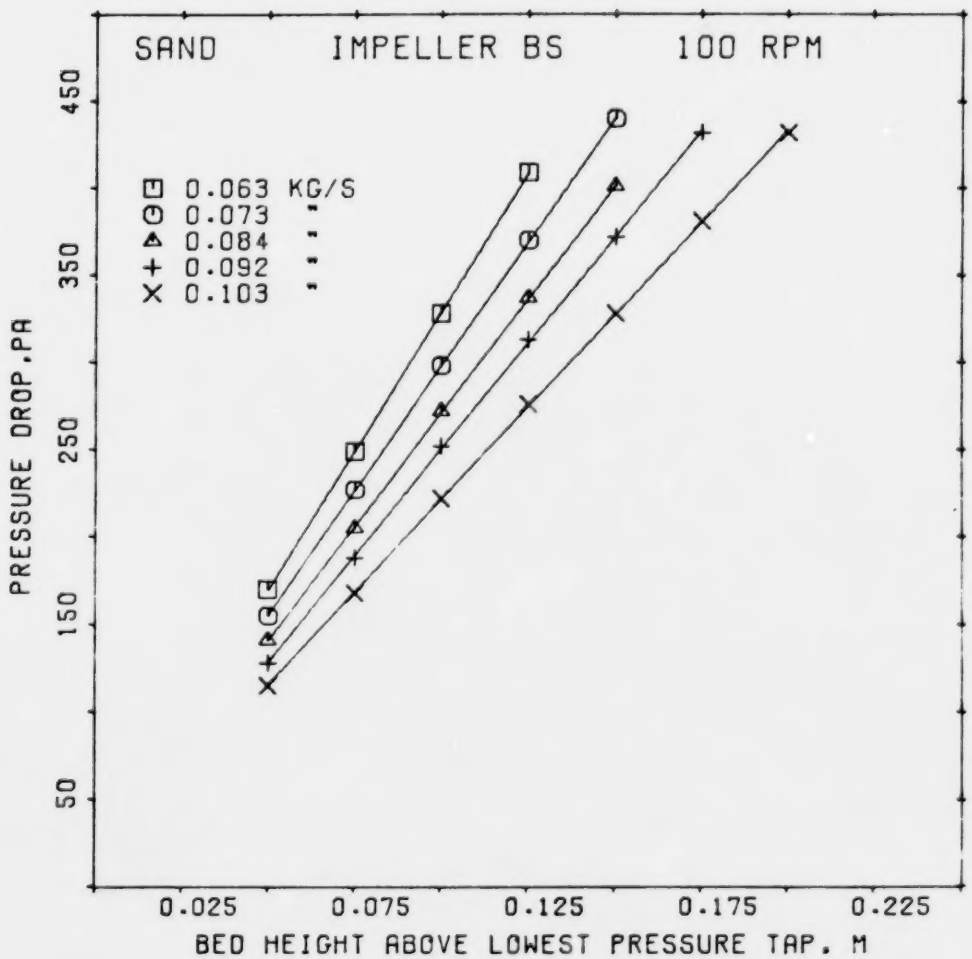

Figure 4 Variation of pressure drop for a sand bed with an impeller at BS location at 100 rpm

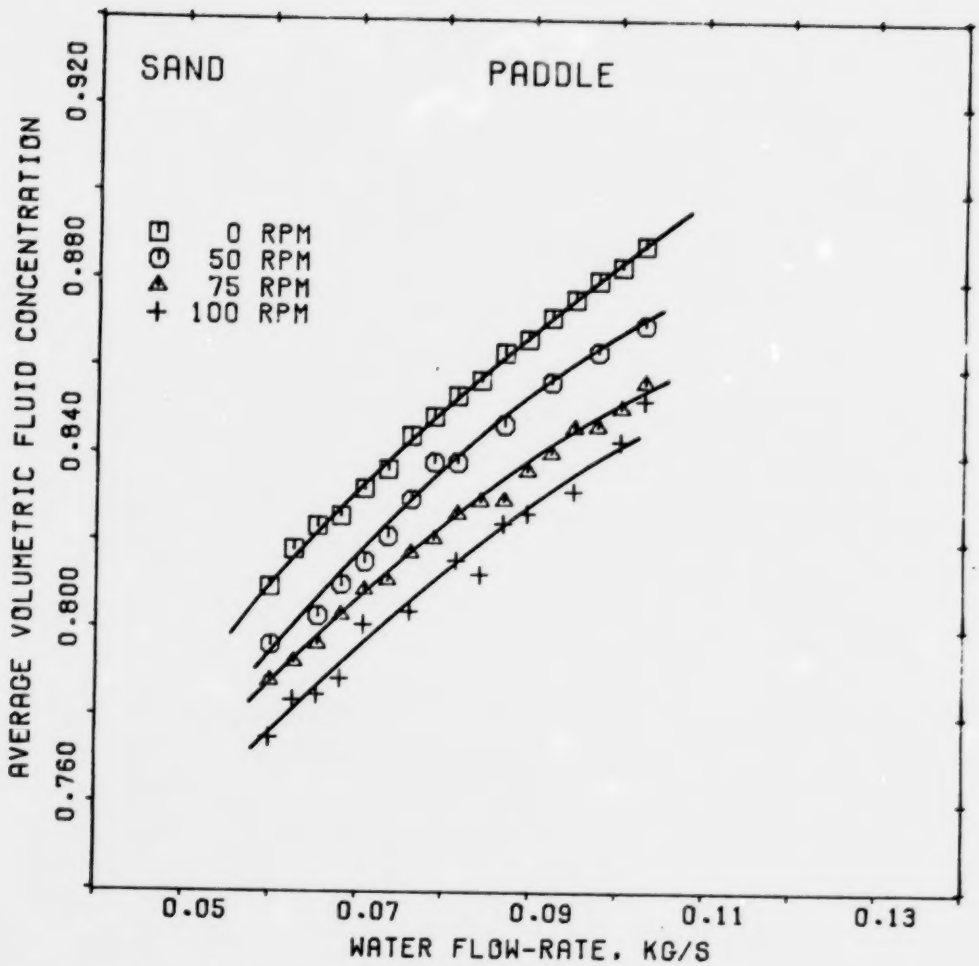

Figure 5(a) Variation of α_f with flow rate for a sand bed with a paddle

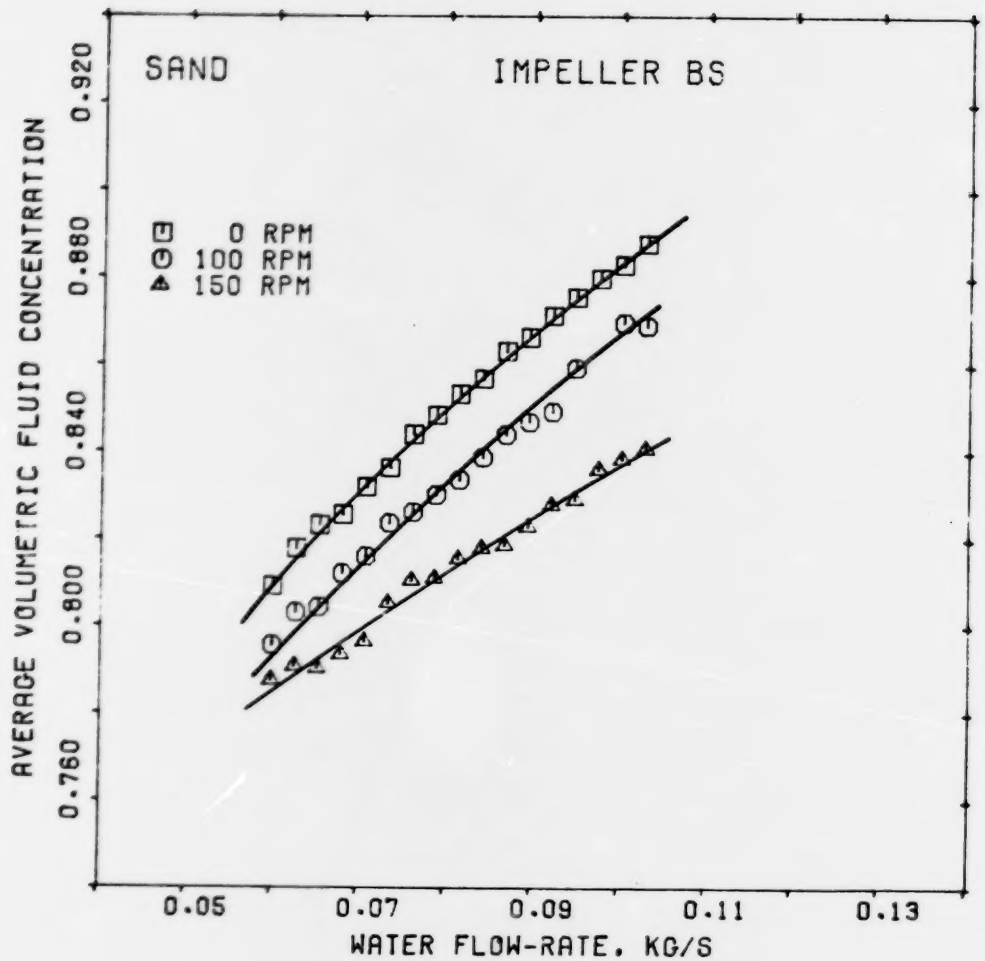

Figure 5(b) Variation of α_f with flow rate for a sand bed with an impeller at location BS

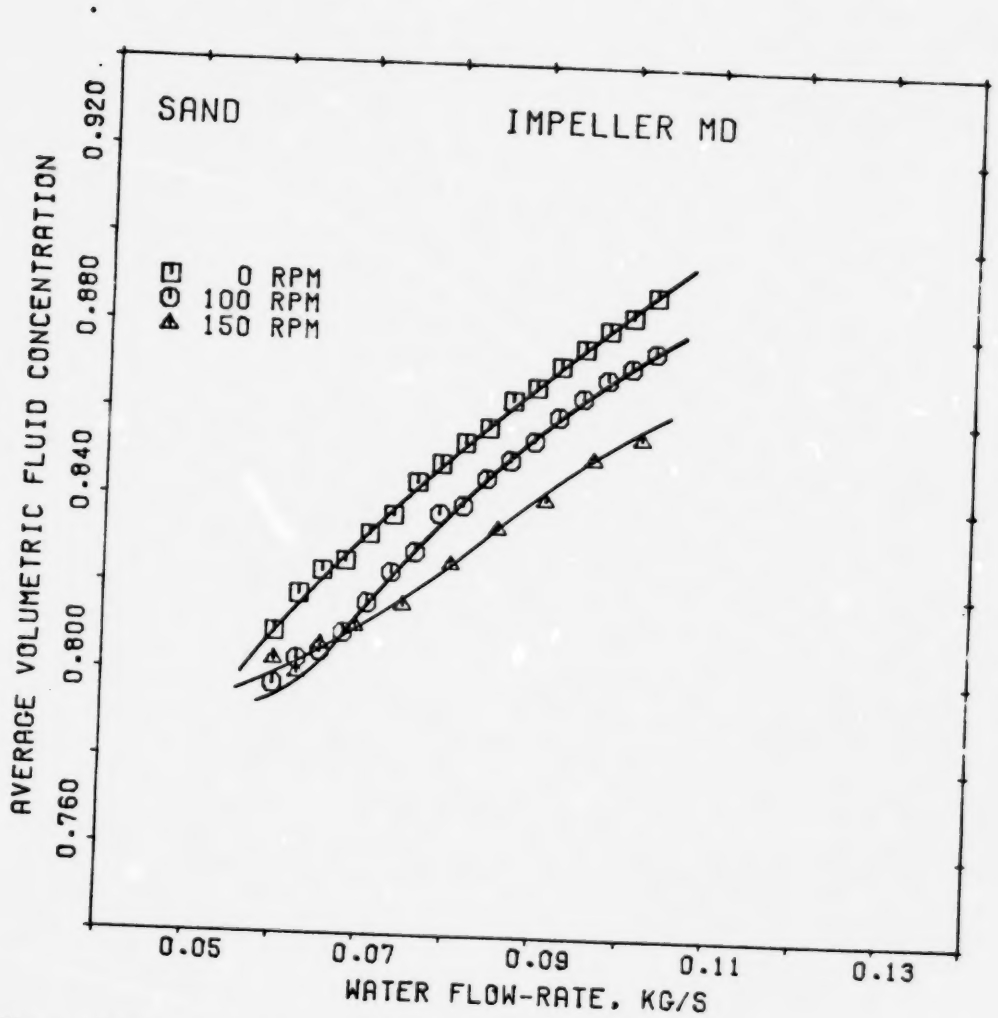

Figure 5(c) Variation of α_f with flow rate for a sand bed with an impeller at location MD

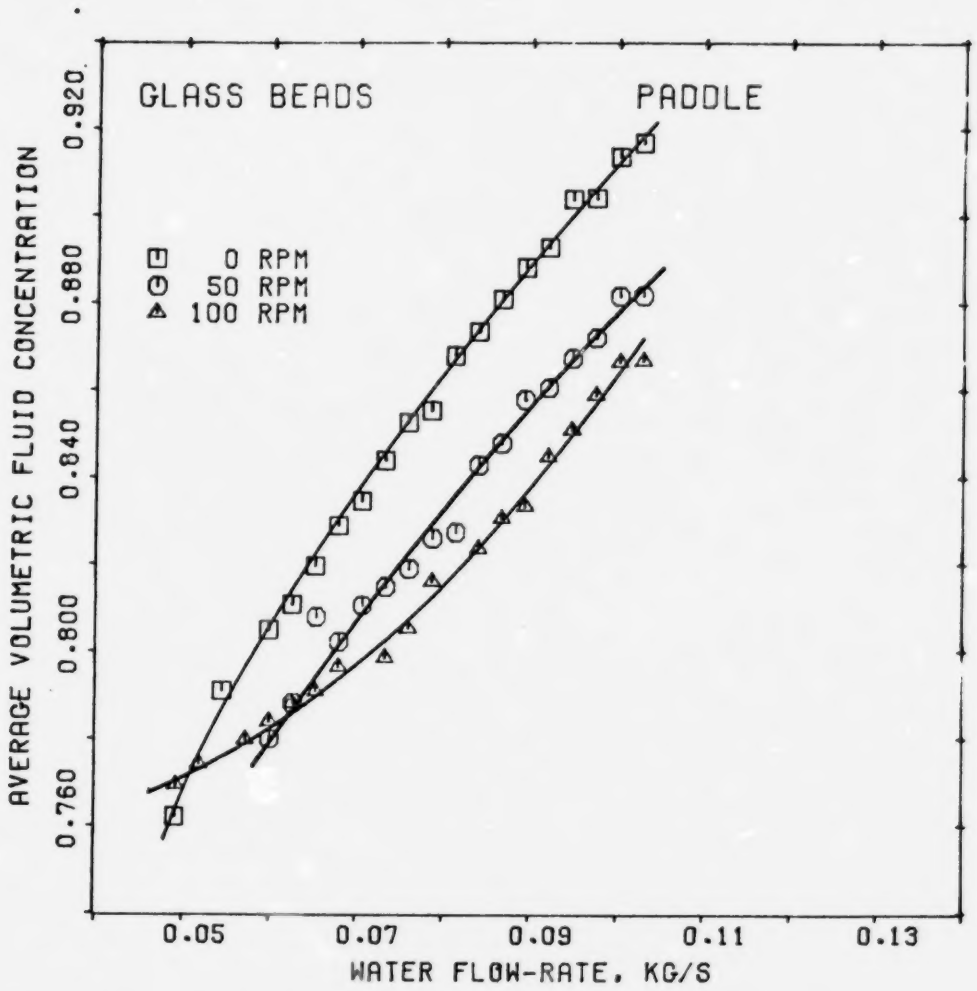

Figure 6(a) Variation of α_f with flow rate for a glass bed with a paddle

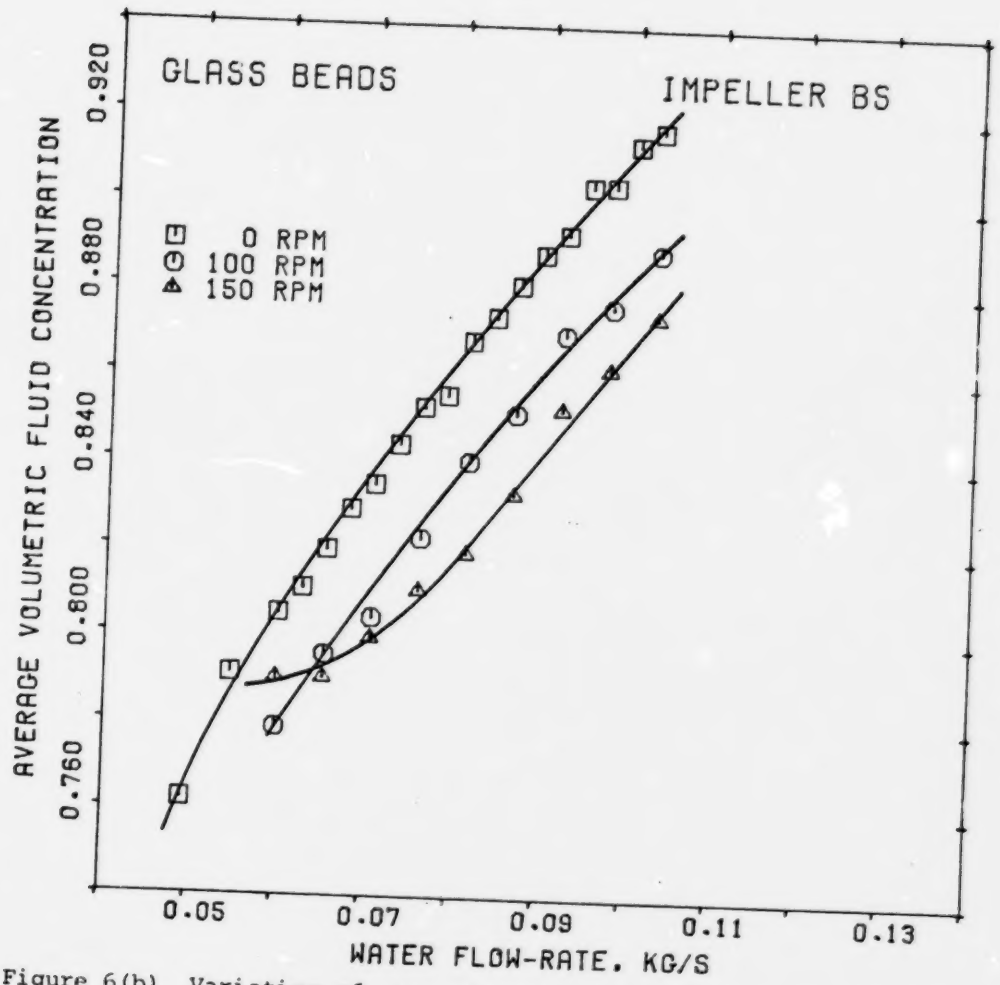

Figure 6(b) Variation of α_f with flow rate for a glass bed with an impeller at location BS

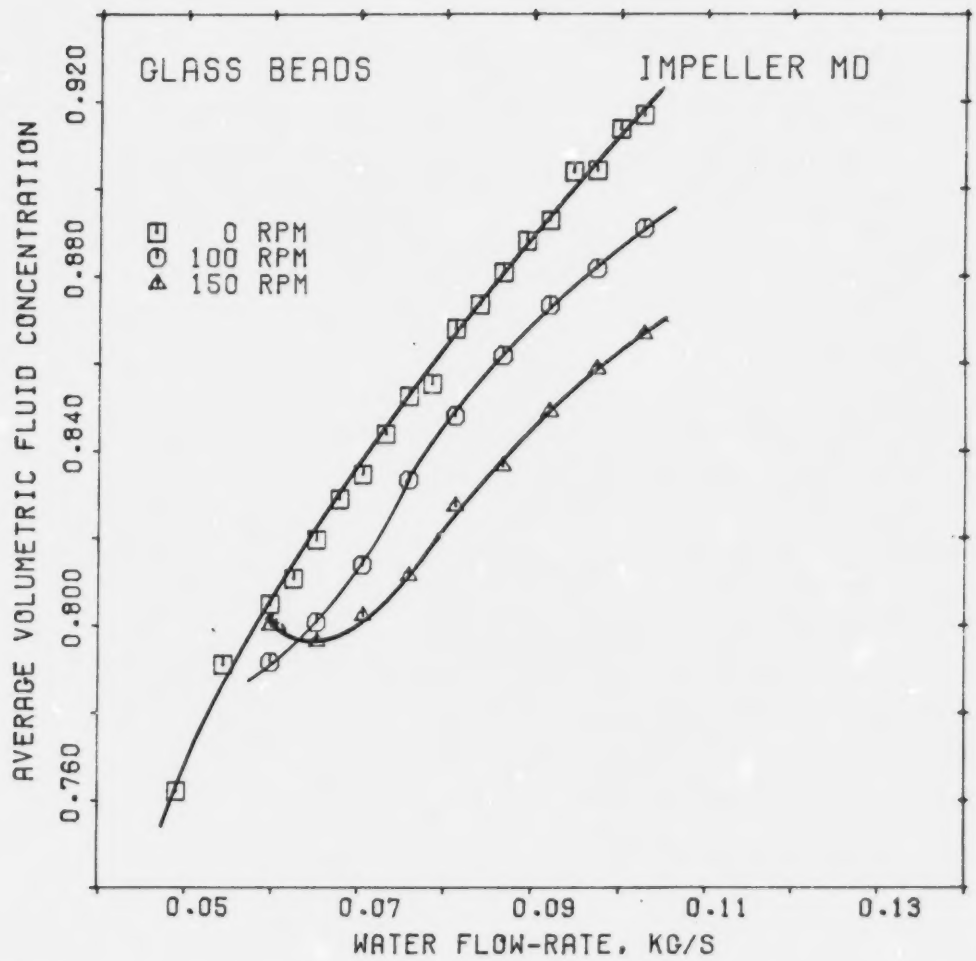

Figure 6(c) Variation of α_f with flow rate for a glass bed with an impeller at location MD

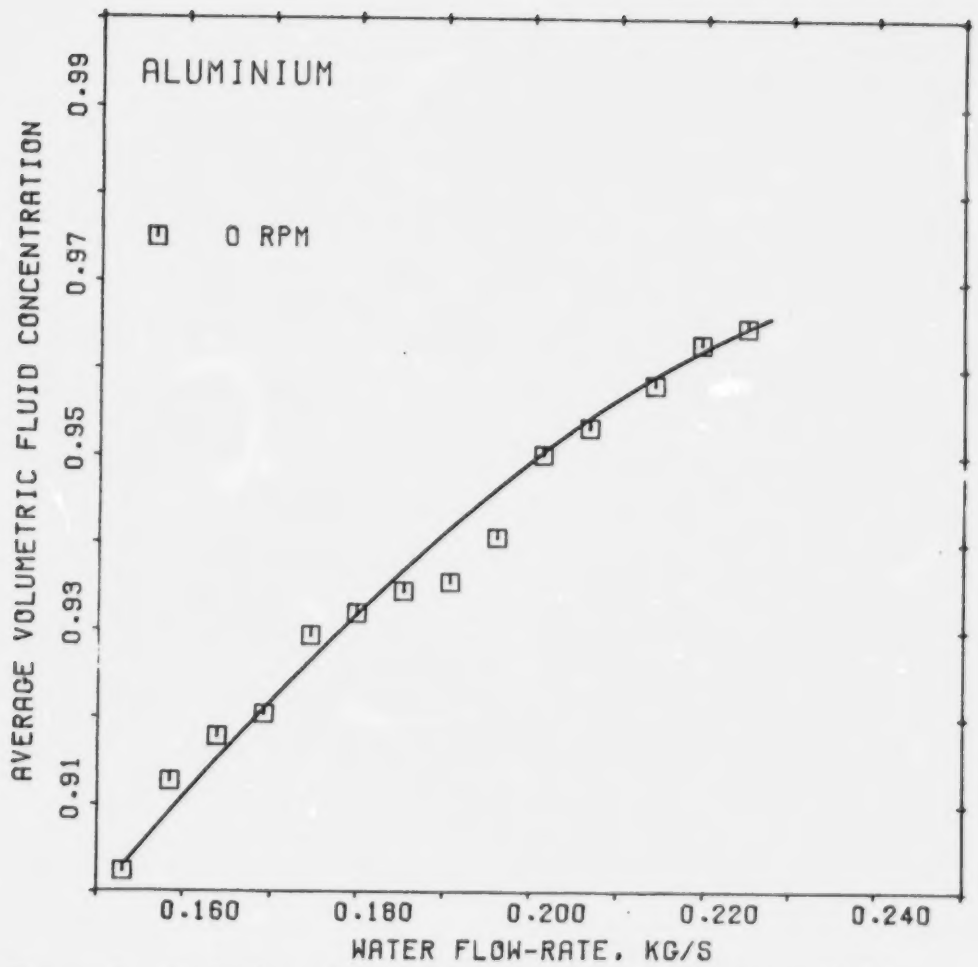

Figure 7 Variation of α_f with water flow rate for rolled aluminum particles

evidenced by the crossing over of the curves. This means that a low fluidization velocity, stirring of the bed enhances bed expansion which is due to the generation of upward lift on the solids particles as would be the case in a non-fluidized system. Such an upward lift is more evident for the case of glass beads bed due to their lower density and smaller particle diameter.

A possible explanation of the decrease of the bed porosity and hence bed height due to stirring could be explained by the presence of solids circulation brought about by the stirring action. Hiby (1967) has shown that a decrease of the total drag could be caused by circulation. Hiby's derivation can be made as follows:

Consider a fluidized bed with an average fluid concentration, α_{fo}, and an average fluid velocity v_{fo} where $Q_o = -A\, v_{fo}\, \alpha_{fo}$. Assume at the central bed region the fluid concentration is higher than that near the bed walls (annular region) by a quantity $\Delta\alpha_f$. The consequence is that the particles in the annular region will move downwards and the fluid velocity will be decreased to v_{f2}. In the central core, the particles will move upwards and the fluid velocity will be increased to v_{f1}. A schematic view of the circulation is shown in Figure 8, after Hiby.

A mass balance for the particles gives

$$A_1 v_{s1} (1-\alpha_{fo}-\Delta\alpha_{fo}) = -v_{s2} (1-\alpha_{fo}+\Delta\alpha_{fo}) A_2 \qquad (16)$$

where A_1 and A_2 are the empty tube areas for the central and annular regions, respectively.

The slip velocity, ignoring inertial effects, is given by

$$v_s - v_f = \frac{g\, d^2 (\rho_s-\rho_f)}{18\, \mu_f}\, \alpha_f^m = F(\alpha_f) \qquad (17)$$

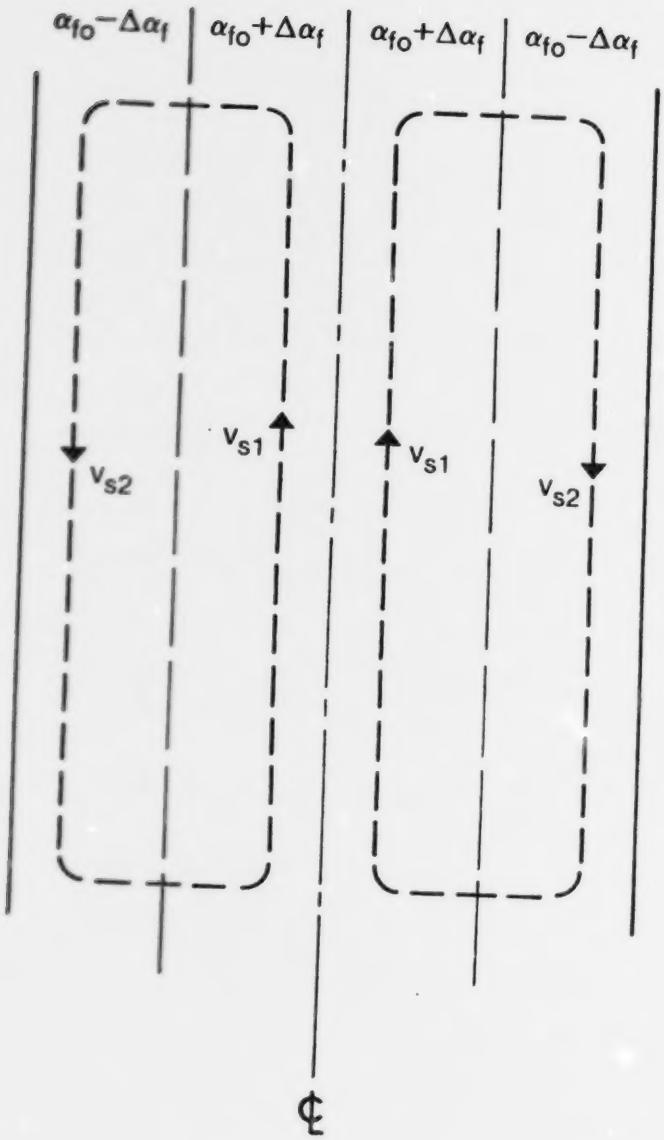

Figure 8 Schematic diagram of particle circulation

where m is a constant. For a uniform bed, the solids velocity, $v_s = 0$ and equation (17) gives

$$-v_{fo} = \frac{g\, d^2}{18\, \mu_f} (\rho_s - \rho_f)\, \alpha_{fo}^m = F(\alpha_{fo}) = F_o \tag{18}$$

For the central and annular regions, one can write using equations (17 and (18)

$$v_{s1} - v_{f1} = F(\alpha_{fo} + \Delta\alpha_f) = -v_{fo} + \frac{d\,F}{d\,\alpha_f}\Big|_{\alpha_f=\alpha_{fo}} \Delta\alpha_f \tag{19a}$$

and

$$v_{s2} - v_{f2} = F(\alpha_{fo} - \Delta\alpha_f) = -v_{fo} - \frac{d\,F}{d\,\alpha_f}\Big|_{\alpha_f=\alpha_{fo}} \Delta\alpha_f \tag{19b}$$

where a downwards velocity is taken as positive. For simplicity, assuming that the flow areas for the central and annular regions are the same, and noting that the volumetric flow rates in the central and annular regions are given by $-A_1 v_{f1} \alpha_{f1}$ and $-A_2 v_{f2} \alpha_{f2}$, respectively, then solution of equations (16) to (19) gives

$$Q = Q_o \left[\, 1 + m \left(\frac{\Delta\,\alpha_f}{\alpha_{fo}}\right)^2\right] + v_{s2} \left[\frac{\alpha_{fo}(1-\alpha_{fo}) + (\Delta\,\alpha_f)^2}{1 - \alpha_{fo} - \Delta\,\alpha_f}\right] A \tag{20}$$

where Q_o and Q are the required water flow rates to maintain the same bed height for uniform and non-uniform porosity beds, respectively. Recognizing that v_{s2} is positive, then equation (20) leads to $Q > Q_o$. This means that in order to maintain the initial average porosity, it is necessary to increase the water flow rate once solids circulation occurs. Consequently, if the water flow rate is not increased, the bed will contract. Similar observations can be made even if $v_{s2} = 0$ as long as $\Delta\,\alpha_f \neq 0$. In other words, for beds having the same average porosity, a higher water flow rate is

required to maintain a bed with non-uniform radial solids distribution as opposed to a bed of uniform solids distribution. It should be noted here that equation (20) is slightly different than that originally presented by Hiby.

During the course of the experimental study, it was noted that stirring of the fluidized bed encouraged the slight build-up of solids over the lead shots near the bed walls. This is an evidence of the downwards movement of the solids in the annular bed region as suggested by equation (20), Leva (1960). We have also conducted preliminary measurements of the bed solids concentration using a conductivity probe. For the case of the impeller at MD location and 100 RPM, the maximum difference of the solids concentration for the case of sand across the bed was found to be 0.02 ± 0.005. The sand concentration is higher near the bed wall.

It has been mentioned earlier that no bed contraction was observed for the case of rolled aluminum solids when the fluidized bed was subjected to a stirring action. To explain the no stirring effect on the aluminum particles the following postulate is put forward.

The contraction of a fluidized bed due to the stirring action can also be thought of in terms of a decrease in the total drag on the solids. Stirring decreases the total drag on the solids due to the creation of solids circulation. When elongated solid particles are fluidized at low Reynolds number, on the average, the particles align themselves along the flow direction. Such an alignment gives the minimum drag on the particles. However, when such elongated particles fluidized bed are subjected to a rotationary motion, a slip velocity is created in the angular direction. This angular slip velocity gives rise to a drag acting in the angular direction which when coupled with the axial drag force, the particles no longer keep their vertical alignment. The non-alignment with the vertical direction gives rise to a higher drag which, in turn, tends to expand the bed. It is

believed that the bed expansion which is due to the change in the particles orientation, coupled with the bed contraction which is due to solids circulation cancel each other. To show that the drag decrease due to circulation and the drag increase due to orientation are of the same order, the following analysis is given.

Consider an axisymetric prolate particle translating with a steady slip velocity $\vec{U}$. The component of drag along the principal axes are

$$F_{D1} = -\mu_f c_1 U \cos\theta \tag{21}$$

and

$$F_{D2} = -\mu_f c_2 U \cos\theta \tag{22}$$

The net drag is given by, Clift, et.al (1978)

$$F_D = -\mu_f U [c_1^2 \cos^2\theta + c_2^2 \sin^2\theta]^{\frac{1}{2}} \tag{23}$$

at angle ϕ to axis of symmetry,

where

$$\tan\theta = (c_2/c_1) \tan\phi \tag{24}$$

the ratio c_2/c_1 is approximately given by

$$c_2/c_1 = (3 + 2E)/(4 + E) \tag{25}$$

where E is the aspect ratio of the prolate spheroid ($E > 1$)

From physical consideration, Figure 9

$$\theta + \alpha = \beta + \phi \qquad \text{where } \alpha = \tan^{-1} U_h/U_v \tag{26}$$

In the absence of an angular slip velocity, the drag is given by

$$F_{Do} = -\mu_f U c_1 \tag{27}$$

The total drag F_D must be directed to counterbalance the net gravity force acting on the particle, hence

$$\left(\frac{F_D}{F_{Do}}\right)_{\text{orientation}} = \frac{1}{\cos\beta} \tag{28}$$

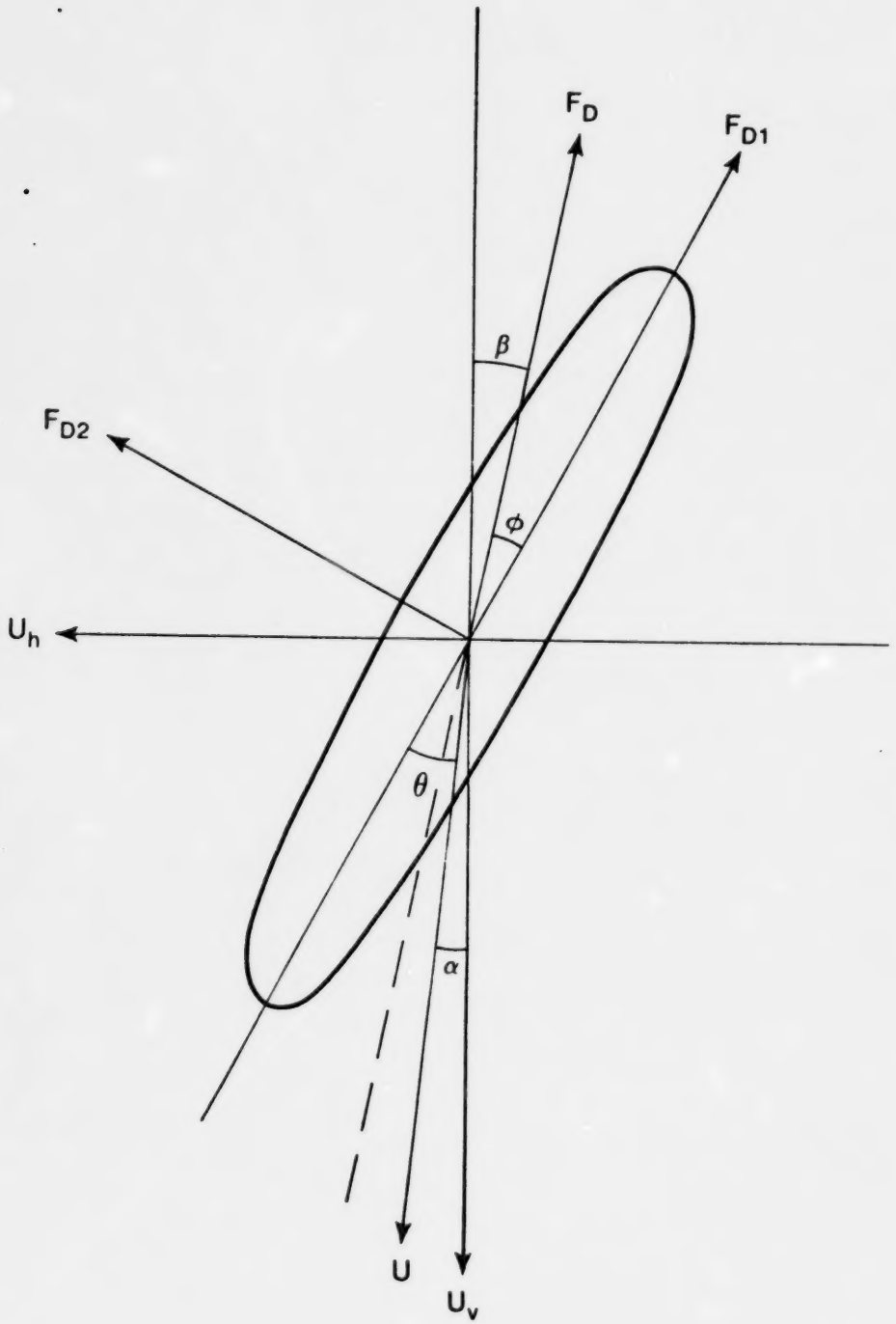

Figure 9 Forces on a suspended elongated particle

Iterative solution of equations (23) to (26) for a given aspect ratio and slip velocity ratio, U_v/U_h, gives the angle β and hence the increase in the drag due to particle non-alignment. Assuming that rolled aluminum particles have the shape of a prolate spheroid with $E=3$ and $U_v \simeq (1-0.1)\ U_h$ the angle β ranges from 50° to 8°, respectively. This indicates that the drag ratio $(F_D/F_{Do})_{orientation}$ varies from 1.56 to 1.01. Although the derivation is strickly correct for an isolated particle, this ratio is assumed to approximately hold for the case of swarms of particles.

The drag force for a particle in a swarm is inversely proportional to the fluidization velocity. An estimate of the change in the drag ratio due to stirring can be made by taking the ratio of the water flow rate for sand with a paddle for different stirring rates at a given fluid concentration. At a volumetric concentration of 0.84, $(F_D/F_{Do})_{circulation}$ varies from 1/1.11 to 1/1.32 for 50 and 100 RPM, respectively. This reduction in the drag ratio is of the same order as that due to orientation increase. It seems reasonable that the compensation effect between drag increase due to orientation and drag decrease due to circulation leads to no observable change in the bed height for the rolled aluminum bed upon stirring.

The hydrodynamic particle diameter was obtained using equation (12). At zero rpm, plots of $\ell n[V_f(\ 1+0.15\ Re^{0.687})]$ versus $\ell n\ \alpha_f$ gave a straight line for cases where stirring rate was low. Figures 10 to 12 show that at higher rpm a plot of equation (12) no longer gives a straight line and consequently it is not possible to relate the fluidization velocity to α_f^a where a is a simple constant.

For the case of zero rpm, the values of N for sand, glass and aluminum are 6.40, 4.35, 6.88, respectively.

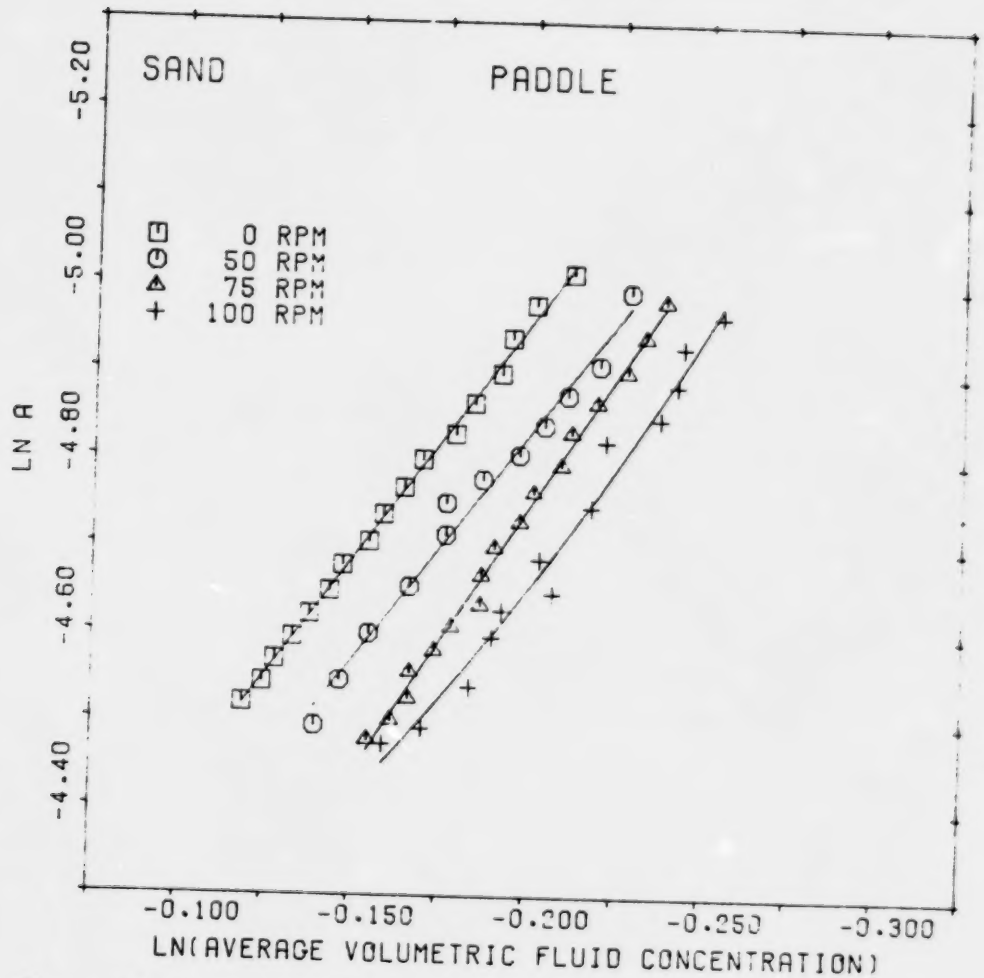

Figure 10(a) Regression plot using equation 12 for a sand bed with a paddle

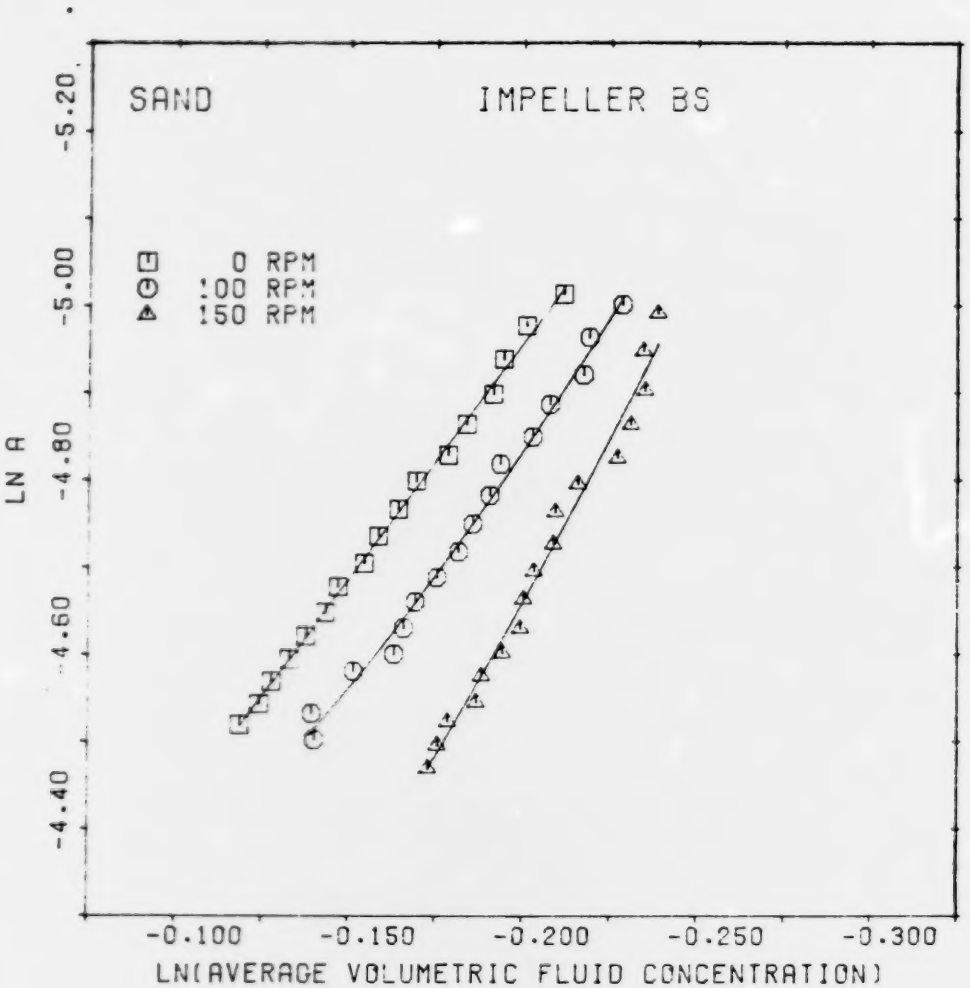

Figure 10(b) Regression plot using equation 12 for a sand bed with an impeller at Bs

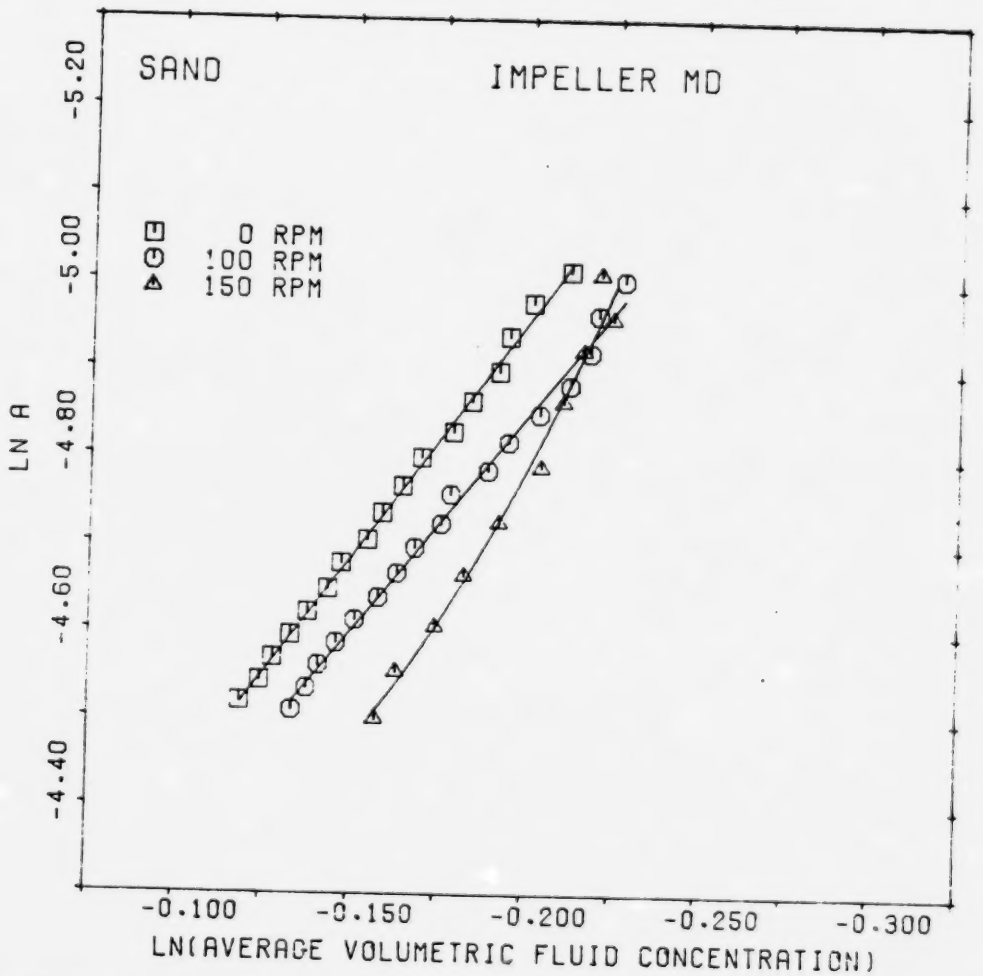

Figure 10(c) Regression plot using equation 12 for a sand bed with an impeller at MD

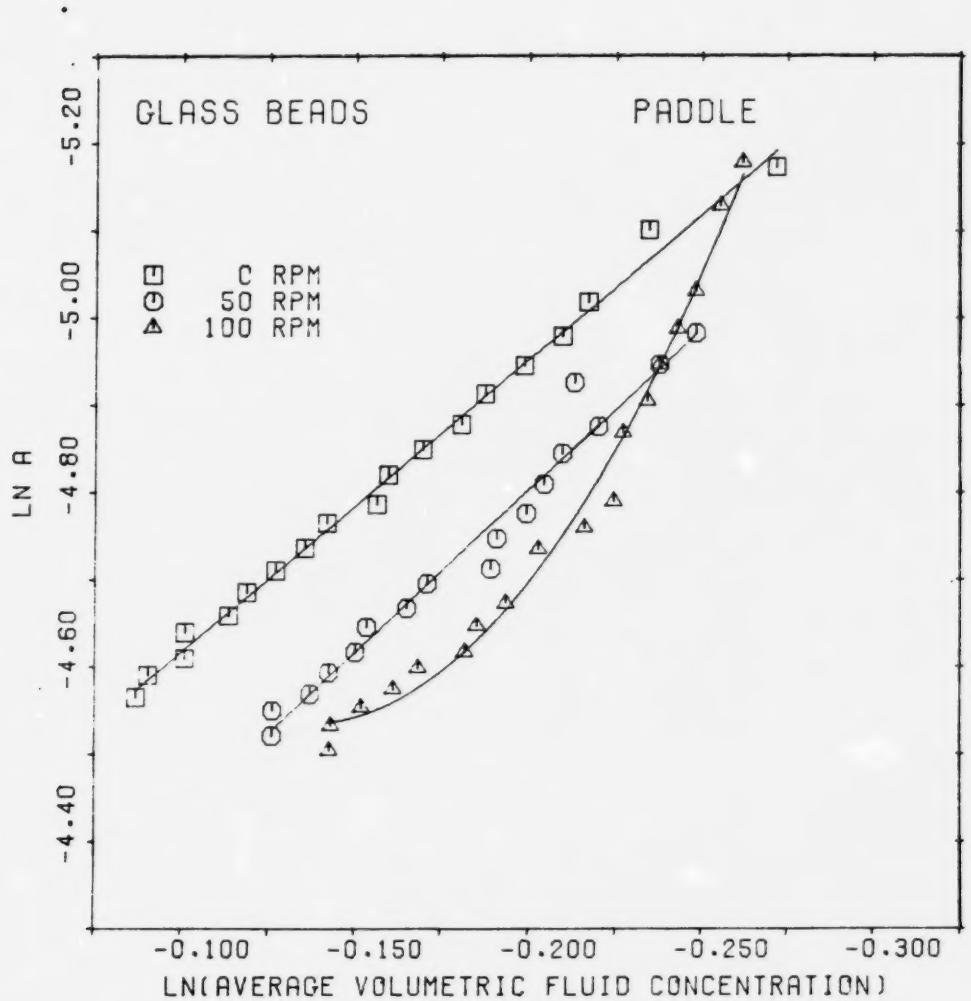

Figure 11(a) Regression plot using equation 12 for a glass bed with a paddle

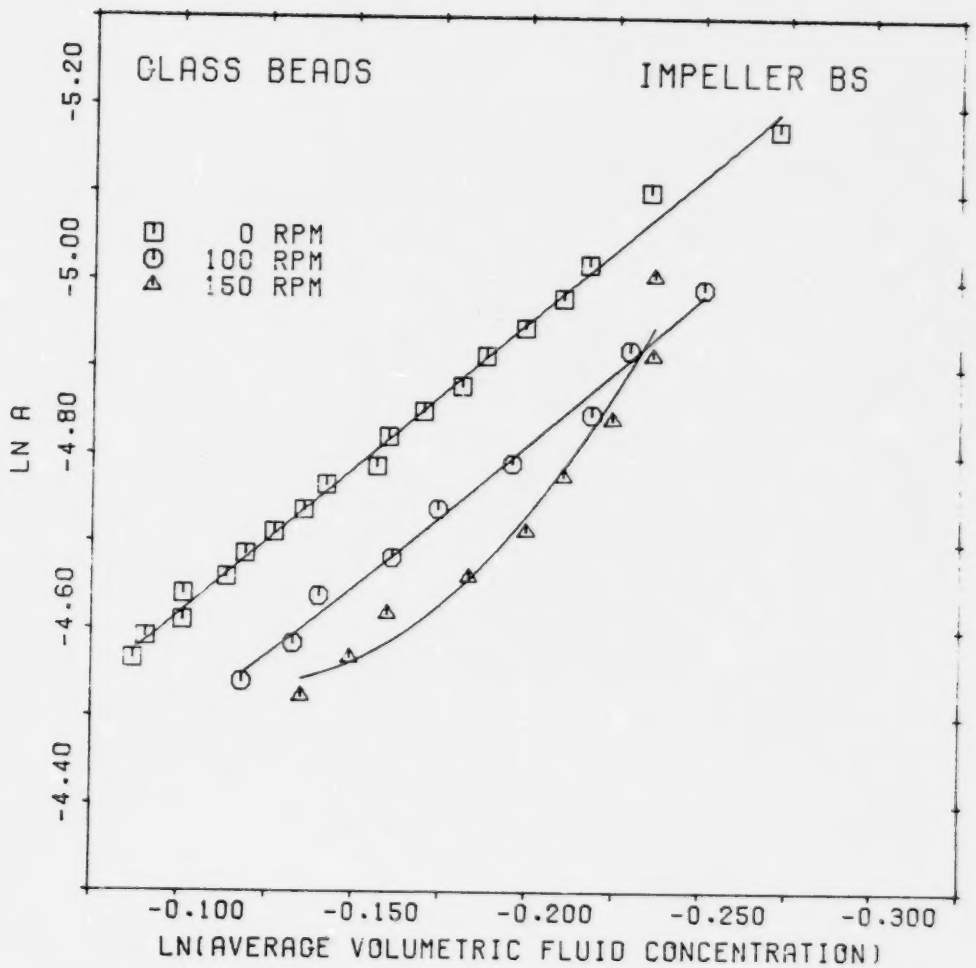

Figure 11(b) Regression plot using equation 12 for a glass bed with an impeller at BS

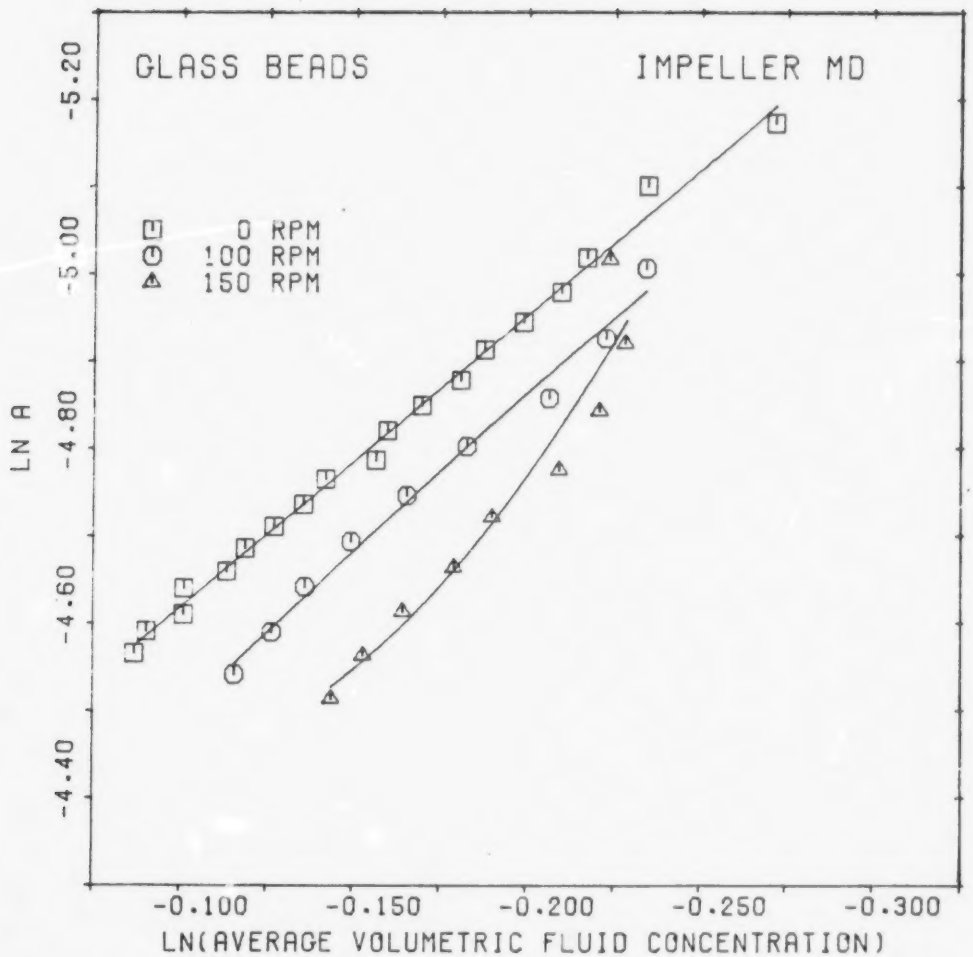

Figure 11(c) Regression plot using equation 12 for a glass bed with an impeller at MD

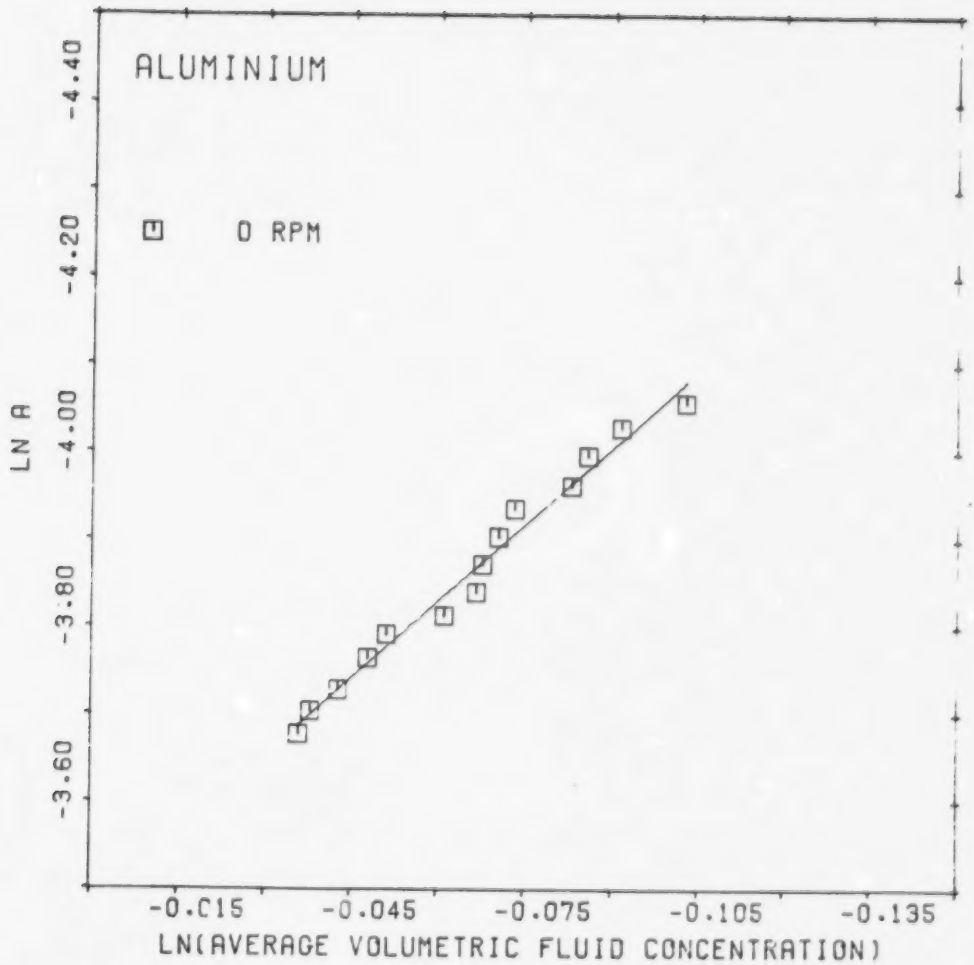

Figure 12 Regression plot using equation 12 for an aluminum bed

Equation (14) is successfully used to correlate the fluidization data. The plotting of equation (14) is made iteratively. The value of K was found such that a slope of 4.6 is obtained. For the case of sand bed, a plot of $\ell n\ B$ vs $(1-K\ \alpha_s)^{4.6}$ was capable to fit the data by a single straight line. Here B is given by

$$B = V_f(1-\alpha_s)^2(1+0.15\ Re_{eff}^{0.687})/(\rho_{eff} - \rho_{susp}) \qquad (29)$$

Figure (13) shows a plot of equation (14) for the case of a sand bed.

For the case of glass beads, equation (14) was also successful in correlating the data but with the exclusion of low water flow rates. For the case of low water flow, different values of K are to be used. Figures 14 and 15 show plots of equation (14) for the case of a glass bed. Figure 16 is the corresponding plot for aluminum particles. Table 2 gives the correlation values of K and γ obtained in using equation (14).

It should be pointed out here that although equation (14) has physical significance in hindered settling for a uniform bed, it should be treated simply as a regression equation for the case of stirring. Moreover, the location of the data points on Figures 13-15 should not be construed to be the order of effectiveness of either the type of stirrer or the stirring rate.

The effectiveness of a particular stirring action can be taken to be the amount by which it causes a bed to contract. In this context it was found that at a given rpm the paddle to be most effective. It is of interest to note that the impeller stirrer located at 8.5 cm above the lead shot was more effective in contracting the fluidized bed than that located just above the lead shot .

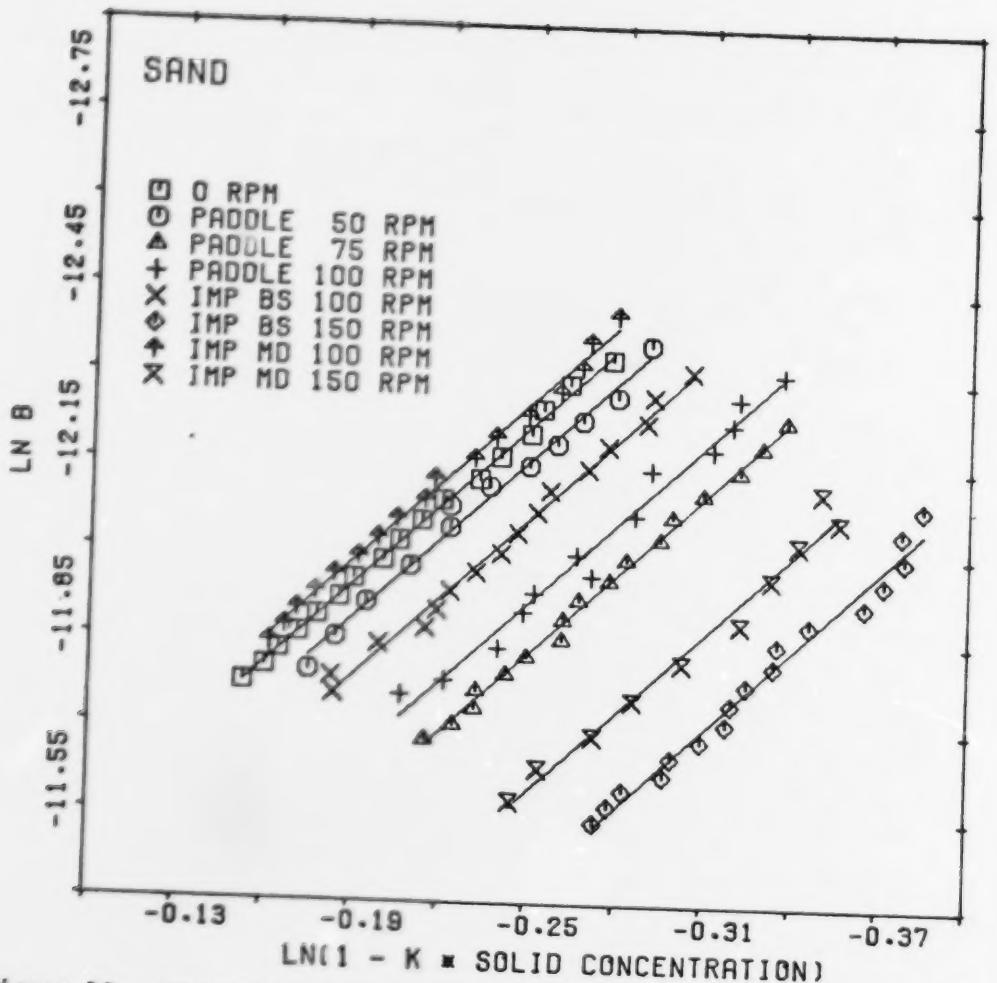

Figure 13 Regression plot using equation 14 for a sand bed at various rpm and stirrers

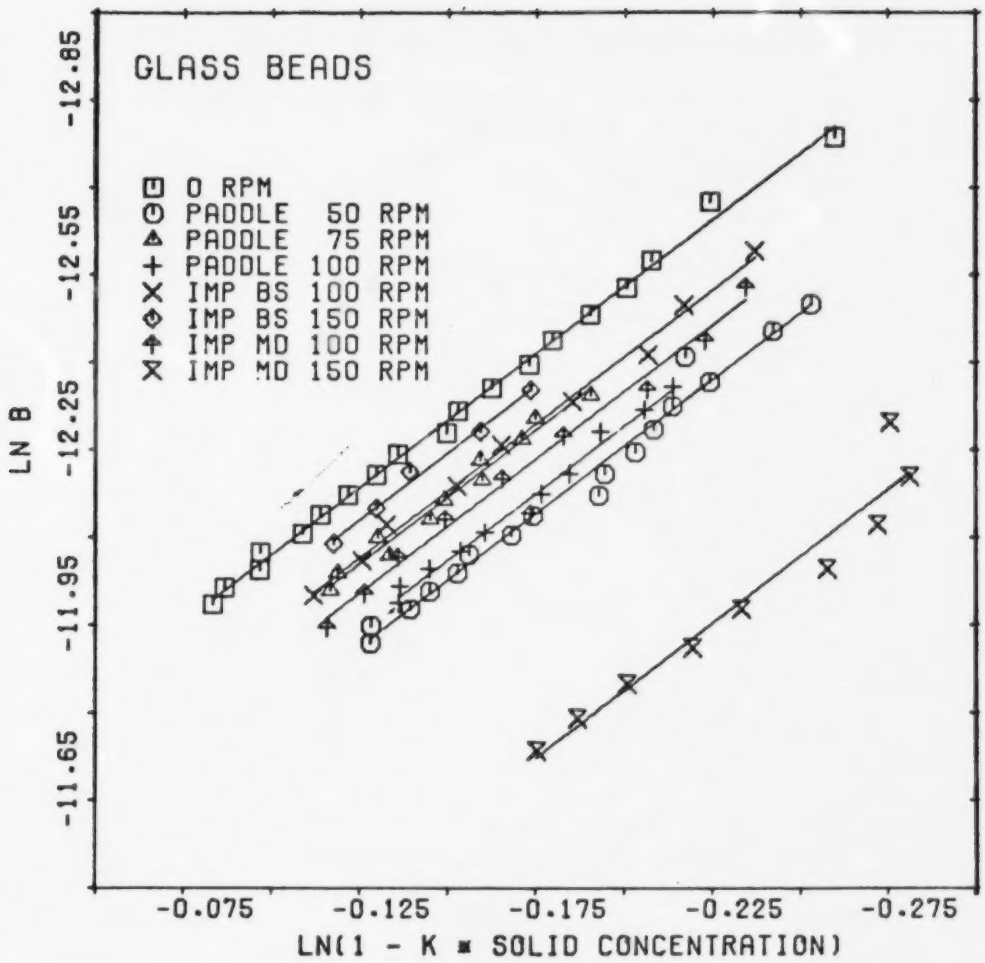

Figure 14 Regression plot using equation 14 for a glass bed at various rpm and stirrers at high water flow rate

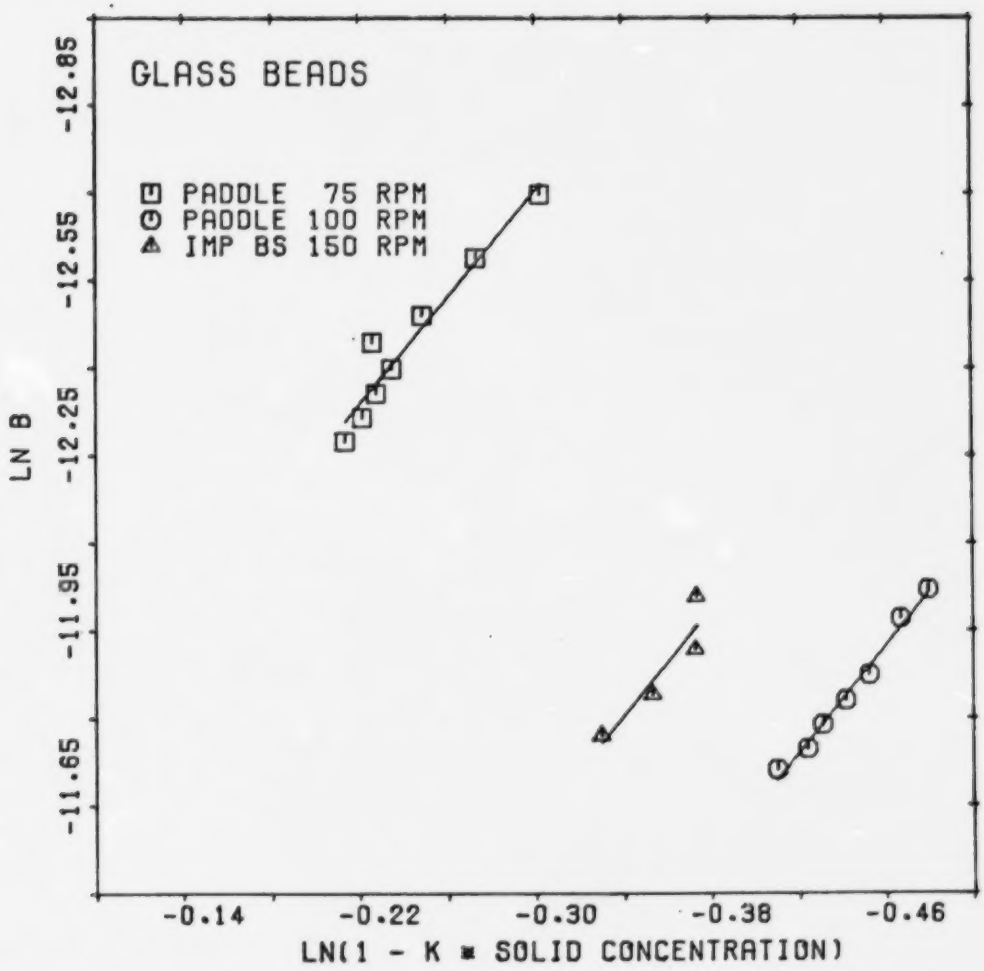

Figure 15 Regression plot using equation 14 for a glass bed at various rpm and stirrers at low water flow rate

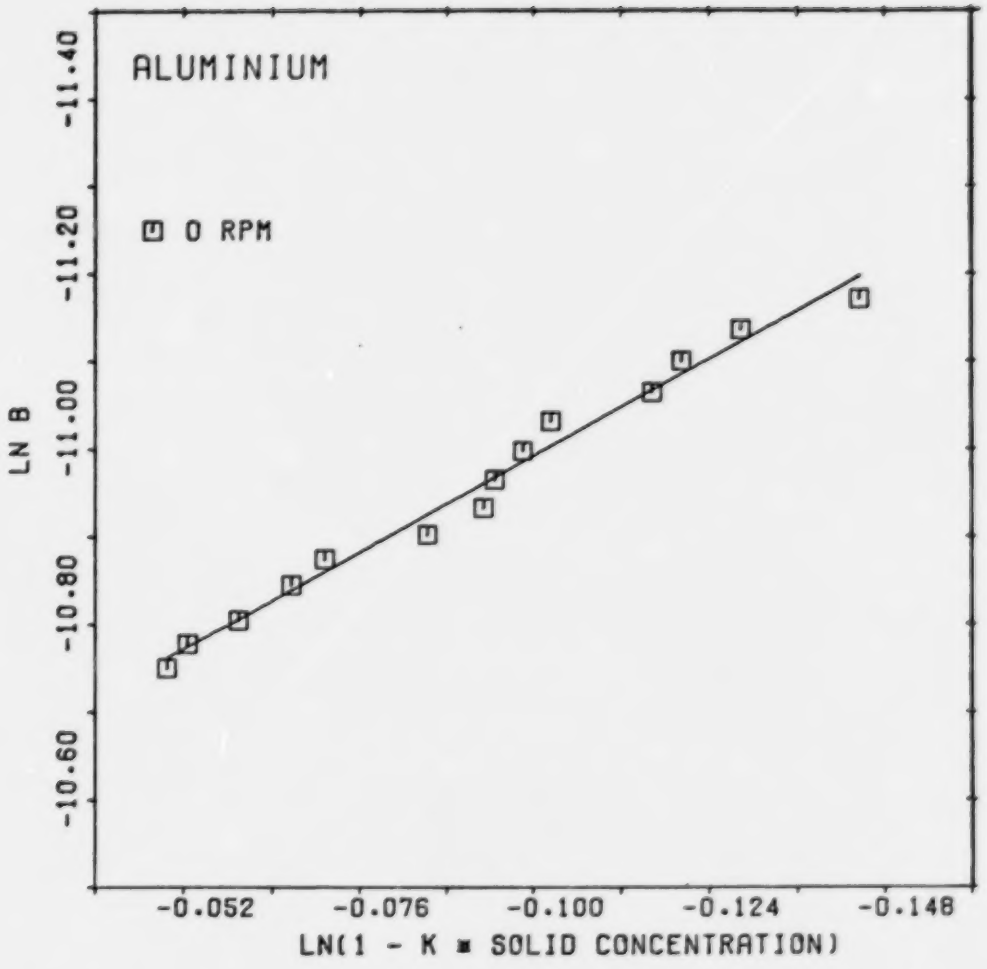

Figure 16 Regression plot using equation 14 for aluminum bed

TABLE 2 : VALUES OF K AND Y OF REGRESSION EQUATION 14

	STIRRER TYPE	STIRRING RATE RPM	SAND 0.060≤M≤0.103kg/s		GLASS BEADS 0.049≤M≤0.103kg/s		GLASS BEADS 0.073≤M≤0.103kg/s		GLASS BEADS 0.049≤M≤0.076kg/s	
			K	Y	K	Y	K	Y	K	Y
(1)	-	0	1.27	16.98	0.96	18.21	-	-	-	-
(2)	Paddle	50	1.23	15.75	1.02	14.35	-	-	-	-
(3)	"	75	1.35	11.99	-	-	0.94	15.74	1.02	14.27
(4)	"	100	1.27	12.55	-	-	0.96	14.30	1.66	4.20
(5)	Impeller (BS)	100	1.28	14.62	0.95	16.05	-	-	-	-
(6)	"	150	1.50	8.63	-	-	0.88	16.33	1.49	6.08
(7)	Impeller (MD)	100	1.19	17.02	1.00	15.58	-	-	-	-
(8)	"	150	1.49	10.11	1.20	10.47	-	-	-	-

Aluminum (ORPM) K = 1.39 Y = 16.06 (0.153 ≤ M ≤ 0.225 kg/s)

M - Mass flow rate of water, kg/s

SIMULATION OF A GRAVITY SEPARATION VESSEL

The details of the simulation of a gravity separation vessel is given by Masliyah et.al (1981). The gravity separation vessel is assumed to be one dimensional and to consist of three zones, Figure 17. A middle zone is assumed to be well mixed whereby the particulates concentration is uniform throughout the zone. The upper and the lower zones are considered to be solid-liquid transport beds. In this model, it is assumed that the middle zone provides the particles, i.e. the sand, clay and bitumen droplets, to the upper and the lower zones of the vessel. Once a particle leaves the middle zone, it is carried away either by the overflow or the tailings stream. The feed is assumed to be composed of several fractions for the sand/clay and bitumen droplets. Each fraction is characterized by a given particle diameter and concentration in the feed. The relevant mathematical treatment is given by Masliyah et.al (1981).

The slip velocity equation used by Masliyah et.al (1981) has been modified to account for possible presence of clays. The modification employs the use of hydraulic volume factor. The slip velocity equation for a given specie is of the same form as that given by equations (14) and (15).

A K-curve was generated using $(1 - K\,\alpha_s)^{4.6} = (1 - \alpha_s)^n$ where n was obtained from literature data, see Epstein (1979). A K-curve variation is shown in Figure 18 . It should be noted that no uniquely defined relationship between the hydrodynamic volume factor K with the particle shape and with the dielectric constant of the liquid has yet emerged. Consequently, Figure 18 represents an estimate only. In order to study the effect of stirring on the sedimentation of sand and floatation of bitumen droplets, it is only necessary to replace the value of '18' by the corresponding γ value of Table 2 with the assumption that the effect of stirring is not a function of particle diameter.

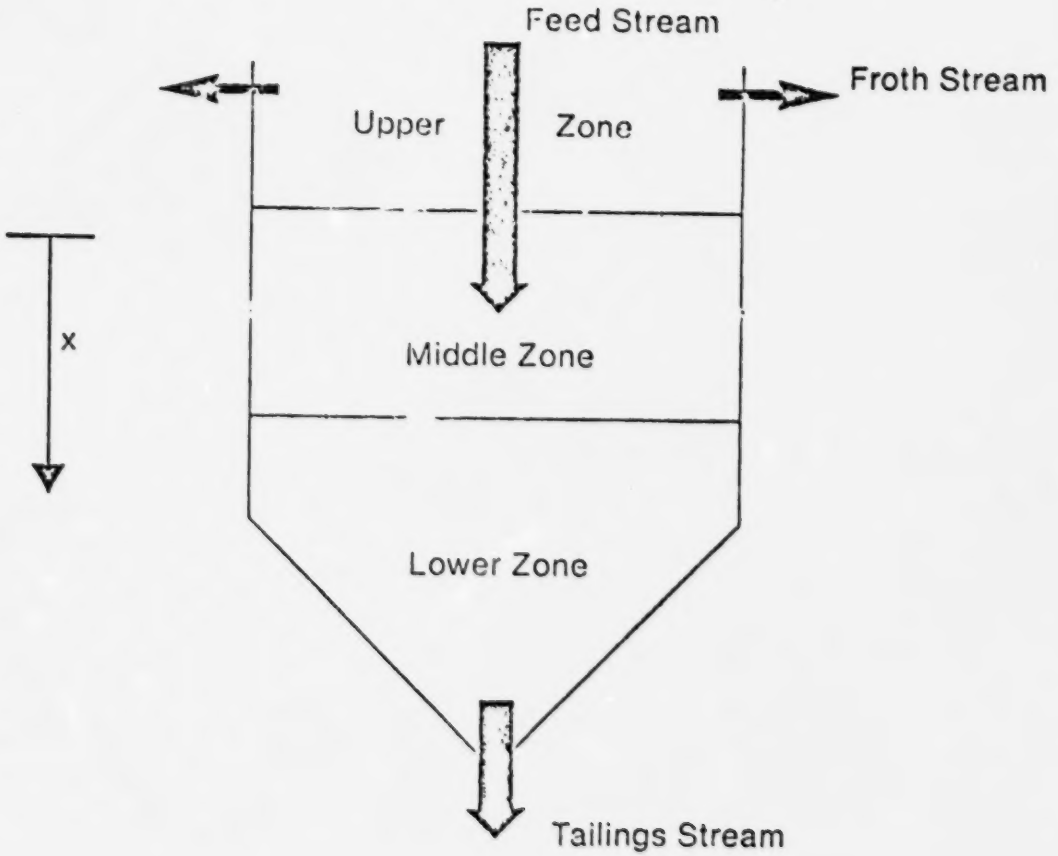

Figure 17 Zone characterization for the mathematical simulation

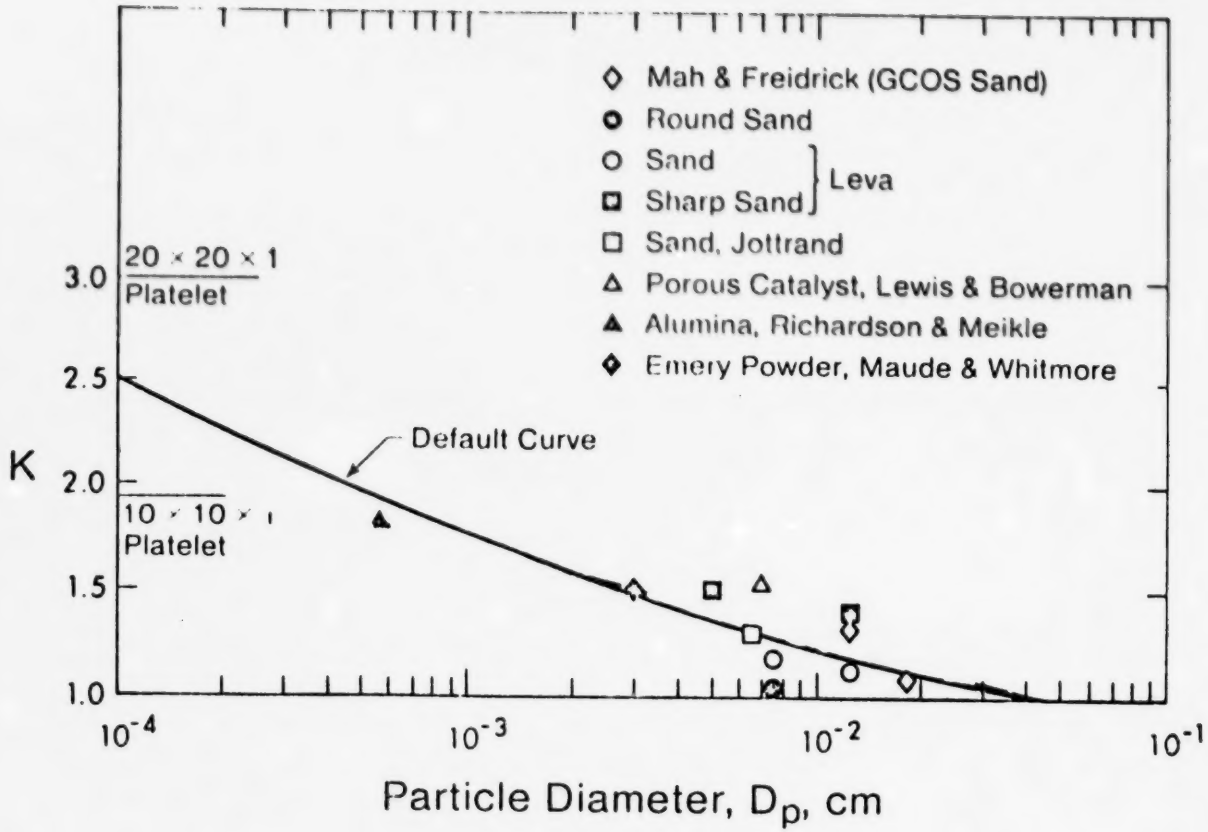

Figure 18 : Variation of K with Particle Diameter

Four simulation runs are made. A particle size distribution, PSD, for the mineral solids was assumed, Camp (1974) and Carrigy (1967). The PSD is for a 10% tar sand quality. Two different PSD for bitumen droplets were utilized; a fine and a coarse PSD were used. The particle size distributions are given in Figure 19.* The gravity separation vessel was assumed to have 1 m^2 free area and has a feed rate of 5 kg/s with a density of 1.4 g/m^3. The results of the simulation runds are summarized in Tables 3 to 6.

In Runs 1A and 2A use is made of the standard hindered settling equation (γ = 18) with coarse and fine PSD for bitumen, respectively. Consequently, Runs 1A and 2A are made for the case where there is no stirring effect. Runs 1B and 2B are for coarse and fine bitumen PSD with stirring, respectively. In these two latter Runs, a K = 12.5 was used to simulate paddle stirring at 100 rpm.

For both types of bitumen PSD used, comparison of Runs 1A with Run 2A and of Runs 1B with 2B, indicates that stirring does affect the separation of sand/bitumen slurry; albeit, the gain is not very significant. For example, for the case of coarse bitumen PSD, the bitumen concentration in the tailings stream is 0.332 for no stirring case as against 0.221 with stirring. This leads to a decrease in bitumen losses of (0.332%* 2.39) - (0.221%* 2.60) = 0.0022 kg/s. Such a decrease in bitumen losses are attributed to the stirring action.

It is of interest to note that the PSD of the bitumen droplets has a marked effect on the separation efficiency irrespective of whether stirring is present or not. For example, comparing the results for Run 1A with Run 2A for the case of no stirring, the effect of bitumen PSD is fairly high, e.g. the bitumen concentration in the tailings is 0.750 for the coarse bitumen PSD as against 0.332 for the fine bitumen PSD. This observation suggests that any conditioning process for the tar sand that leads itself to a situation where large bitumen droplets are present, a higher bitumen recovery and a lower bitumen loss would be expected.

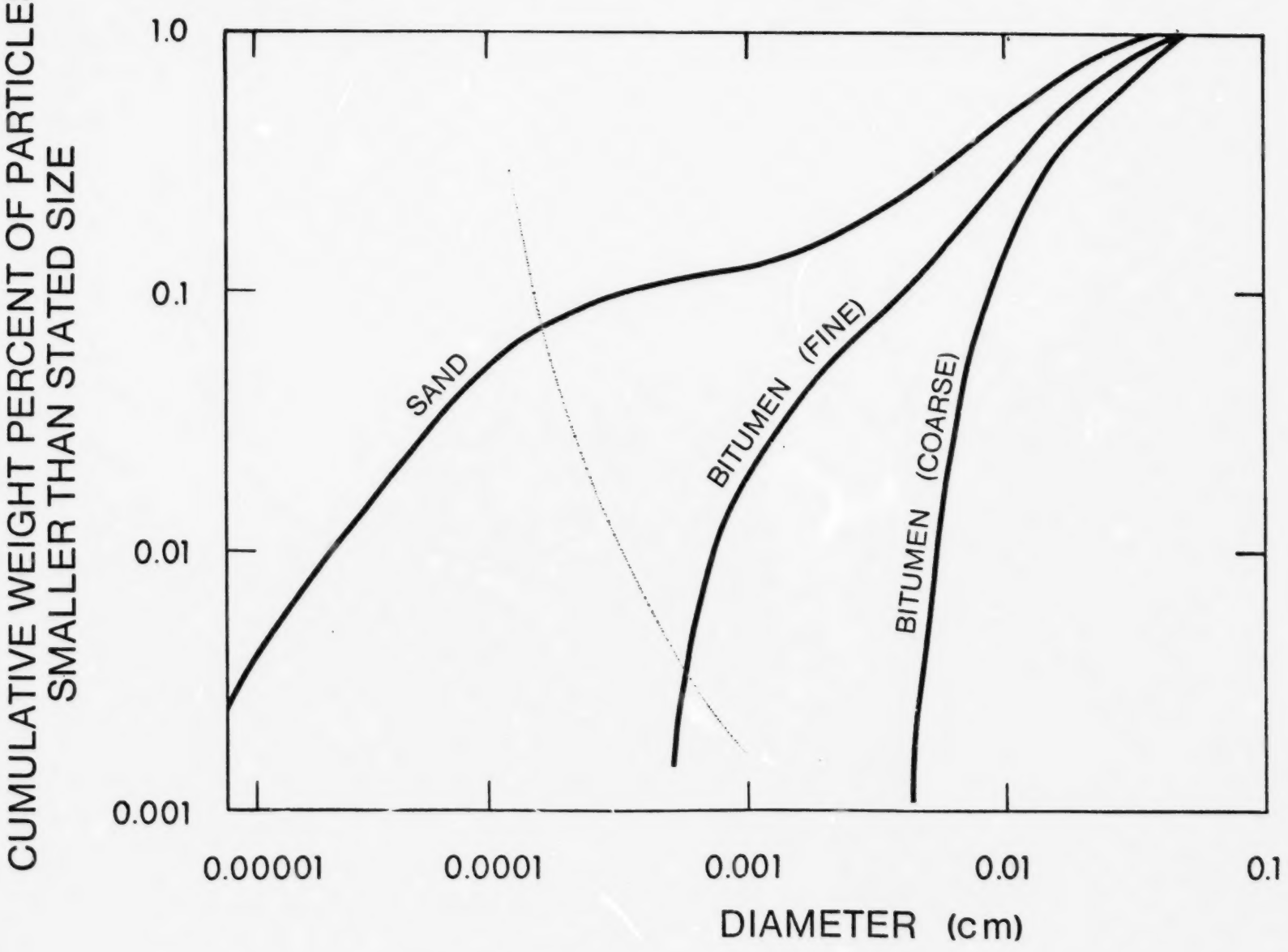

Figure 19 Particle size distribution of mineral solids and bitumen droplets used in the mathematical simulation

TABLE 3

Simulation Summary for the Case of No Stirring
for Coarse Bitumen PSD (Run 1A)

	FEED	FROTH	TAILINGS
TOTAL STREAM FLOW RATE,KG/S	5.00	2.60	2.39
WATER FLOW RATE,KG/S	2.39	1.71	0.67
SAND FLOW RATE,KG/S	2.34	0.62	1.72
BITUMEN FLOW RATE,KG/S	0.27	0.27	0.01
STREAM DENSITY,KG/DM3,(G/CM3)	1.400	1.164	1.799
SAND DISTRIBUTION	100.00	26.56	73.48
BITUMEN DISTRIBUTION	100.00	97.12	2.89
SAND CONCENTRATION,BY WEIGHT	46.760	23.901	71.808
BITUMEN CONCENTRATION,BY WEIGHT	5.500	10.279	0.332

VESSEL AREA,M2 1.000
BITUMEN DENSITY ,G/CM3 0.990
SAND/CLAY DENSITY ,G/CM3 2.650
FLUID(LIQUID) DENSITY ,G/CM3 0.990
FLUID VISCOSITY ,POISE 0.00800
RELAXATION FACTORS 0.300 0.300 0.300 1.330
NO DETAILED OUTPUT GENERATED
TAILINGS DENSITY SPECIFIED
"18" CONSTANT VALUE 18.000
DEFAULT K VALUES USED , R-Z POWER= 4.70

MASL.1 VERSION 3 APRIL / 1982 RUN NUMBER 1 A

TABLE 4

Simulation Summary for the Case of Stirring at 100 RPM for Coarse Bitumen PSD (Run 1B)

	FEED	FROTH	TAILINGS
TOTAL STREAM FLOW RATE,KG/S	5.00	2.40	2.60
WATER FLOW RATE,KG/S	2.39	1.66	0.73
SAND FLOW RATE,KG/S	2.34	0.47	1.87
BITUMEN FLOW RATE,KG/S	0.27	0.27	0.01
STREAM DENSITY,KG/DM3,(G/CM3)	1.400	1.129	1.800
SAND DISTRIBUTION	100.00	20.24	79.78
BITUMEN DISTRIBUTION	100.00	97.91	2.09
SAND CONCENTRATION,BY WEIGHT	46.760	19.701	71.820
BITUMEN CONCENTRATION,BY WEIGHT	5.500	11.211	0.221

VESSEL AREA,M2 1.000
BITUMEN DENSITY ,G/CM3 0.990
SAND/CLAY DENSITY ,G/CM3 2.650
FLUID(LIQUID) DENSITY ,G/CM3 0.990
FLUID VISCOSITY ,POISE 0.00800
RELAXATION FACTORS 0.300 0.300 0.300 1.330
NO DETAILED OUTPUT GENERATED
TAILINGS DENSITY SPECIFIED
"18" CONSTANT VALUE 12.500
DEFAULT K VALUES USED , R-Z POWER= 4.70

RUN NUMBER 1B

MASL.1 VERSION 3 APRIL / 1982

TABLE 5

Simulation Summary for the Case of No Stirring
for Fine Bitumen PSD (Run 2A)

	FEED	FROTH	TAILINGS
TOTAL STREAM FLOW RATE,KG/S	5.00	2.64	2.35
WATER FLOW RATE,KG/S	2.39	1.74	0.65
SAND FLOW RATE,KG/S	2.34	0.65	1.69
BITUMEN FLOW RATE,KG/S	0.27	0.26	0.02
STREAM DENSITY,KG/DM3,(G/CM3)	1.400	1.169	1.800
SAND DISTRIBUTION	100.00	27.64	72.32
BITUMEN DISTRIBUTION	100.00	93.53	6.42
SAND CONCENTRATION,BY WEIGHT	46.760	24.453	71.819
BITUMEN CONCENTRATION,BY WEIGHT	5.500	9.732	0.750

VESSEL AREA.M2 1.000
BITUMEN DENSITY ,G/CM3 0.990
SAND/CLAY DENSITY ,G/CM3 2.650
FLUID(LIQUID) DENSITY ,G/CM3 0.990
FLUID VISCOSITY ,POISE 0.00800
RELAXATION FACTORS 0.400 0.400 0.400 1.450
NO DETAILED OUTPUT GENERATED
TAILINGS DENSITY SPECIFIED
"18" CONSTANT VALUE 18.000
DEFAULT K VALUES USED , R-Z POWER= 4.70

RUN NUMBER 2 A

MASL.1 VERSION 3 APRIL / 1982

TABLE 6

Simulation Summary for the Case of Stirring at 100 RPM for Fine Bitumen PSD (Run 2B)

	FEED	FROTH	TAILINGS
TOTAL STREAM FLOW RATE,KG/S	5.00	2.46	2.54
WATER FLOW RATE,KG/S	2.39	1.69	0.70
SAND FLOW RATE,KG/S	2.34	0.51	1.83
BITUMEN FLOW RATE,KG/S	0.27	0.26	0.02
STREAM DENSITY,KG/DM3,(G/CM3)	1.400	1.138	1.800
SAND DISTRIBUTION	100.00	21.85	78.17
BITUMEN DISTRIBUTION	100.00	94.29	5.71
SAND CONCENTRATION,BY WEIGHT	46.760	20.789	71.823
BITUMEN CONCENTRATION,BY WEIGHT	5.500	10.555	0.617

VESSEL AREA,M2 1.000
BITUMEN DENSITY ,G/CM3 0.990
SAND/CLAY DENSITY ,G/CM3 2.650
FLUID(LIQUID) DENSITY ,G/CM3 0.990
FLUID VISCOSITY ,POISE 0.00800
RELAXATION FACTORS 0.400 0.400 0.400 1.450
NO DETAILED OUTPUT GENERATED
TAILINGS DENSITY SPECIFIED
"18" CONSTANT VALUE 12.500
DEFAULT K VALUES USED , R-Z POWER= 4.70

RUN NUMBER 2 B

MASL.1 VERSION 3 APRIL / 1982

NOMENCLATURE

A	Empty tube area
A_1	Central region area
A_2	Annular region area
BS	Stirrer located at base
C_D	Drag coefficient
d	Particle diameter
E	Aspect ratio of a prolate spheroid, $E > 1$
F_D	Drag force on a particle
F_{Do}	Drag force on a particle in absence of either stirring or orientation
F_{D1} F_{D2}	Principle axes drag force
g	Gravitational acceleration
K	Hydrodynamic volume factor; regression coefficient
L	Bed height
M	Mass flow rate of water
MD	Stirrer located well above base
Q_o	Volumetric flow rate of water required to maintain a uniform bed at a fluid concentration α_f
Q	Volumetric flow rate of water required to maintain a non-uniform bed at a fluid concentration α_f
Re	Reynolds number
$\vec{U}$	Slip velocity vector
U_h	Horizontal component of slip velocity
U_v	Vertical component of slip velocity
v_f	Fluid velocity relative to a stationary observer
v_{fo}	Fluid velocity relative to a stationary observer for a uniform bed
v_{f1}	Fluid velocity in the central region relative to a stationary observer
v_{f2}	Fluid velocity in the annular region relative to a stationary observer

v_f	Fluidization water velocity, $\|v_f\|$
v_s	Solids velocity relative to a stationary observer
v_{s1}	Solids velocity in the central region relative to a stationary observer
v_{s2}	Solids velocity in the annular region relative to a stationary observer
v_{susp}	Suspension settling velocity
v_∞	Settling velocity of a particle in infinite medium

GREEK SYMBOLS

α_f	Fluid volumetric concentration (bed porosity)
α_{fo}	Uniform bed fluid volumetric concentration
α_s	Solids volumetric concentration
ΔP	Pressure drop over a distance L
$\Delta\alpha_f$	Increment change in fluid concentration between central and annular regions
ρ_f	Fluid density
ρ_s	Solids density
μ_f	Fluid viscosity

ACKNOWLEDGEMENT

The author wishes to thank Mr. S. Mohamed for conducting the experimental study and Dr. D.K. Faurschou for his encouragement and interest throughout the study.

REFERENCES

Arastoopour, H., S. Lin and S.A. Weil, "Analysis of Vertical Pneumatic Conveying of Solids Using Multiphase Flow Models", AIChE J., 28, 467-473, (1982).

Camp, F.W., "The Tar Sands of Alberta, Canada", 2nd Ed. Cameron Engineers, Inc. Denver, Col. (1974).

Carrigy, M.A., "The Physical and Chemical Nature of a Typical Tar Sand". The proceedings of the 7th World Petroleum Congress, Research Council of Alberta, contribution no. 346.

Clark, K.A., Can. Min. Met. Bull. No. 212, 1385-1395 (1930). See also The K.A. Clark Volume Athabasca Oil Sands (1963), Alberta Research Council, Edmonton, Alberta.

Clift, R., J.R. Grace and M.E. Weber, "Bubbles, Drops, and Particles", Academic Press, N.Y. (1978).

Epstein, N., "Hydrodynamic Particle Volume Factor and Settled Bed Volume", Can. J. Chem. Eng., 57, 383 (1979).

Fouda, A.E. and C.E. Capes, "Hydrodynamic Particle Volume and Fluidized Bed Expansion", Can. J. Chem. Eng., 57, 120-121 (1979).

Ibid, "Hydrodynamic Particle Volume and Fluidized Bed Expansion", Can. J. Chem. Eng., 55, 386-391 (1977).

Hiby, J.W., "Proceedings of the International Symposium on Fluidization (Eindhoven)", Netherlands University Press, Amsterdam, 21-30 (1967).

Jottrand, R., J. Appl. Chem., 2, S17 (1952).

Juma, A.K.A. and J.F. Richardson, "Particle Segregation in Liquid-Solid Fluidized Beds", Chem. Eng. Sci., 34, 137-143 (1979).

Leva, M., "Pressure Drop and Power Requirements in a Stirred Fluidized Bed", AIChE J., 6, 688-692 (1960).

Leva, M., "Fluidization", 89, McGraw Hill, N.Y. (1959).

Mah, M. and B.D. Friedrick, Ch.E. 552 Project, Department of Chemical Engineering, University of Alberta (1979).

Masliyah, J.H., T.K. Kwong and F.A. Seyer, "Theoretical and Experimental Studies of a Gravity Separation Vessel", I & E C Process Design and Development, 20, 154-160 (1981).

Maude, A.D. and R.L. Whitmore, Trans. Inst. Chem. Engrs., 36, 296 (1958).

Richardson, J.F. and M.A. Jeronimo, "Velocity-Voidage Relations for Sedimentation and Fluidization", Chem. Eng. Sci., 34, 1419-1422 (1979).

Richardson, J.F. and W.N. Zaki, "Sedimentation and Fluidization: Part I", Trans. Instn. Chem. Engrs., 32, 35-53 (1954).

Richardson, J.F. and R. Meikle, Trans. Inst. Chem. Engrs., 39, 348 (1961).

Rowe, P.N. and G.A. Henwood, "Drag Force in a Hydraulic Model of a Fluidized Bed - Part I", Trans. Instn. Chem. Engrs., 39, 43-54 (1961).

Ibid, "Drag Force in a Hydraulic MOdel of a Fluidized Bed - Part II", Trans. Instn. Chem. Engrs., 39, 175-180 (1961).

Wallis, G.B., "One-dimensional Two-phase Flow", McGraw-Hill Book Co., Inc., N.Y. (1969).

LIST OF FIGURES

Figure 1	Schematic Diagram of Equipment
Figure 2	Stirrers description
Figure 3	Variation of apparent bed height with rpm
Figure 4	Variation of pressure drop along the fluidized bed
Figure 5(a)	Variation of α_f with flow rate for a sand bed with a paddle
Figure 5(b)	Variation of α_f with flow rate for a sand bed with an impeller at location BS
Figure 5(c)	Variation of α_f with flow rate for a sand bed with an impeller at location MD
Figure 6(a)	Variation of α_f with flow rate for a glass bed with a paddle
Figure 6(b)	Variation of α_f with flow rate for a glass bed with an impeller at location BS
Figure 6(c)	Variation of α_f with flow rate for a glass bed with an impeller at location MD
Figure 7	Variation of α_f with water flow rate for rolled aluminum particles
Figure 8	Schematic diagram of particle circulation
Figure 9	Forces on a suspended elongated particle
Figure 10(a)	Regression plot using equation 12 for a sand bed with a paddle
Figure 10(b)	Regression plot using equation 12 for a sand bed with an impeller at BS
Figure 10(c)	Regression plot using equation 12 for a sand bed with an impeller at MD
Figure 11(a)	Regression plot using equation 12 for a glass bed with a paddle
Figure 11(b)	Regression plot using equation 12 for a glass bed with an impeller at BS
Figure 11(c)	Regression plot using equation 12 for a glass bed with an impeller at MD
Figure 12	Regression plot using equation 12 for an aluminum bed

Figure 13 Regression plot using equation 14 for a sand bed at various rpm and stirrers

Figure 14 Regression plot using equation 14 for a glass bed at various rpm and stirrers at high water flow rate

Figure 15 Regression plot using equation 14 for a glass bed at various rpm and stirrers at low water flow rate

Figure 16 Regression plot using equation 14 for aluminum bed

Figure 17 Zone characterization for the mathematical simulation

Figure 18 Variation of K with particle diameter

Figure 19 Particle size distribution of mineral solids and bitumen droplets used in the mathematical simulation

LIST OF TABLES

Table 1	Particle Properties
Table 2	Values of K and γ of Regression Equation 14
Table 3	Simulation Summary for the Case of No Stirring for Coarse Bitumen PSD (Run 1A)
Table 4	Simulation Summary for the Case of Stirring at 100 RPM for Coarse Bitumen PSD (Run 1B)
Table 5	Simulation Summary for the Case of No Stirring for Fine Bitumen PSD (Run 2A)
Table 6	Simulation Summary for the Case of Stirring at 100 RPM for Fine Bitumen PSD (Run 2B)

APPENDIX A

CONDUCTIVITY CELL

Conductivity cells are used to measure the specific conductance of electrolytes. It is possible to make use of the conductivity cell to measure solids concentration in a fluidized bed when there is a difference between the fluid and the solid conductance. A conductivity cell consists of a pair of electrodes of given area and spacing. A high frequency ac current is applied to the conductivity cell. The working media in which the cell is immersed completes the electrical circuit. The voltage drop across the cell gives an estimate of the resistance (or conductance) of the working medium. Figure A-1 and A-2 show the details of the cell and the electric circuit.

In this work the calibration of the cell was made by simply measuring the voltage drop across the cell at zero rpm at various water flow rates. This procedure gave the rate of voltage drop with fluid concentration. Table A-1 shows that typically a change of 0.2 volts per 0.122 of concentration change. It was also found that no measurable change in voltage drop could be detected at zero rpm between the cell located near the wall and near the centre of the bed.

For the case of the impeller stirrer (BS) at 100 rpm it was found that the solids concentration at the bed wall was 0.018 higher than that towards the bed centre.

In order to make more precise solid concentration measurements, it becomes necessary to measure the voltage drop across the cell via a much complicated electrical circuitary. The conductivity measurements in this study is only preliminary in nature.

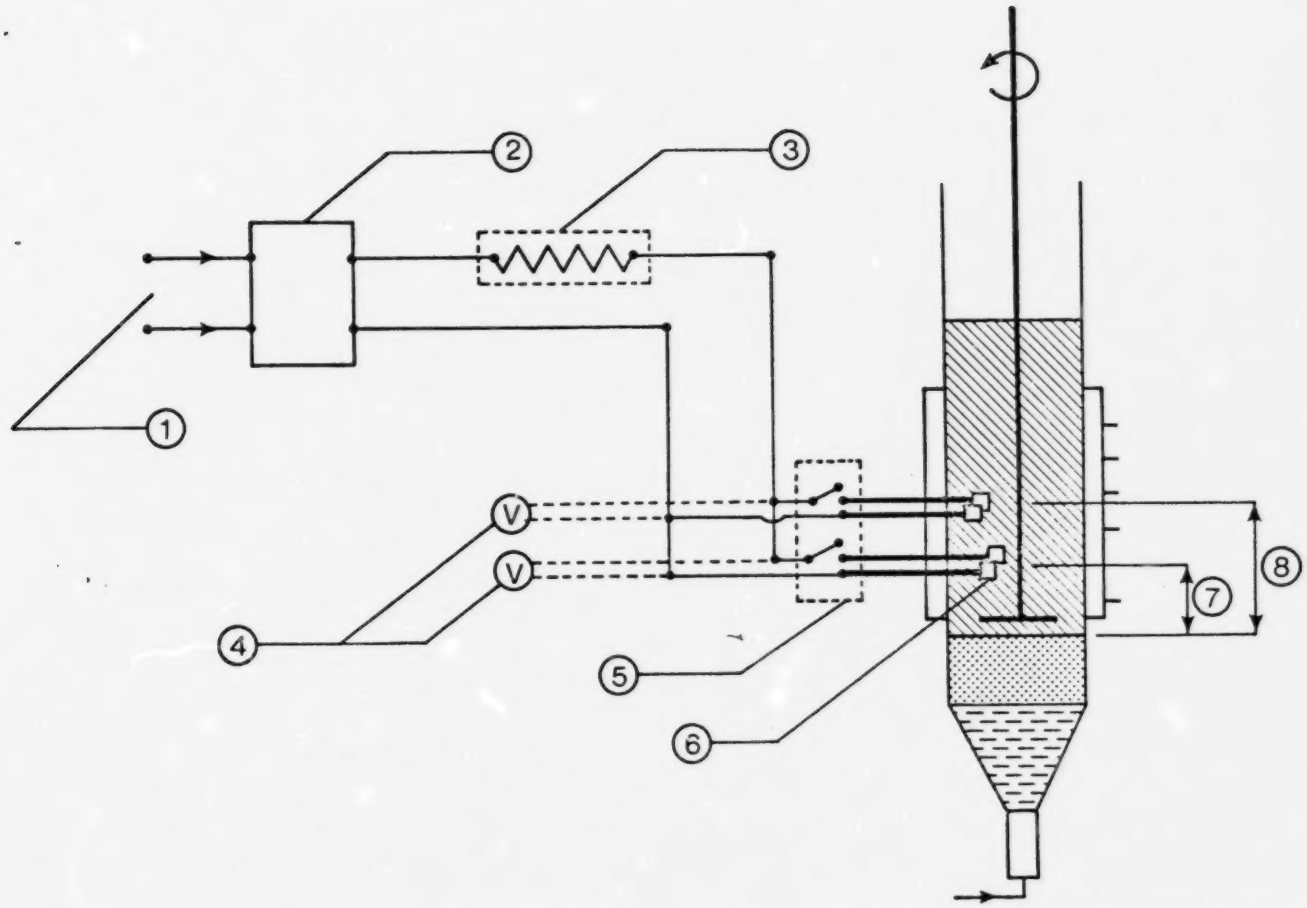

(1) Power source (115 v ac, 60 cys)
(2) Wide range oscillator
(3) Variable resistor (50 k ohms max.)
(4) Voltmeter (ac)
(5) Switch box
(6) Copper probe plates
(7) 0.06 m
(8) 0.11 m

Figure A-1 Schematic Diagram of the Conductivity Probe Set-up

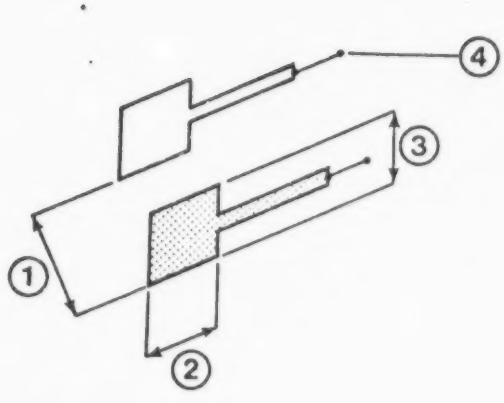

(A)

(1) 0.005 m
(2) 0.01 m
(3) 0.02 m
(4) Soldered contact wire

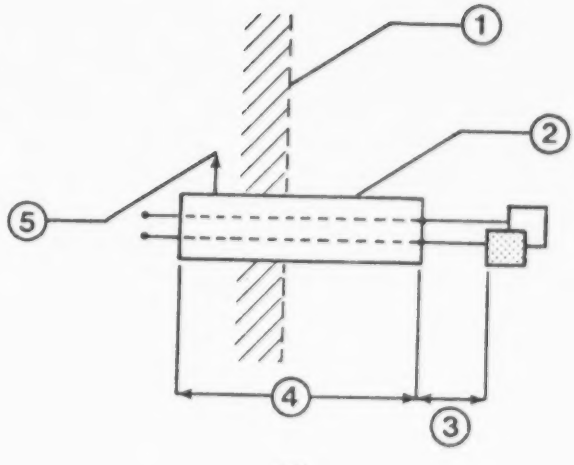

(B)

(1) Column wall
(2) Sliding solid lucite rod (0.006 m O.D.)
(3) 0.005 m
(4) 0.10 m
(5) Stainless steel pointer

Figure A-2 Detail Conductivity Probe Design

Table A-1 : Measurement of change in radial solid concentration using a conductivity cell setup.

Particle : Sand Stirrer : Impeller (bs)

Frequency = 1000 cy/s Probe Constant = 25 m^{-1}

Applied Voltage = 5.00 V

RPM	FLOW RATE KG/S	HEIGHT OF BED M	FLUID CONC.	WALL V	MIDDLE V	CHANGE IN VOLTAGE
0	0.06	0.135	0.733	4.62	4.61	+0.01
	0.07	0.155	0.767	4.53	4.52	+0.01
	0.08	0.181	0.801	4.47	4.46	+0.01
	0.09	0.210	0.828	4.43	4.44	-0.01
	0.10	0.249	0.855	4.42	4.42	0.00
			AVERAGE CHANGE IN VOLTAGE =			0.00 V
100	0.06	0.135	0.733	4.60	4.58	+0.02
	0.07	0.151	0.761	4.53	4.51	+0.02
	0.08	0.170	0.787	4.48	4.44	+0.04
	0.09	0.196	0.815	4.46	4.43	+0.03
	0.10	0.231	0.844	4.43	4.41	+0.02
			AVERAGE CHANGE IN VOLTAGE =			+0.03 V
150	0.06	0.132	0.725	4.57	4.54	+0.03
	0.07	0.149	0.757	4.54	4.51	+0.03
	0.08	0.167	0.783	4.50	4.47	+0.03
	0.09	0.187	0.806	4.47	4.45	+0.02
	0.10	0.220	0.836	4.45	4.44	+0.01
			AVERAGE CHANGE IN VOLTAGE =			+0.02 V

NOTE:

WALL AT 0 RPM:

FROM 0.06 TO 0.10 KG/S:

CHANGE IN VOLTAGE = (4.62-4.42) = 0.20 V
CHANGE IN FLUID CONCENTRATION = (0.855-0.733) = 0.122
CHANGE IN SOLID CONCENTRATION = 0.122

COMPARING DIFFERENCE BETWEEN WALL AND MIDDLE:

AT 0 RPM, WITH AVERAGE CHANGE IN VOLTAGE = 0.00 V,
CHANGE IN FLUID CONCENTRATION = 0.00
CHANGE IN SOLID CONCENTRATION = 0.00

AT 100 RPM, WITH AVERAGE CHANGE IN VOLTAGE = +0.03 V,
CHANGE IN FLUID CONCENTRATION = (0.122*0.03)/0.20 = 0.0183
CHANGE IN SOLID CONCENTRATION = 0.0183

AT 150 RPM, WITH AVERAGE CHANGE IN VOLTAGE = +0.02 V,
CHANGE IN FLUID CONCENTRATION = (0.122*0.02)/0.20 = 0.0122
Change in solid concentration = 0.0122

A P P E N D I X B

PRESSURE DROP PLOTS

LIST OF FIGURES FOR APPENDIX B

Figure B- 1	Variation of pressure drop for a sand bed at zero rpm
Figure B- 2	Variation of pressure drop for a sand bed with a paddle at 50 rpm
Figure B- 3	Variation of pressure drop for a sand bed with a paddle at 75 rpm
Figure B- 4	Variation of pressure drop for a sand bed with a paddle at 100 rpm
Figure B- 5	Variation of pressure drop for a sand bed with an impeller at BS location at 100 rpm
Figure B- 6	Variation of pressure drop for a sand bed with an impeller at BS location at 150 rpm
Figure B- 7	Variation of pressure drop for a sand bed with an impeller at MD location at 100 rpm
Figure B- 8	Variation of pressure drop for a sand bed with an impeller at MD location at 150 rpm
Figure B- 9	Variation of pressure drop for a glass bed at zero rpm
Figure B-10	Variation of pressure drop for a glass bed with a paddle at 50 rpm
Figure B-11	Variation of pressure drop for a glass bed with a paddle at 75 rpm
Figure B-12	Variation of pressure drop for a glass bed with a paddle at 100 rpm
Figure B-13	Variation of pressure drop for a glass bed with an impeller at BS location at 100 rpm
Figure B-14	Variation of pressure drop for a glass bed with an impeller at BS location at 150 rpm
Figure B-15	Variation of pressure drop for a glass bed with an impeller at MD location at 100 rpm
Figure B-16	Variation of pressure drop for a glass bed with an impeller at MD location at 150 rpm
Figure B-17	Variation of pressure drop for an aluminum bed at zero rpm

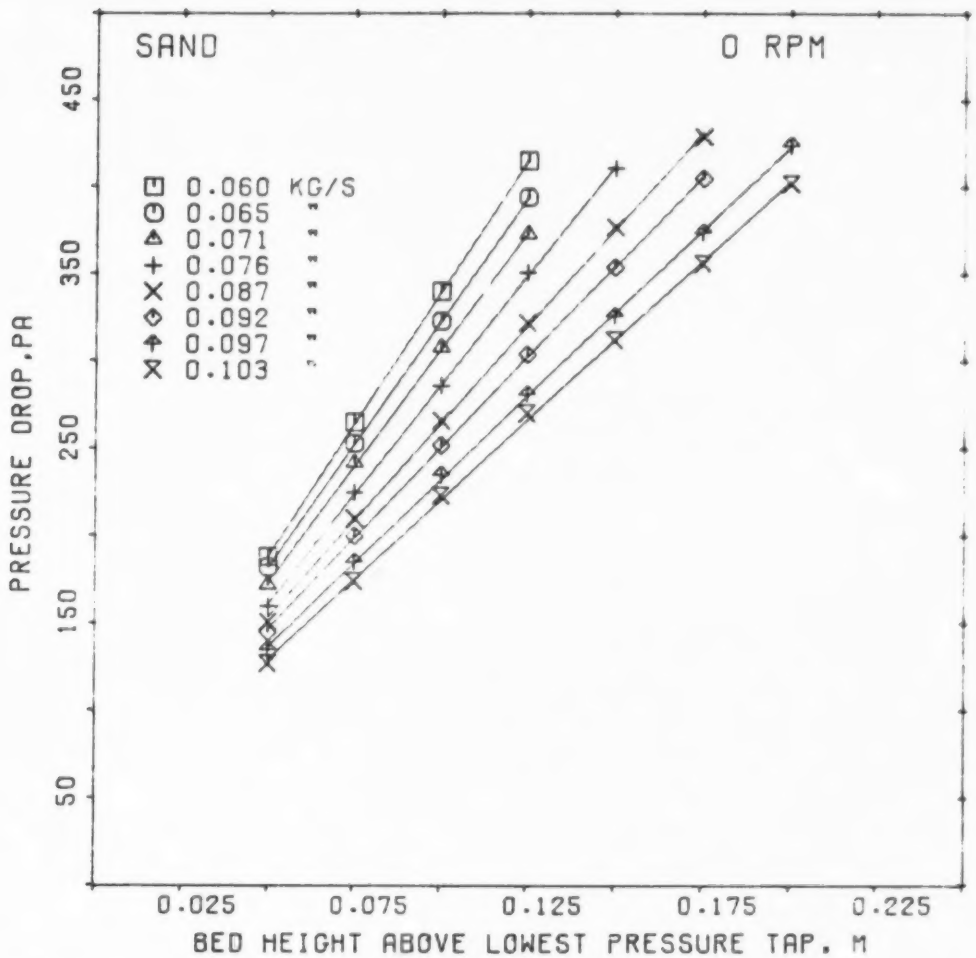

Figure B- 1 Variation of pressure drop for a sand bed at zero rpm

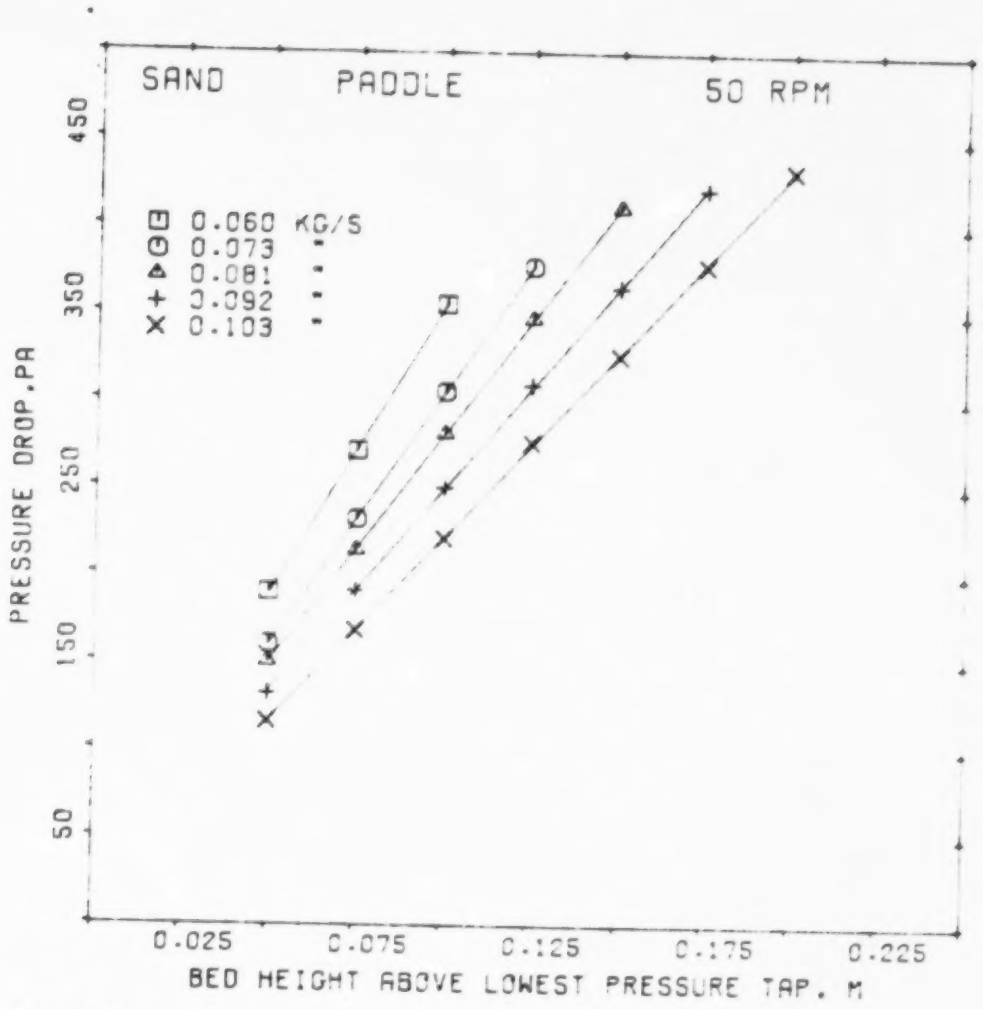

Figure B-2 Variation of pressure drop for a sand bed with a paddle at 50 rpm

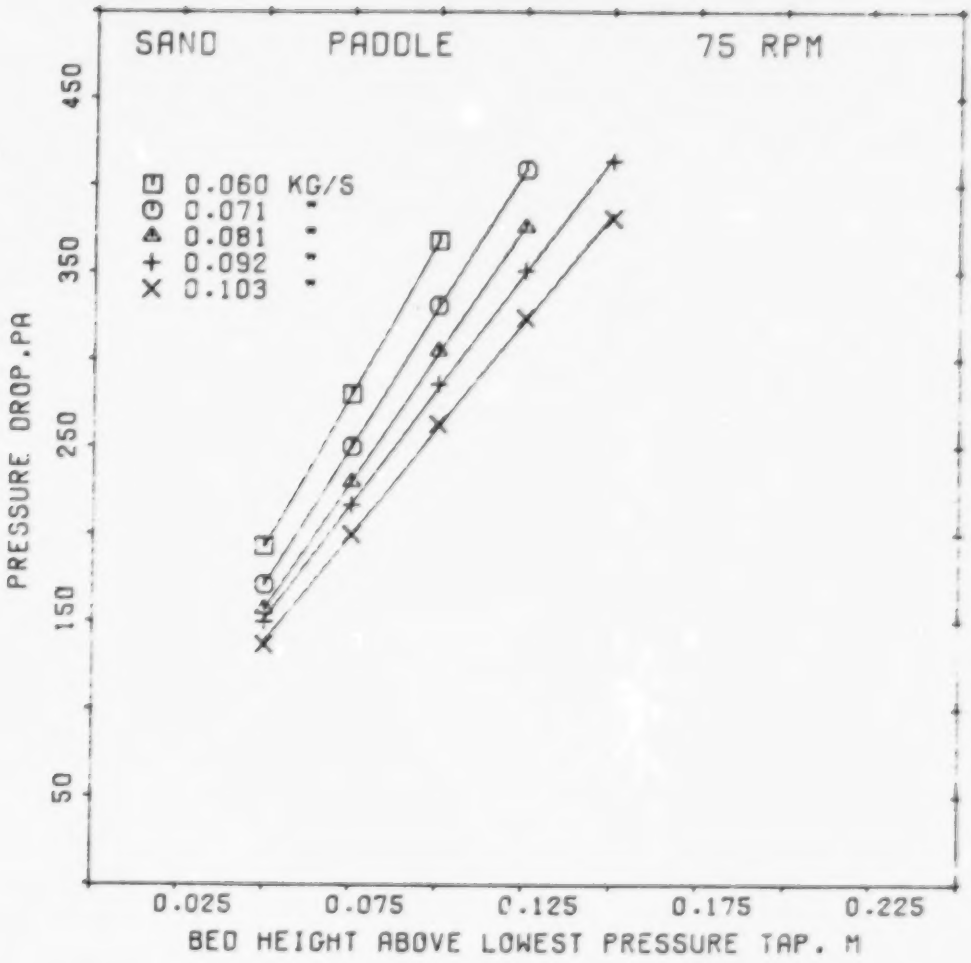

Figure B-3 Variation of pressure drop for a sand bed with a paddle at 75 rpm

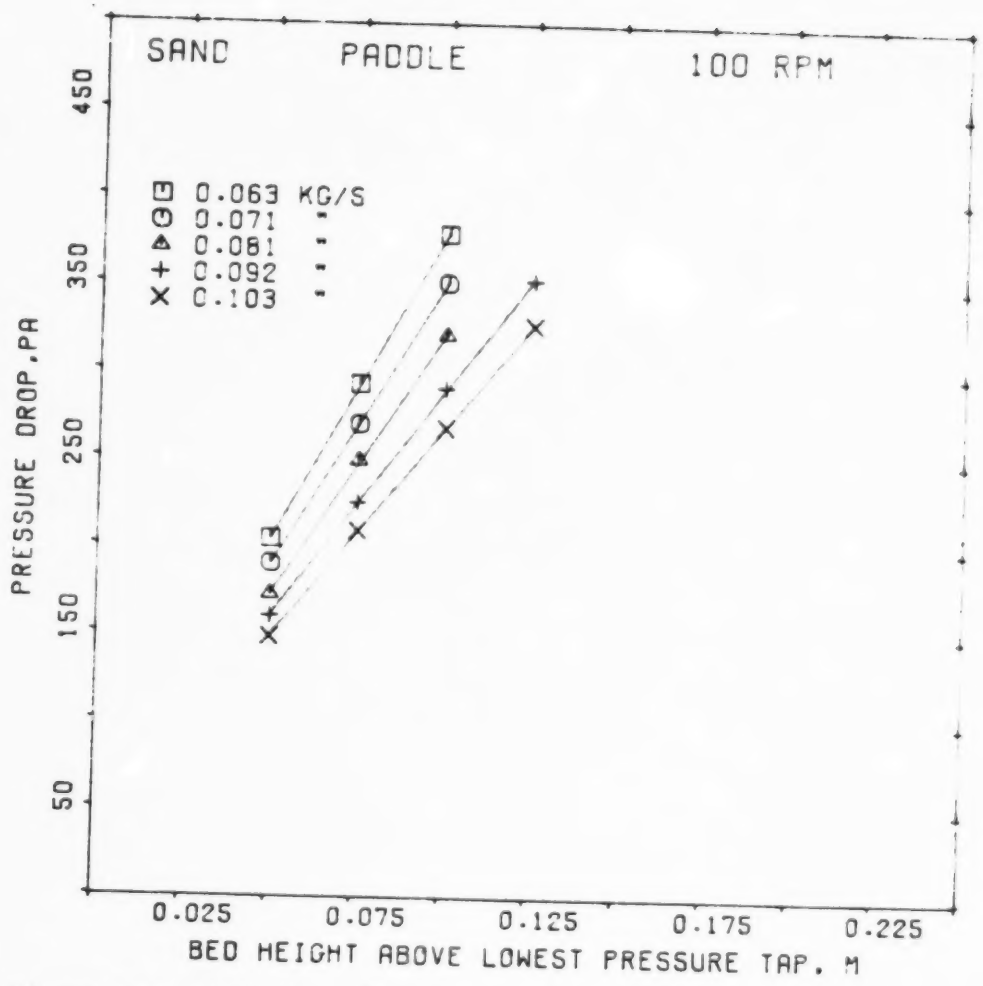

Figure B-4 Variation of pressure drop for a sand bed with a paddle at 100 rpm

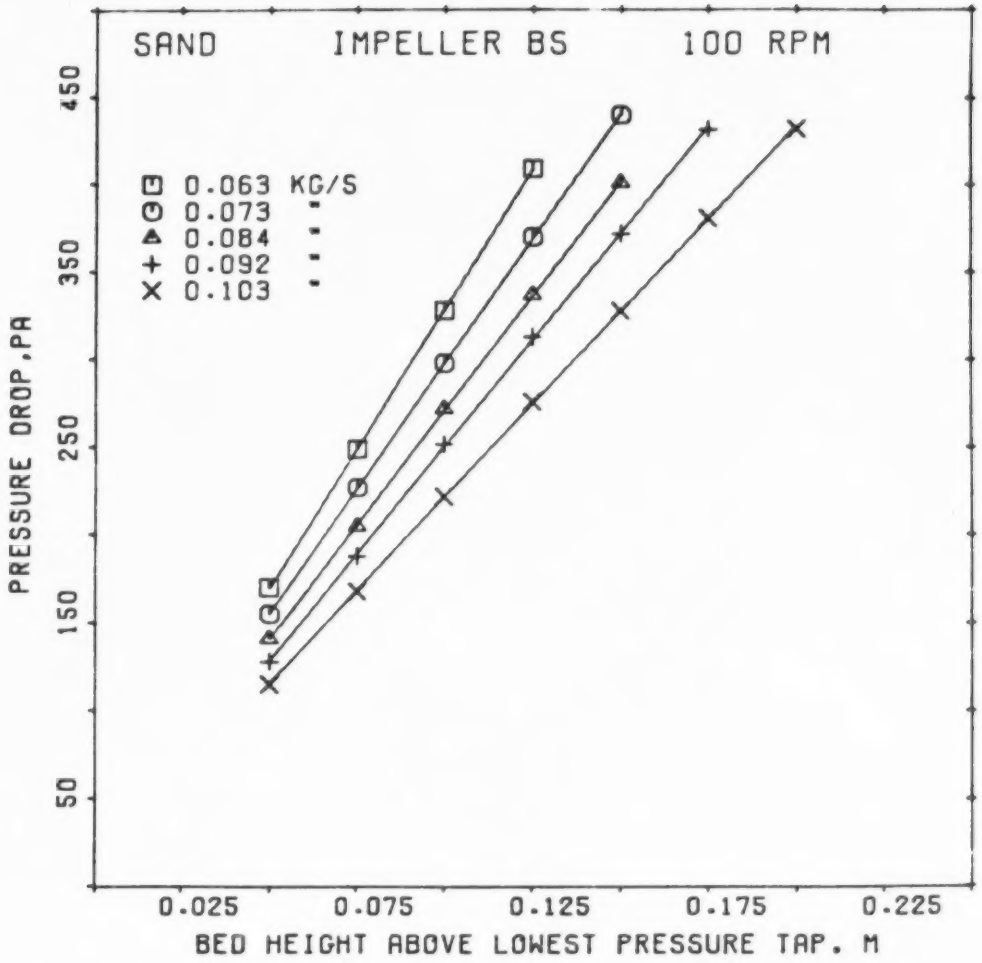

Figure B-5 Variation of pressure drop for a sand bed with an impeller at BS location at 100 rpm

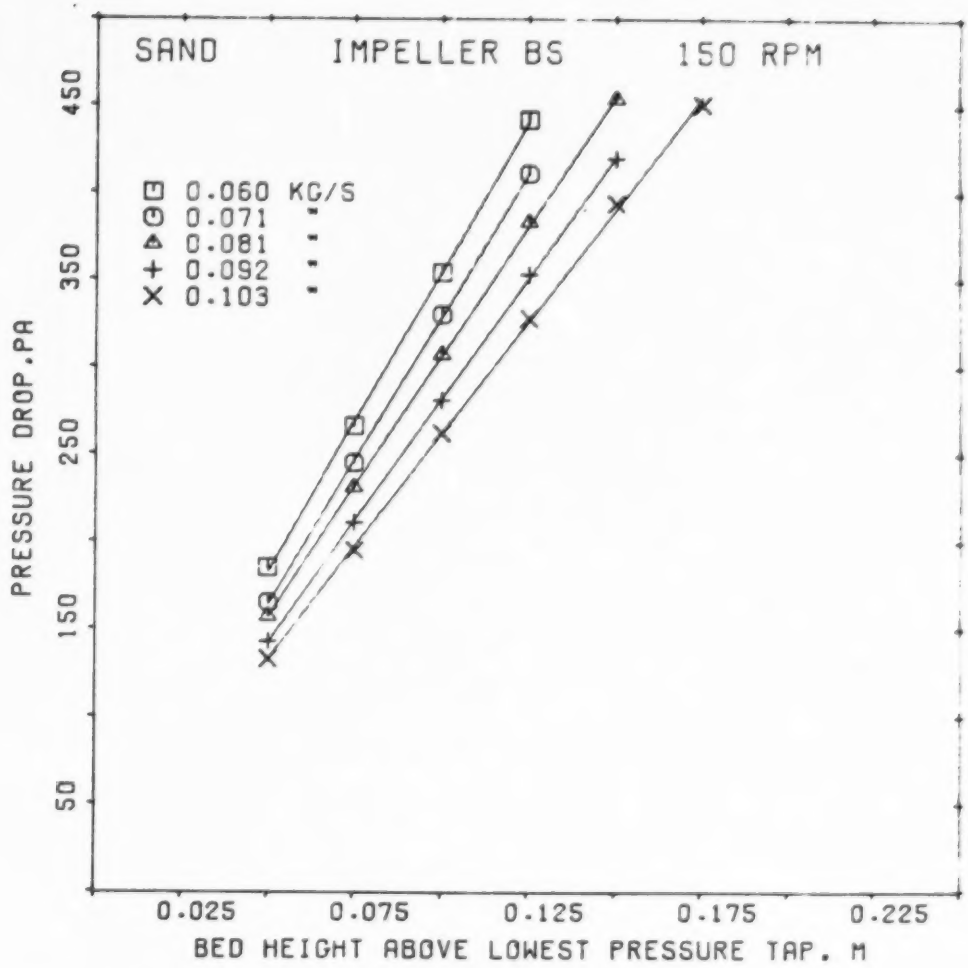

Figure B-6 Variation of pressure drop for a sand bed with an impeller at BS location at 150 rpm

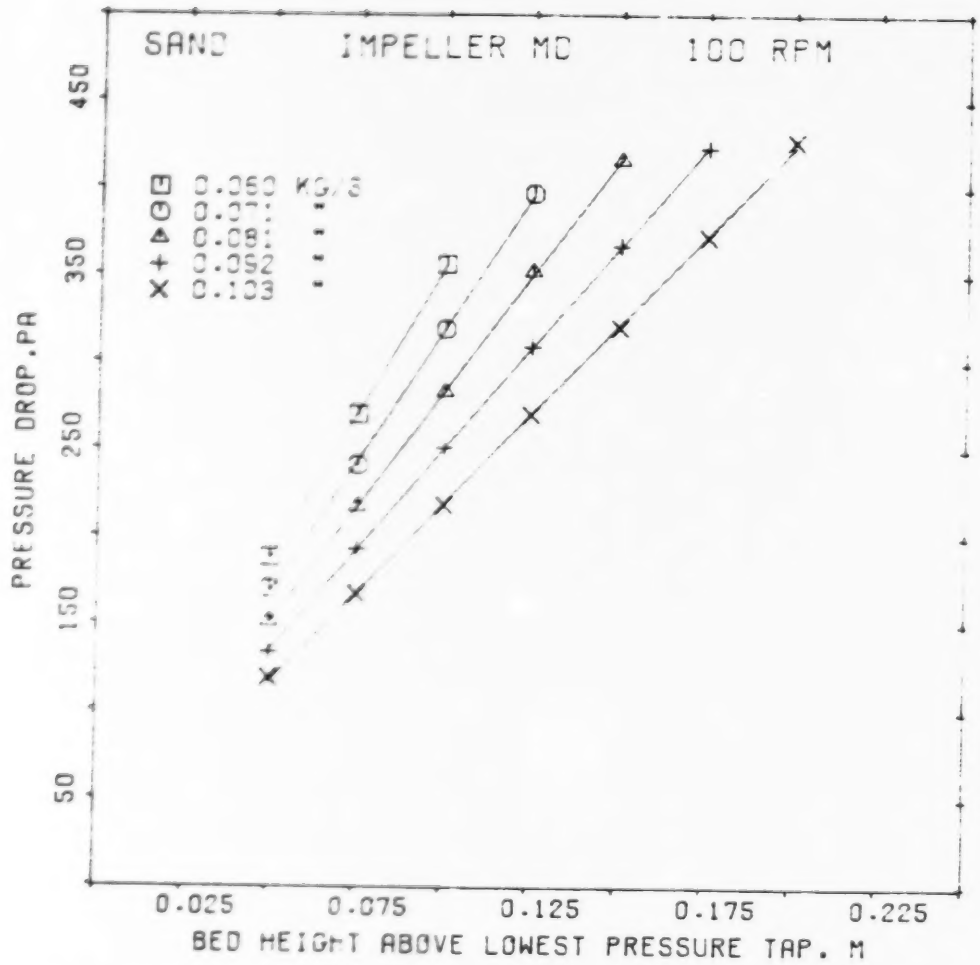

Figure B-7 Variation of pressure drop for a sand bed with an impeller at MD location at 100 rpm

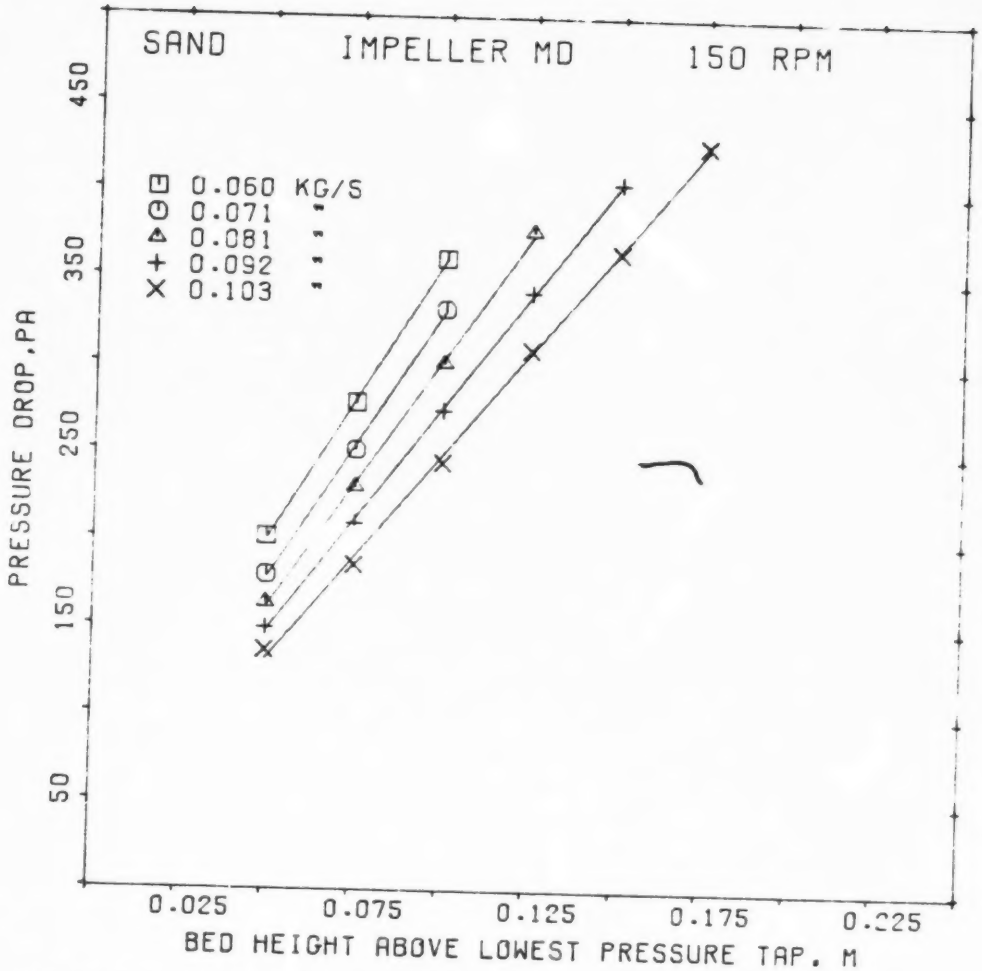

Figure B-8 Variation of pressure drop for a sand bed with an impeller at MD location at 150 rpm

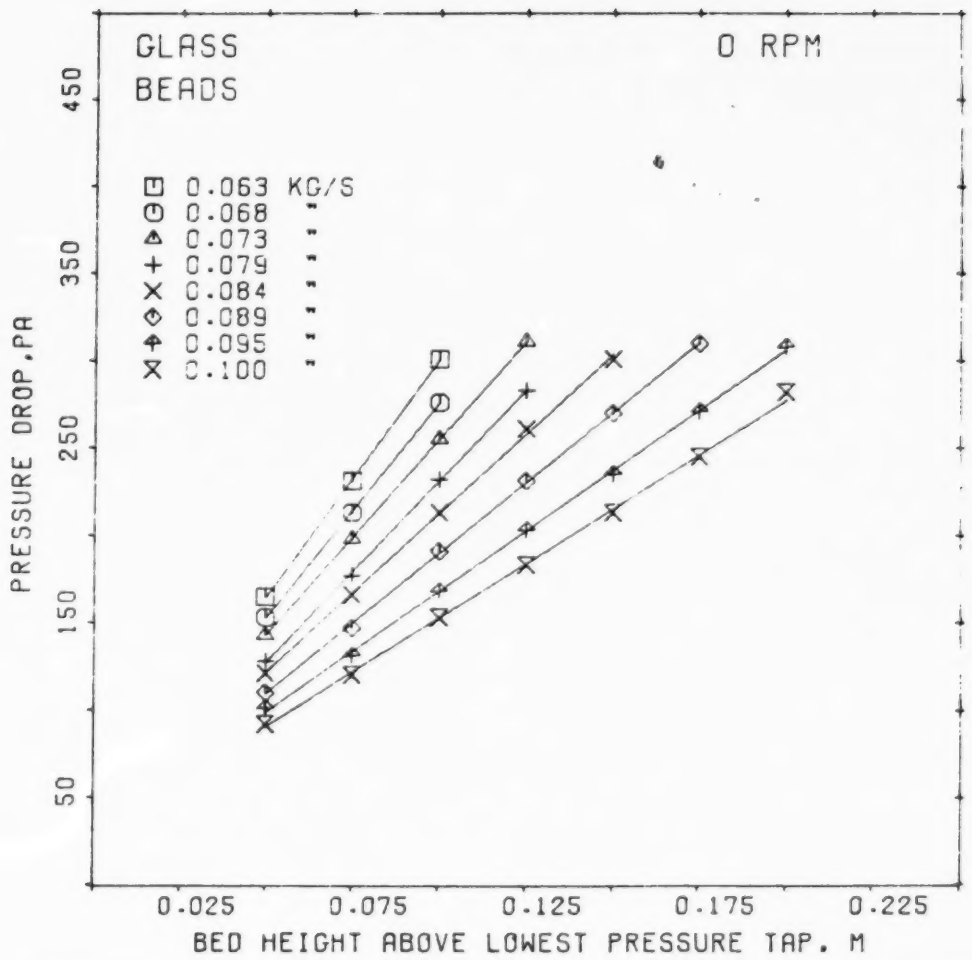

Figure B-9 Variation of pressure drop for a glass bed at zero rpm

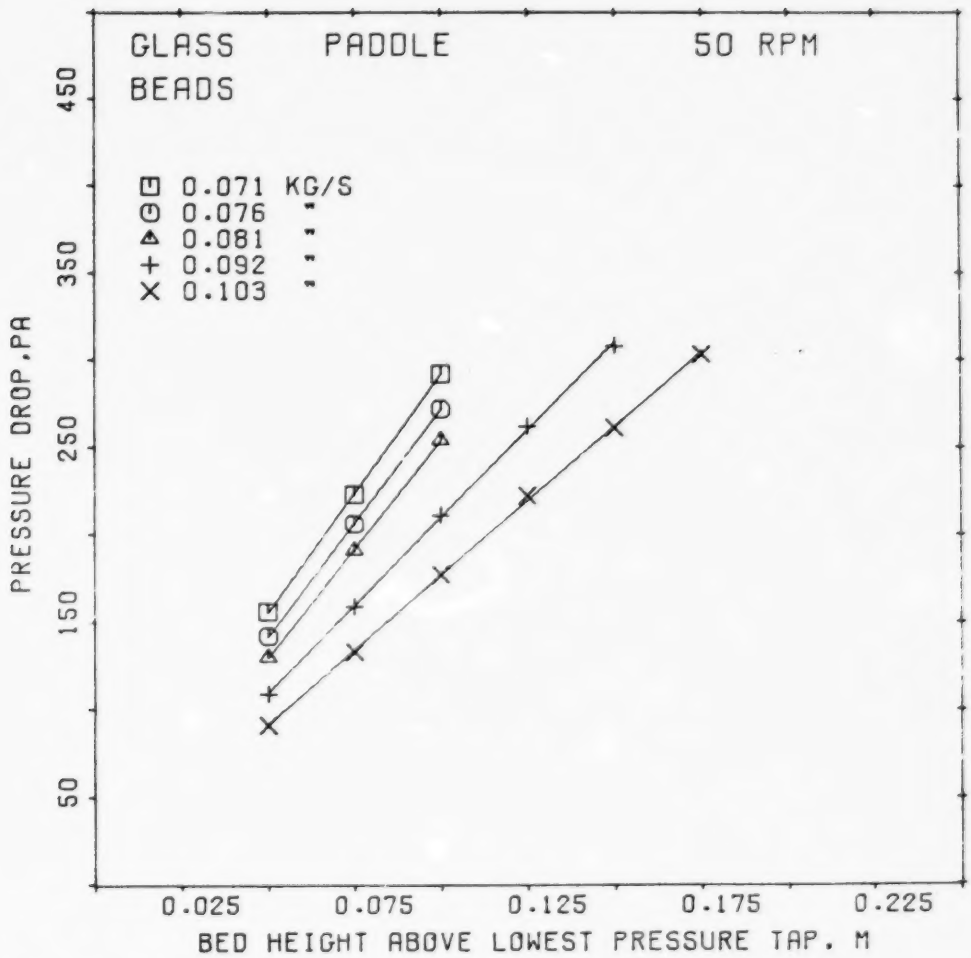

Figure B-10 Variation of pressure drop for a glass bed with a paddle at 50 rpm

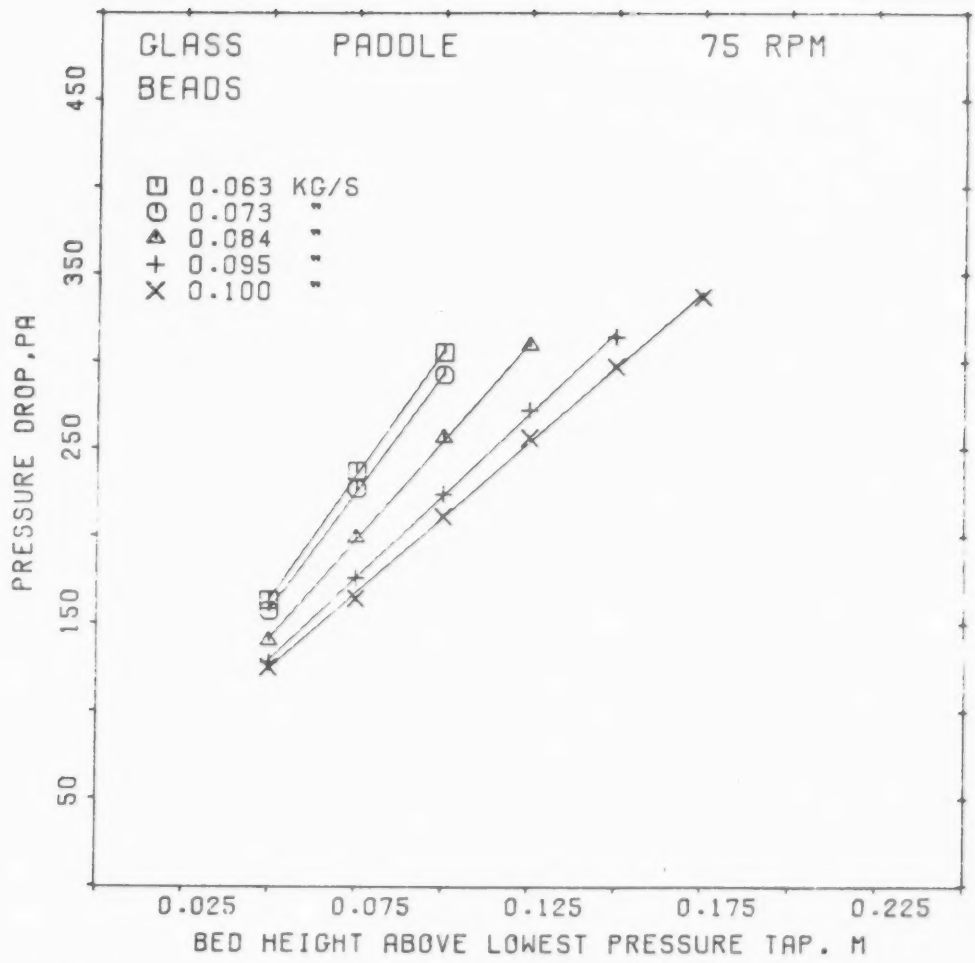

Figure B-11 Variation of pressure drop for a glass bed with a paddle at 75 rpm

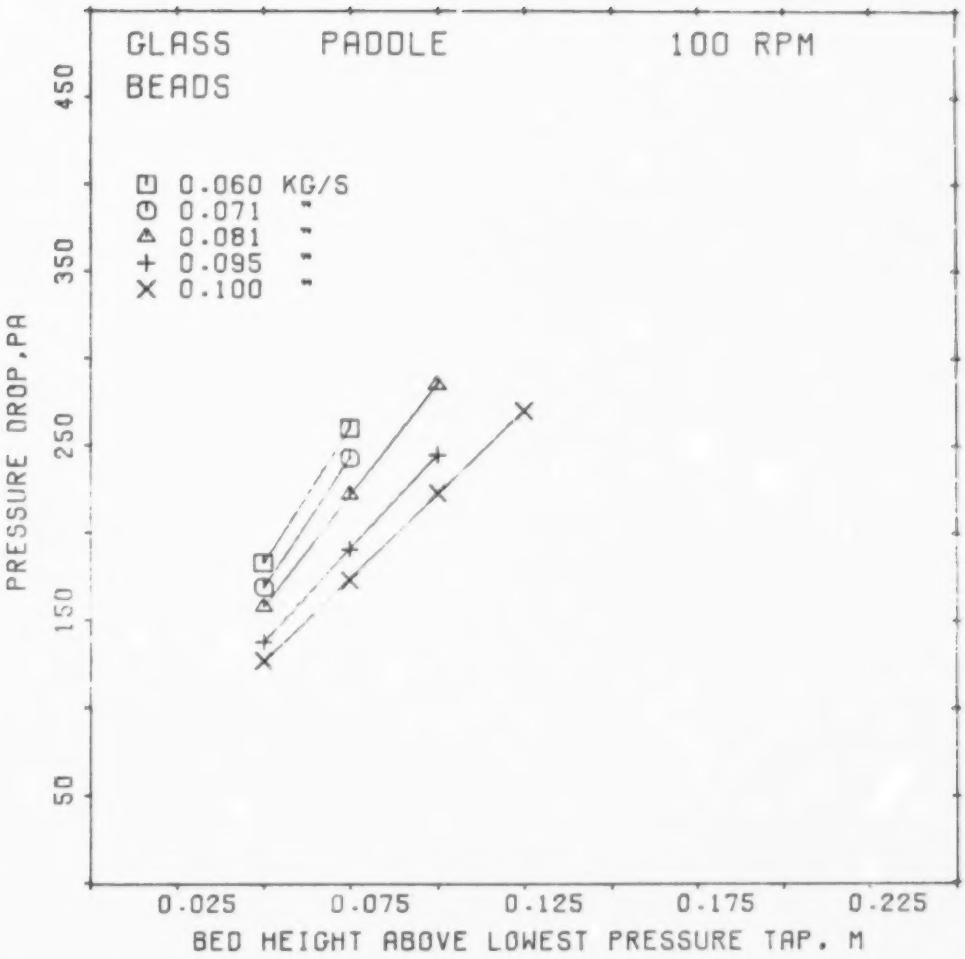

Figure B-12 Variation of pressure drop for a glass bed with a paddle at 100 rpm

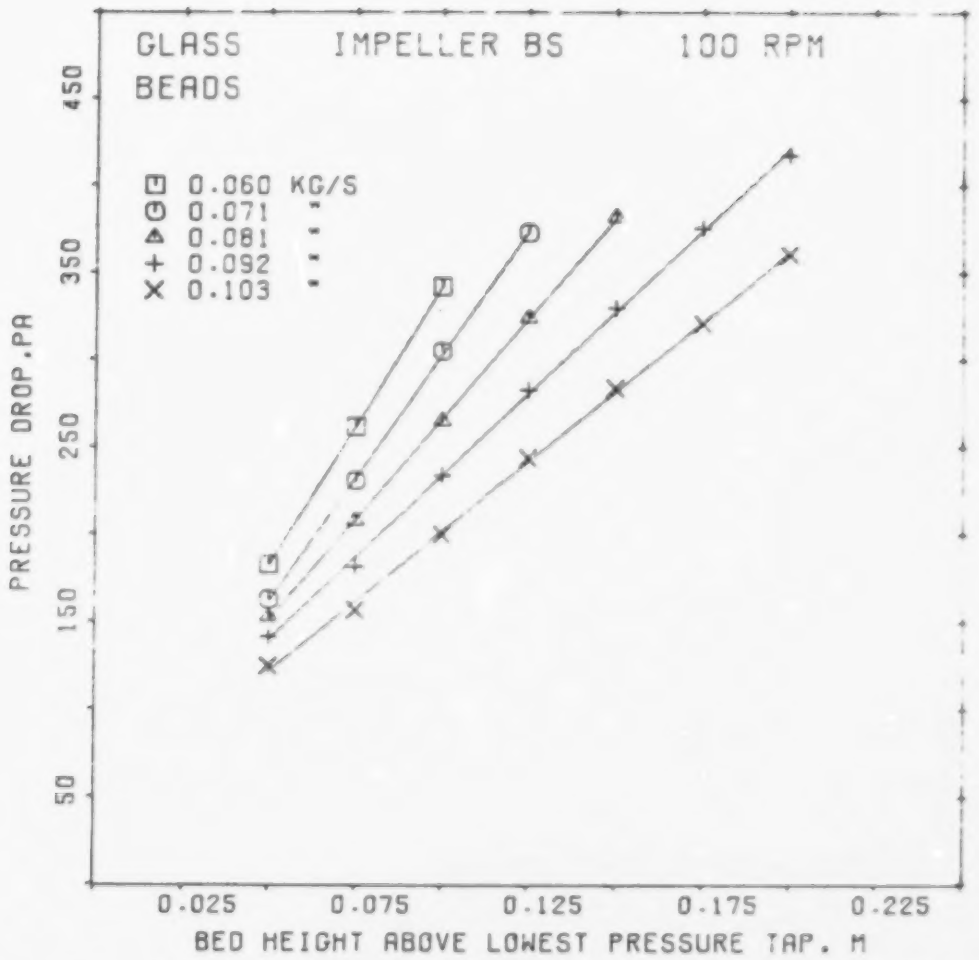

Figure B-13 Variation of pressure drop for a glass bed with an impeller at BS location at 100 rpm

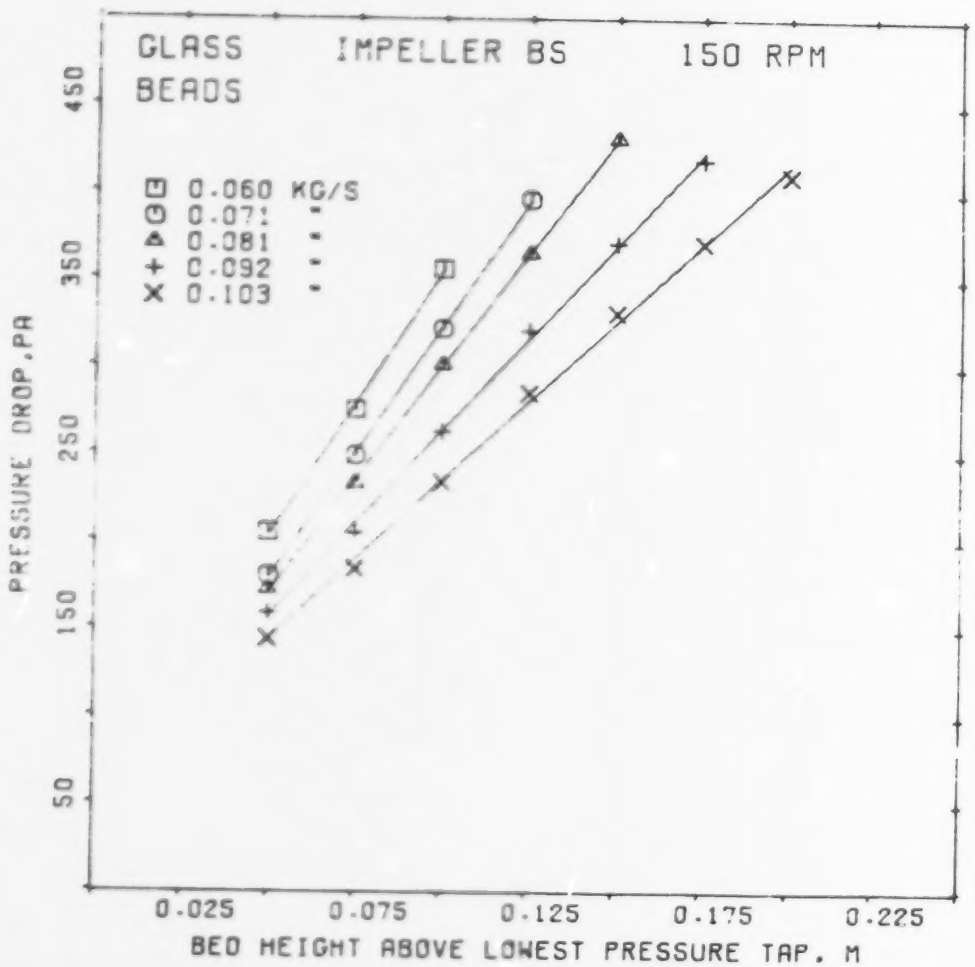

Figure B-14 Variation of pressure drop for a glass bed with an impeller at BS location at 150 rpm

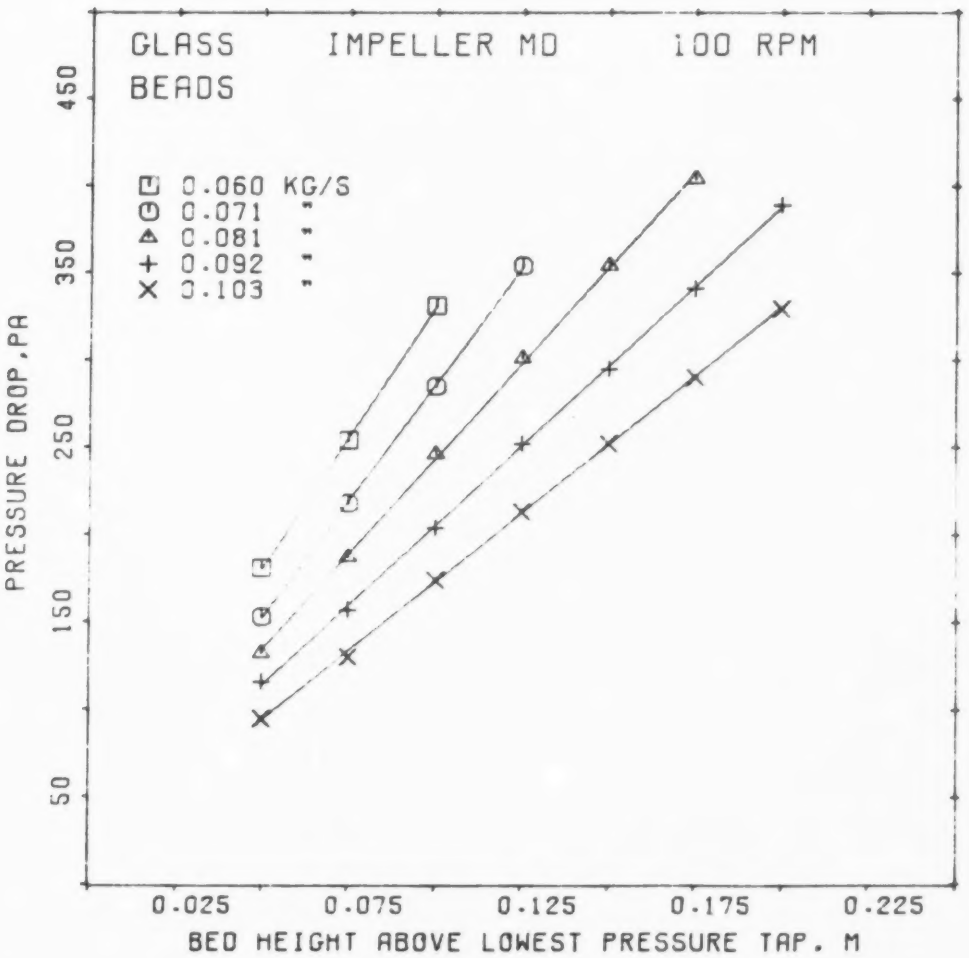

Figure B-15 Variation of pressure drop for a glass bed with an impeller at MD location at 100 rpm

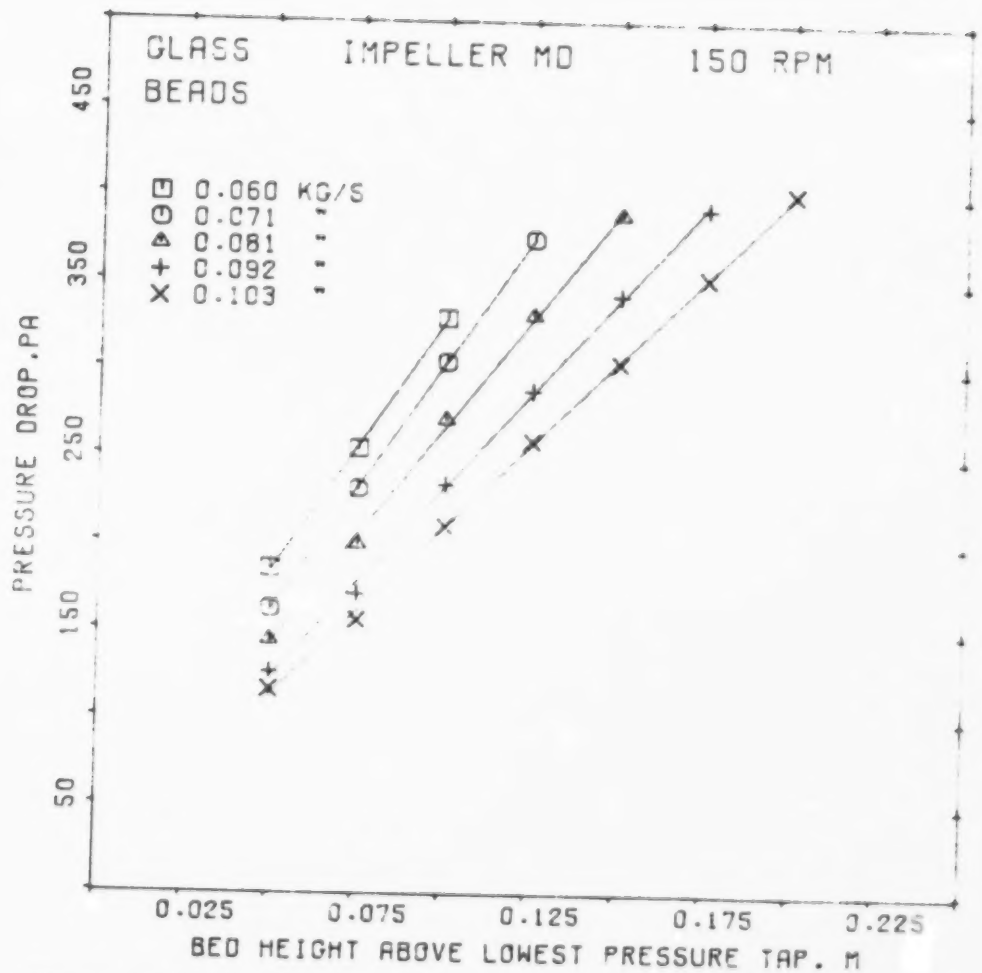

Figure B-16 Variation of pressure drop for a glass bed with an impeller at MD location at 150 rpm

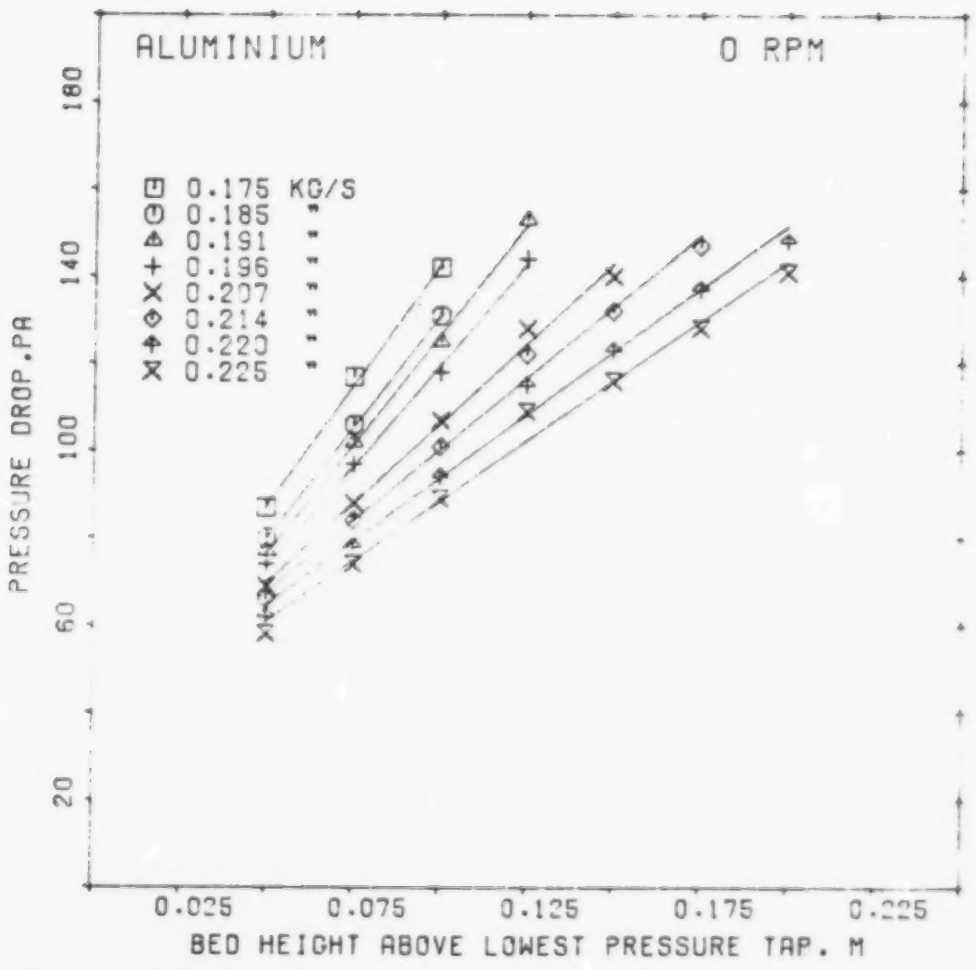

Figure B-17 Variation of pressure drop for an aluminum bed at zero rpm

APPENDIX C

RAW EXPERIMENTAL DATA

SAND 0 RPM

SETTINGS OF CARRIER DEMODULATOR
SPAN = 412 ± 1
ZERO = 290 ± 1

RF,%	(NO STIR) SCALE HEIGHT M	(STIR) SCALE HEIGHT M	PRESSURE DROP, PA AT BED HEIGHT ABOVE LOWEST PRESSURE TAP, M 0.050	0.075	0.100	0.125	0.150	0.175	0.200
12.00	0.3800	------	176.0	252.0	325.0	399.0			
13.00	0.3895	------	168.0	239.0	308.0	377.0			
14.00	0.3980	------	161.0	228.0	293.0	358.0			
15.00	0.4085	------	153.0	216.0	277.0	339.0	397.0		
16.00	0.4205	------	146.0	204.0	262.0	318.0	374.0		
17.00	0.4330	------	136.0	191.0	247.0	302.0	354.0	406.0	
18.00	0.4505	------	129.0	180.0	230.0	281.0	330.0	377.0	425.0
19.00	0.4663	------	123.0	170.0	216.0	263.0	310.0	356.0	402.0
20.00	0.4850	------	115.0	162.0	201.0	247.0	291.0	334.0	376.0
12.50	0.3770	------	181.0	259.0	334.0	410.0			
13.50	0.3855	------	171.0	245.0	316.0	387.0			
14.50	0.3950	------	165.0	230.0	302.0	371.0			
15.50	0.4050	------	159.0	220.0	286.0	350.0	411.0		
16.50	0.4155	------	149.0	208.0	268.0	328.0	387.0		
17.50	0.4285	------	139.0	194.0	252.0	310.0	364.0	417.0	
18.50	0.4420	------	133.0	188.0	243.0	296.0	347.0	398.0	
19.50	0.4575	------	127.0	179.0	232.0	284.0	331.0	379.0	424.0
12.00	0.3780	------	182.0	259.0	334.0	406.0			
12.50	0.3825	------	178.0	253.0	326.0	397.0			
13.00	0.3860	------	176.0	248.0	317.0	386.0			
13.50	0.3900	------	170.0	240.0	309.0	380.0			
14.00	0.3960	------	166.0	233.0	298.0	364.0			
14.50	0.4010	------	161.0	226.0	291.0	353.0	416.0		
15.00	0.4060	------	157.0	219.0	282.0	345.0	405.0		
15.50	0.4110	------	153.0	215.0	275.0	335.0	395.0		
16.00	0.4180	------	150.0	208.0	267.0	326.0	382.0		
16.50	0.4250	------	144.0	201.0	257.0	312.0	368.0	422.0	
17.00	0.4335	------	140.0	194.0	248.0	302.0	355.0	408.0	
17.50	0.4385	------	137.0	191.0	244.0	297.0	349.0	399.0	
18.00	0.4450	------	135.0	186.0	238.0	290.0	340.0	389.0	
18.50	0.4535	------	128.0	181.0	231.0	280.0	326.0	375.0	422.0
19.00	0.4640	------	126.0	174.0	221.0	268.0	314.0	361.0	405.0
19.50	0.4730	------	122.0	169.0	216.0	263.0	305.0	349.0	394.0
20.00	0.4843	------	118.0	162.0	206.0	253.0	297.0	338.0	382.0
12.00	0.3745	------	188.0	265.0	340.0	415.0			
12.50	0.3785	------	187.0	260.0	332.0	405.0			
13.00	0.3838	------	182.0	253.0	323.0	394.0			
13.50	0.3878	------	176.0	248.0	318.0	387.0			
14.00	0.3930	------	172.0	242.0	308.0	373.0			
14.50	0.3983	------	166.0	232.0	302.0	365.0			
15.00	0.4040	------	160.0	225.0	286.0	351.0	411.0		
15.50	0.4100	------	157.0	214.0	275.0	337.0	397.0		
16.00	0.4118	------	161.0	222.0	283.0	343.0	400.0		
16.50	0.4195	------	155.0	214.0	271.0	330.0	384.0		
17.00	0.4260	------	151.0	210.0	266.0	322.0	377.0	429.0	

17.50	0.4315	------	148.0	205.0	262.0	314.0	366.0	417.0		
18.00	0.4383	------	145.0	200.0	252.0	304.0	354.0	405.0		
18.50	0.4495	------	138.0	189.0	242.0	294.0	340.0	388.0	435.0	
19.00	0.4580	------	135.0	185.0	235.0	281.0	326.0	374.0	424.0	
19.50	0.4638	------	131.0	181.0	229.0	275.0	320.0	367.0	415.0	
20.00	0.4715	------	127.0	174.0	223.0	270.0	312.0	356.0	402.0	
12.00	0.3750	------	192.0	270.0	344.0	418.0				
12.50	0.3788	------	187.0	260.0	334.0	406.0				
13.00	0.3833	------	182.0	253.0	324.0	395.0				
13.50	0.3875	------	176.0	247.0	317.0	385.0				
14.00	0.3920	------	171.0	241.0	308.0	376.0				
14.50	0.3980	------	167.0	232.0	296.0	363.0				
15.00	0.4030	------	162.0	226.0	289.0	352.0	413.0			
15.50	0.4095	------	158.0	219.0	279.0	341.0	399.0			
16.00	0.4150	------	153.0	213.0	271.0	330.0	387.0			
16.50	0.4208	------	150.0	208.0	264.0	320.0	380.0			
17.00	0.4273	------	147.0	202.0	256.0	312.0	365.0	420.0		
17.50	0.4343	------	142.0	197.0	252.0	305.0	356.0	407.0		
18.00	0.4415	------	138.0	192.0	241.0	293.0	344.0	394.0		
18.50	0.4490	------	133.0	186.0	237.0	285.0	333.0	382.0	428.0	
19.00	0.4603	------	128.0	178.0	228.0	274.0	320.0	365.0	413.0	
19.50	0.4670	------	125.0	172.0	222.0	269.0	313.0	358.0	402.0	
20.00	0.4793	------	122.0	167.0	212.0	258.0	301.0	342.0	389.0	
12.00	0.3770	------	189.0	271.0	348.0	420.0				
12.50	0.3815	------	189.0	262.0	336.0	410.0				
13.00	0.3850	------	183.0	257.0	329.0	399.0				
13.50	0.3895	------	178.0	250.0	321.0	390.0				
14.00	0.3950	------	173.0	244.0	312.0	379.0				
14.50	0.3995	------	169.0	238.0	304.0	368.0	429.0			
15.00	0.4035	------	166.0	230.0	296.0	358.0	420.0			
15.50	0.4100	------	162.0	224.0	287.0	349.0	407.0			
16.00	0.4155	------	158.0	219.0	280.0	339.0	397.0			
16.50	0.4195	------	154.0	213.0	273.0	331.0	387.0			
17.00	0.4265	------	150.0	207.0	264.0	321.0	375.0	429.0		
17.50	0.4340	------	146.0	203.0	257.0	311.0	364.0	419.0		
18.00	0.4405	------	142.0	196.0	249.0	302.0	354.0	405.0		
18.50	0.4485	------	139.0	190.0	243.0	294.0	342.0	392.0		
19.00	0.4545	------	136.0	186.0	236.0	286.0	333.0	383.0	430.0	
19.50	0.4625	------	134.0	183.0	232.0	279.0	325.0	373.0	421.0	
20.00	0.4755	------	130.0	174.0	219.0	266.0	311.0	355.0	401.0	
12.00	0.3760	------	191.0	267.0	346.0	422.0				
13.00	0.3845	------	183.0	258.0	330.0	400.0				
14.00	0.3940	------	172.0	239.0	312.0	377.0				
15.00	0.4030	------	162.0	232.0	294.0	357.0	417.0			
16.00	0.4140	------	158.0	217.0	279.0	339.0	396.0			
17.00	0.4270	------	148.0	205.0	261.0	318.0	372.0	426.0		
18.00	0.4400	------	136.0	194.0	247.0	299.0	350.0	401.0		
19.00	0.4540	------	129.0	184.0	234.0	284.0	333.0	382.0	428.0	
20.00	0.4725	------	122.0	171.0	220.0	266.0	310.0	355.0	403.0	

SAND PADDLE 50 RPM

SETTINGS OF CARRIER DEMODULATOR
SPAN = 412 ± 1
ZERO = 290 ± 1

RF,%	(NO STIR) SCALE HEIGHT M	(STIR) SCALE HEIGHT M	PRESSURE DROP, PA AT BED HEIGHT ABOVE LOWEST PRESSURE TAP, M 0 050	0 075	0 100	0 125	0 150	0 175	0 200
12.00	0.3745	0.3685	192.0	274.0	364.0				
12.50	0.3780	0.3715	189.0	268.0	353.0				
13.00	0.3830	0.3765	177.0	258.0	342.0	417.0			
13.50	0.3890	0.3815	171.0	249.0	328.0	401.0			
14.00	0.3950	0.3870	166.0	240.0	314.0	390.0			
14.50	0.4005	0.3925	160.0	232.0	305.0	377.0			
15.00	0.4080	0.3990	155.0	223.0	294.0	362.0	427.0		
15.50	0.4170	0.4055	150.0	215.0	283.0	348.0	411.0		
16.00	0.4265	0.4125	144.0	207.0	273.0	336.0	397.0		
16.50	0.4325	0.4185	138.0	200.0	261.0	321.0	381.0		
17.00	0.4410	0.4240	133.0	194.0	255.0	316.0	372.0	440.0	
17.50	0.4495	0.4320	130.0	186.0	245.0	304.0	359.0	414.0	
18.00	0.4590	0.4400	124.0	181.0	237.0	293.0	347.0	401.0	
18.50	0.4740	0.4515	120.0	170.0	222.0	277.0	328.0	381.0	436.0
19.00	0.4880	0.4640	114.0	163.0	214.0	264.0	313.0	363.0	412.0
19.50	0.4940	0.4690	112.0	159.0	210.0	259.0	308.0	357.0	409.0
20.00	0.5070	0.4800	105.0	154.0	201.0	250.0	296.0	344.0	393.0
12.00	0.3770	0.3710	190.0	271.0	355.0				
13.00	0.3850	0.3780	174.0	255.0	336.0	413.0			
14.00	0.3950	0.3865	166.0	240.0	317.0	390.0			
15.00	0.4070	0.3965	159.0	228.0	297.0	368.0			
16.00	0.4180	0.4060	150.0	214.0	281.0	347.0	411.0		
17.00	0.4300	0.4165	143.0	204.0	264.0	330.0	390.0		
18.00	0.4450	0.4285	132.0	191.0	250.0	309.0	365.0	422.0	
19.00	0.4620	0.4415	124.0	178.0	231.0	286.0	345.0	399.0	
20.00	0.4800	0.4545	116.0	168.0	221.0	276.0	326.0	378.0	433.0

SAND PADDLE 75 RPM

SETTINGS OF CARRIER DEMODULATOR
SPAN = 412 ± 1
ZERO = 290 ± 1

RF,%	(NO STIR) SCALE HEIGHT M	(STIR) SCALE HEIGHT M	PRESSURE DROP, PA AT BED HEIGHT ABOVE LOWEST PRESSURE TAP, M 0.050	0 075	0 100	0.125	0 150	0 175	0 200
12.00	0.3800	0.3690	194.0	283 0	373 0				
13.00	0.3880	0.3745	188.0	272 0	358 0	435 0			
14.00	0.3980	0 3805	181.0	261 0	341 0	419 0			
15.00	0.4100	0.3900	171.0	246 0	325 0	395 0			
16.00	0.4225	0.3995	166.0	234 0	305 0	375 0	437 0		
17.00	0.4420	0.4115	158.0	221 0	286 0	351 0	413 0		
18.00	0 4600	0.4225	149.0	208 0	270 0	332 0	389 0	443 0	
19.00	0.4810	0.4360	135.0	197 0	255 0	316 0	369 0	423 0	
20.00	0.5120	0.4525	125 0	181 0	237 0	291 0	344 0	393 0	443 0
12.00	0.3790	0.3685	193 0	280 0	368 0				
12.50	0.3815	0.3705	186.0	273 0	361 0				
13.00	0.3855	0.3740	185.0	267 0	356 0				
13.50	0.3905	0.3765	179.0	262 0	347 0	424 0			
14.00	0.3975	0.3815	171.0	250 0	331 0	409 0			
14.50	0.3995	0.3815	175 0	257 0	335 0	412 0			
15.00	0.4075	0.3875	167.0	241 0	317 0	391 0			
15.50	0.4140	0.3925	159 0	234 0	308 0	382 0			
16.00	0.4175	0.3940	157.0	230.0	305 0	376 0			
16.50	0 4210	0 3960	156 0	231 0	301 0	372 0			
17.00	0.4270	0.4005	152.0	224 0	295 0	364 0	425 0		
17.50	0.4315	0.4030	151 0	221 0	291 0	359 0	422 0		
18.00	0.4375	0 4065	150 0	217 0	286 0	351 0	414 0		
18.50	0.4450	0.4100	146 0	214 0	281 0	344 0	404 0		
19.00	0.4510	0 4135	142 0	209 0	274 0	337 0	399 0		
19 50	0 4610	0 4180	138 0	204 0	269 0	332 0	390 0		
20.00	0.4675	0 4245	137 0	200 0	263 0	324 0	381 0		
12.00	0.3845	0 3745	187 0	267 0	353 0	426 0			
13.00	0.3955	0.3805	181 0	257 0	335 0	410 0			
14.00	0 4090	0.3870	174 0	247 0	323 0	392 0			
15.00	0.4170	0.3945	165 0	237 0	311 0	379 0			
16.00	0 4310	0 4035	154 0	224 0	291 0	362 0	421 0		
17.00	0 4485	0 4140	146 0	214 0	278 0	342 0	401 0		
18.00	0 4695	0 4250	139 0	202 0	264 0	323 0	387 0		
19.00	0 4870	0 4350	132 0	193 0	254 0	311 0	369 0	421 0	
20.00	0.5100	0 4500	125 0	182 0	238 0	292 0	342 0	394 0	
12.50	0 3885	0 3775	184 0	268 0	350 0	425 0			
13 50	0 3995	0 3825	176 0	256 0	333 0	408 0			
14 50	0 4110	0 3905	167 0	244 0	317 0	389 0			
15 50	0.4240	0 3985	161.0	234 0	303 0	374 0			
16.50	0.4375	0.4065	154 0	223 0	290 0	357 0	418 0		
17 50	0 4560	0 4175	146 0	211 0	275 0	338 0	397 0		
18 50	0 4730	0.4275	140 0	202 0	264 0	322 0	377 0	431 0	
19 50	0 4925	0 4413	130 0	190 0	247 0	303 0	358 0	410 0	

SAND PADDLE 100 RPM

SETTINGS OF CARRIER DEMODULATOR
SPAN = 412 ± 1
ZERO = 290 ± 1

RF,%	(NO STIR) SCALE HEIGHT M	(STIR) SCALE HEIGHT M	PRESSURE DROP, PA AT BED HEIGHT ABOVE LOWEST PRESSURE TAP, M 0.050	0 075	0 100	0 125	0 150	0 175	0.200
12.00	0.3825	0.3650	204.0	297 0	385 0				
13.00	0.3920	0.3700	197.0	284.0	369 0				
14.00	0 4035	0.3790	190.0	270 0	351 0	419 0			
15.00	0.4150	0.3870	180.0	262.0	336 0	404 0			
16.00	0.4280	0.3940	172.0	249 0	321 0	386 0			
17.00	0.4445	0.4010	165.0	236 0	307 0	371 0	426 0		
18.00	0.4620	0.4125	160.0	225 0	291 0	353 0	411 0		
19.00	0.4790	0.4210	156.0	217 0	282 0	342 0	397 0		
20.00	0.4990	0.4315	148 0	209 0	268 0	327 0	380 0	426.0	
12.50	0.3825	0.3655	204 0	293 0	373 0				
13.50	0.3900	0.3695	197.0	284 0	368.0				
14.50	0.4000	0.3770	189.0	273 0	355 0	422 0			
15.50	0.4100	0.3820	181.0	261 0	341 0	410 0			
16.50	0.4275	0.3930	165.0	243.0	316.0	383 0			
17.50	0.4405	0.3995	160 0	230.0	304.0	369 0			
18.50	0.4535	0.4070	155.0	224.0	294 0	358 0	415 0		
19.50	0.4740	0.4175	151.0	215.0	279 0	341 0	396 0		
12.00	0.3770	0.3620	201.0	294 0	384 0				
13.00	0.3865	0.3675	194.0	282.0	370 0				
14.00	0.3945	0.3725	186 0	274 0	359.0				
15.00	0 4050	0.3795	183.0	264 0	344 0	415 0			
16.50	0.4215	0.3900	171.0	251 0	323 0	392 0			
17.50	0.4345	0.3980	165.0	241.0	311.0	378 0			
18.50	0.4475	0 4040	159.0	232 0	298 0	364 0	420 0		
19.50	0.4650	0 4105	152.0	221.0	287 0	350.0	407.0		

SAND IMPELLER BS 100 RPM

SETTINGS OF CARRIER DEMODULATOR :
SPAN = 412 ± 1
ZERO = 290 ± 1

RF,%	(NO STIR) SCALE HEIGHT M	(STIR) SCALE HEIGHT M	PRESSURE DROP, PA AT BED HEIGHT ABOVE LOWEST PRESSURE TAP, M. 0.050	0.075	0.100	0.125	0.150	0.175	0.200
12.00	0.3780	0.3780	175.0	259.0	340.0	424.0			
13.00	0.3865	0.3845	168.0	246.0	326.0	408.0			
14.00	0.3970	0.3935	160.0	233.0	307.0	384.0			
15.00	0.4100	0.4025	150.0	219.0	290.0	362.0	431.0		
16.00	0.4220	0.4120	143.0	210.0	278.0	348.0	413.0		
17.00	0.4390	0.4225	134.0	197.0	261.0	325.0	387.0		
18.00	0.4510	0.4320	128.0	188.0	252.0	313.0	372.0	432.0	
19.00	0.4660	0.4455	122.0	178.0	236.0	294.0	350.0	406.0	
20.00	0.4880	0.4590	115.0	168.0	222.0	276.0	328.0	381.0	432.0
12.50	0.3770	0.3755	182.0	269.0	353.0	439.0			
13.50	0.3855	0.3810	177.0	259.0	343.0	426.0			
14.50	0.3945	0.3895	167.0	240.0	316.0	395.0			
15.50	0.4045	0.3970	156.0	227.0	302.0	377.0			
16.50	0.4160	0.4085	146.0	214.0	285.0	352.0	418.0		
17.50	0.4400	0.4265	133.0	194.0	258.0	321.0	382.0	441.0	
18.50	0.4700	0.4470	121.0	178.0	236.0	294.0	349.0	405.0	
19.50	0.4950	0.4655	114.0	167.0	222.0	275.0	327.0	380.0	429.0
12.00	0.3850	0.3825	174.0	255.0	342.0	420.0			
12.50	0.3895	0.3860	170.0	249.0	328.0	409.0			
13.00	0.3940	0.3905	166.0	243.0	323.0	400.0			
13.50	0.3985	0.3940	162.0	238.0	314.0	390.0			
14.00	0.4045	0.3980	158.0	231.0	307.0	380.0			
14.50	0.4105	0.4030	155.0	227.0	298.0	370.0	440.0		
15.00	0.4150	0.4065	151.0	221.0	291.0	362.0	431.0		
15.50	0.4215	0.4115	147.0	214.0	283.0	353.0	421.0		
16.00	0.4285	0.4165	143.0	210.0	278.0	346.0	409.0		
16.50	0.4355	0.4210	141.0	205.0	272.0	337.0	401.0		
17.00	0.4440	0.4265	140.0	200.0	264.0	329.0	390.0	452.0	

SAND IMPELLER BS 150 RPM

SETTINGS OF CARRIER DEMODULATOR :
SPAN = 412 ± 1
ZERO = 290 ± 1

RF,%	(NO STIR) SCALE HEIGHT M	(STIR) SCALE HEIGHT M	PRESSURE DROP, PA AT BED HEIGHT ABOVE LOWEST PRESSURE TAP, M. 0.050	0.075	0.100	0.125	0.150	0.175	0.200
12.00	0.3845	0.3800	185.0	266.0	354.0	442.0			
12.50	0.3895	0.3830	177.0	260.0	347.0	430.0			
13.00	0.3935	0.3845	174.0	255.0	344.0	427.0			
13.50	0.3980	0.3873	172.0	252.0	337.0	422.0			
14.00	0.4035	0.3915	165.0	245.0	330.0	411.0			
14.50	0.4110	0.3945	165.0	240.0	319.0	401.0			
15.00	0.4165	0.3988	162.0	235.0	311.0	392.0			
15.50	0.4225	0.4005	159.0	231.0	310.0	387.0	463.0		
16.00	0.4315	0.4050	157.0	231.0	307.0	383.0	454.0		
16.50	0.4360	0.4065	151.0	225.0	299.0	375.0	444.0		
17.00	0.4400	0.4105	147.0	221.0	292.0	370.0	439.0		
17.50	0.4490	0.4155	146.0	217.0	288.0	363.0	431.0		
18.00	0.4565	0.4205	143.0	211.0	281.0	353.0	420.0		
18.50	0.4640	0.4245	142.0	207.0	279.0	348.0	417.0		
19.00	0.4760	0.4285	139.0	201.0	270.0	339.0	405.0	467.0	
19.50	0.4835	0.4310	136.0	199.0	269.0	333.0	398.0	461.0	
20.00	0.4940	0.4380	133.0	195.0	262.0	328.0	394.0	451.0	

SAND IMPELLER MD 100 RPM

SETTINGS OF CARRIER DEMODULATOR :
SPAN = 412 ± 1
ZERO = 290 ± 1

RF,%	(NO STIR) SCALE HEIGHT M	(STIR) SCALE HEIGHT M	PRESSURE DROP, PA AT BED HEIGHT ABOVE LOWEST PRESSURE TAP, M. 0.050	0.075	0.100	0.125	0.150	0.175	0.200
12.00	0.3750	0.3700	188.0	270.0	356.0				
12.50	0.3800	0.3735	185.0	264.0	346.0				
13.00	0.3845	0.3775	177.0	257.0	336.0	419.0			
13.50	0.3885	0.3815	174.0	250.0	329.0	410.0			
14.00	0.3950	0.3855	170.0	241.0	319.0	397.0			
14.50	0.4005	0.3915	167.0	236.0	309.0	385.0			
15.00	0.4055	0.3965	160.0	230.0	301.0	376.0			
15.50	0.4125	0.4020	156.0	223.0	290.0	363.0	427.0		
16.00	0.4180	0.4065	151.0	217.0	283.0	352.0	416.0		
16.50	0.4245	0.4130	147.0	211.0	273.0	342.0	402.0		
17.00	0.4315	0.4195	142.0	204.0	266.0	331.0	391.0		
17.50	0.4400	0.4265	137.0	197.0	259.0	320.0	378.0	435.0	
18.00	0.4475	0.4330	134.0	193.0	251.0	309.0	367.0	423.0	
18.50	0.4570	0.4415	133.0	184.0	241.0	297.0	352.0	408.0	
19.00	0.4635	0.4480	125.0	177.0	233.0	289.0	340.0	394.0	
19.50	0.4765	0.4560	120.0	171.0	222.0	276.0	327.0	380.0	433.0
20.00	0.4850	0.4605	119.0	167.0	218.0	270.0	320.0	372.0	427.0
12.00	0.3825	0.3763	184.0	260.0	341.0	425.0			
13.00	0.3925	0.3845	173.0	249.0	328.0	406.0			
14.00	0.4030	0.3935	163.0	237.0	308.0	383.0			
15.00	0.4145	0.4045	157.0	222.0	289.0	360.0	425.0		
16.00	0.4270	0.4165	146.0	207.0	272.0	338.0	400.0		
17.00	0.4405	0.4305	137.0	196.0	256.0	318.0	376.0	431.0	
18.00	0.4585	0.4423	130.0	184.0	241.0	298.0	351.0	408.0	
19.00	0.4790	0.4578	121.0	169.0	222.0	278.0	328.0	381.0	433.0
20.00	0.5000	0.4730	113.0	157.0	208.0	259.0	308.0	358.0	411.0
12.50	0.3900	0.3825	173.0	252.0	330.0	411.0			
13.50	0.3985	0.3890	164.0	239.0	314.0	392.0			
14.50	0.4100	0.4000	154.0	226.0	296.0	369.0	435.0		
15.50	0.4250	0.4150	147.0	210.0	275.0	341.0	401.0		
16.50	0.4345	0.4230	140.0	200.0	264.0	328.0	387.0	443.0	
17.50	0.4490	0.4350	133.0	192.0	251.0	311.0	366.0	424.0	
18.50	0.4665	0.4483	126.0	182.0	232.0	291.0	344.0	399.0	
19.50	0.4880	0.4610	117.0	165.0	216.0	271.0	320.0	372.0	428.0

SAND IMPELLER MD 150 RPM

SETTINGS OF CARRIER DEMODULATOR :
SPAN = 412 ± 1
ZERO = 290 ± 1

RF,%	(NO STIR) SCALE HEIGHT M	(STIR) SCALE HEIGHT M	PRESSURE DROP, PA AT BED HEIGHT ABOVE LOWEST PRESSURE TAP, M. 0.050	0.075	0.100	0.125	0.150	0.175
12.00	0.3775	0.3675	201.0	278.0	361.0			
13.00	0.3865	0.3735	187.0	266.0	344.0			
14.00	0.3990	0.3810	179.0	251.0	332.0			
15.00	0.4085	0.3875	172.0	243.0	319.0	397.0		
16.00	0.4220	0.3970	163.0	230.0	301.0	377.0		
17.00	0.4365	0.4055	158.0	221.0	286.0	360.0	427.0	
18.00	0.4500	0.4160	149.0	209.0	274.0	342.0	405.0	
19.00	0.4670	0.4275	143.0	198.0	256.0	321.0	383.0	
20.00	0.4870	0.4380	136.0	185.0	244.0	309.0	365.0	427.0
12.50	0.3915	0.3755	186.0	261.0	344.0	429.0		
13.50	0.4015	0.3825	177.0	251.0	328.0	408.0		
14.50	0.4135	0.3905	167.0	240.0	311.0	391.0		
15.50	0.4265	0.4000	160.0	228.0	295.0	372.0		
16.50	0.4400	0.4110	154.0	216.0	282.0	354.0	421.0	
17.50	0.4550	0.4205	144.0	201.0	265.0	336.0	401.0	
18.50	0.4725	0.4305	140.0	193.0	256.0	321.0	381.0	444.0
19.50	0.4925	0.4395	135.0	188.0	244.0	306.0	366.0	428.0

GLASS BEADS 0 RPM

SETTINGS OF CARRIER DEMODULATOR :
SPAN = 412 ± 1
ZERO = 306 ± 1
ZERO = 290 ± 1

RF,%	(NO STIR) SCALE HEIGHT M	(STIR) SCALE HEIGHT M	PRESSURE DROP, PA AT BED HEIGHT ABOVE LOWEST PRESSURE TAP, M. 0.050	0.075	0.100	0.125	0.150	0.175	0.200	0.250	0.300
(ZERO = 306 ± 1)											
12.00	0.3678	------	187.0	256.0	325.0						
13.00	0.3805	------	174.0	237.0	301.0	361.0					
14.00	0.3960	------	162.0	219.0	280.0	334.0					
15.00	0.4165	------	152.0	206.0	259.0	309.0	357.0				
16.00	0.4383	------	145.0	190.0	239.0	286.0	331.0	374.0			
17.00	0.4675	------	135.0	175.0	218.0	260.0	297.0	338.0	382.0		
18.00	0.5010	------	118.0	157.0	199.0	236.0	273.0	313.0	351.0	403.0	
19.00	0.5430	------	112.0	145.0	182.0	218.0	249.0	281.0	317.0	371.0	
20.00	0.5930	------	103.0	129.0	161.0	193.0	221.0	250.0	285.0	333.0	377.0
(ZERO = 290 ± 1)											
12.00	0.3813	------	163.0	231.0	305.0	370.0					
13.00	0.3948	------	156.0	218.0	283.0	342.0					
14.00	0.4125	------	135.0	194.0	256.0	315.0	365.0				
15.00	0.4330	------	129.0	182.0	236.0	287.0	335.0	382.0			
16.00	0.4593	------	120.0	162.0	208.0	256.0	302.0	342.0	383.0		
17.00	0.4845	------	112.0	149.0	196.0	238.0	278.0	319.0	360.0		
18.00	0.5250	------	102.0	137.0	175.0	211.0	247.0	284.0	322.0	378.0	
19.00	0.5735	------	96.0	125.0	163.0	191.0	224.0	255.0	289.0	343.0	387.0
20.00	0.6420	------	86.0	111.0	142.0	171.0	197.0	226.0	256.0	305.0	348.0
12.00	0.3625	------	180.0	250.0	321.0						
13.00	0.3740	------	165.0	231.0	298.0						
14.00	0.3910	------	150.0	209.0	271.0	330.0					
15.00	0.4095	------	140.0	195.0	249.0	302.0	350.0				
16.00	0.4295	------	128.0	178.0	228.0	277.0	324.0	371.0			
17.00	0.4570	------	119.0	162.0	209.0	255.0	298.0	340.0	377.0		
18.00	0.4940	------	106.0	145.0	186.0	227.0	266.0	303.0	342.0		
19.00	0.5260	------	94.0	131.0	169.0	206.0	242.0	279.0	316.0	368.0	
20.00	0.6073	------	86.0	115.0	145.0	178.0	209.0	243.0	273.0	318.0	362.0
12.00	0.3565	------	170.0	240.0	310.0						
12.50	0.3585	------	165.0	231.0	301.0						
13.00	0.3650	------	159.0	221.0	288.0						
13.50	0.3710	------	153.0	213.0	276.0						
14.00	0.3780	------	148.0	205.0	266.0	325.0					
14.50	0.3855	------	143.0	198.0	255.0	311.0					
15.00	0.3935	------	137.0	188.0	243.0	298.0					
15.50	0.4035	------	128.0	177.0	232.0	283.0	327.0				
16.00	0.4125	------	126.0	173.0	222.0	270.0	314.0				
16.50	0.4215	------	121.0	166.0	213.0	261.0	301.0				
17.00	0.4350	------	115.0	155.0	200.0	242.0	283.0	324.0			
17.50	0.4465	------	110.0	147.0	191.0	231.0	270.0	310.0			
18.00	0.4610	------	108.0	142.0	183.0	220.0	256.0	294.0	335.0		
18.50	0.4840	------	101.0	131.0	168.0	203.0	235.0	271.0	308.0		
19.00	0.4985	------	96.0	126.0	162.0	195.0	227.0	259.0	295.0		

19.50	0.5160	------	92.0	120.0	153.0	183.0	213.0	245.0	282.0	337.0								
20.00	0.5380	------	87.0	112.0	145.0	173.0	201.0	231.0	265.0	318.0								
10.00	0.3803	------	202.0	289.0	373.0	448.0												
11.00	0.3915	------	195.0	270.0	349.0	419.0												
12.00	0.4090	------	178.0	246.0	320.0	389.0	452.0											
13.00	0.4263	------	163.0	226.0	296.0	363.0	424.0	479.0										
14.00	0.4478	------	151.0	209.0	273.0	334.0	391.0	446.0										
15.00	0.4765	------	137.0	191.0	248.0	303.0	356.0	409.0	457.0									
16.00	0.5068	------	128.0	177.0	228.0	276.0	323.0	373.0	421.0	494.0								
17.00	0.5453	------	115.0	162.0	208.0	251.0	294.0	339.0	384.0	456.0	505.0							
18.00	0.5945	------	105.0	145.0	188.0	224.0	263.0	302.0	343.0	412.0	473.0							
19.00	0.6685	------	96.0	131.0	168.0	201.0	235.0	270.0	310.0	370.0	426.0							

GLASS BEADS PADDLE 50 RPM

SETTINGS OF CARRIER DEMODULATOR :
SPAN = 412 ± 1
ZERO = 290 ± 1

RF.%	(NO STIR) SCALE HEIGHT M	(STIR) SCALE HEIGHT M	PRESSURE DROP, PA AT BED HEIGHT ABOVE LOWEST PRESSURE TAP, M. 0.050	0.075	0.100	0.125	0.150	0.175	0.200
12.00	0.3435	0.3370	177.0	256.0					
13.00	0.3530	0.3450	168.0	237.0					
14.00	0.3635	0.3535	156.0	223.0	292.0				
15.00	0.3780	0.3645	142.0	206.0	272.0				
16.00	0.3905	0.3740	130.0	191.0	254.0	308.0			
17.00	0.4100	0.3895	121.0	176.0	231.0	285.0			
18.00	0.4275	0.4050	109.0	159.0	211.0	262.0	308.0		
19.00	0.4500	0.4230	99.0	144.0	192.0	238.0	282.0		
20.00	0.4750	0.4420	91.0	133.0	177.0	222.0	261.0	303.0	
12.00	0.3370	0.3330	186.0	264.0					
12.50	0.3435	0.3360	180.0	256.0					
13.00	0.3500	0.3415	174.0	245.0					
13.50	0.3575	0.3470	167.0	238.0					
14.00	0.3630	0.3525	159.0	227.0	296.0				
14.50	0.3690	0.3575	153.0	219.0	286.0				
15.00	0.3770	0.3635	144.0	210.0	274.0				
15.50	0.3855	0.3705	137.0	199.0	262.0				
16.00	0.3935	0.3765	134.0	193.0	253.0	310.0			
16.50	0.4040	0.3860	126.0	181.0	239.0	295.0			
17.00	0.4140	0.3945	120.0	173.0	227.0	281.0			
17.50	0.4225	0.4010	116.0	167.0	221.0	272.0	319.0		
18.00	0.4300	0.4080	111.0	160.0	211.0	261.0	309.0		
18.50	0.4445	0.4195	103.0	151.0	199.0	246.0	294.0		
19.00	0.4600	0.4300	99.0	144.0	189.0	234.0	278.0	322.0	
19.50	0.4790	0.4410	96.0	138.0	181.0	224.0	267.0	308.0	
20.00	0.4875	0.4475	93.0	134.0	177.0	219.0	261.0	301.0	336.0

GLASS BEADS PADDLE 75 RPM

SETTINGS OF CARRIER DEMODULATOR :
SPAN = 412 ± 1
ZERO = 290 ± 1

RF,%	(NO STIR) SCALE HEIGHT M	(STIR) SCALE HEIGHT M	PRESSURE DROP, PA AT BED HEIGHT ABOVE LOWEST PRESSURE TAP, M. 0.050	0.075	0.100	0.125	0.150	0.175	0.200
10.00	0.3820	0.3745	206.0	294.0	389.0	470.0			
11.00	0.3980	0.3865	192.0	279.0	362.0	445.0			
12.00	0.4120	0.3945	187.0	267.0	351.0	429.0			
13.00	0.4330	0.4070	183.0	254.0	331.0	404.0	474.0		
14.00	0.4580	0.4215	174.0	243.0	313.0	384.0	452.0		
15.00	0.4860	0.4350	163.0	229.0	298.0	365.0	427.0	492.0	
16.00	0.5200	0.4525	154.0	217.0	281.0	340.0	398.0	459.0	514.0
17.00	0.5580	0.4695	148.0	205.0	265.0	323.0	377.0	434.0	489.0
10.00	0.3750	0.3670	195.0	288.0	378.0				
11.00	0.3950	0.3775	184.0	268.0	353.0	434.0			
12.00	0.4060	0.3865	173.0	254.0	336.0	413.0			
13.00	0.4270	0.4040	165.0	232.0	310.0	383.0	449.0		
14.00	0.4475	0.4175	162.0	235.0	307.0	379.0	446.0		
15.00	0.4730	0.4325	157.0	220.0	290.0	355.0	418.0	481.0	
16.00	0.4995	0.4500	153.0	206.0	270.0	333.0	392.0	451.0	507.0
17.00	0.5380	0.4675	146.0	197.0	258.0	314.0	369.0	426.0	480.0
12.00	0.3470	0.3395	183.0	259.0					
13.00	0.3600	0.3525	176.0	253.0	326.0				
14.00	0.3730	0.3630	167.0	236.0	307.0				
15.00	0.3880	0.3695	160.0	229.0	297.0				
16.00	0.4105	0.3835	149.0	214.0	275.0	332.0			
17.00	0.4305	0.3965	139.0	198.0	255.0	310.0			
18.00	0.4550	0.4075	134.0	186.0	240.0	292.0	338.0		
19.00	0.4820	0.4225	125.0	175.0	226.0	274.0	320.0		
20.00	0.5300	0.4450	122.0	163.0	207.0	251.0	292.0	332.0	
12.00	0.3515	0.3415	177.0	249.0					
13.00	0.3625	0.3515	166.0	237.0	311.0				
14.00	0.3750	0.3610	157.0	226.0	293.0				
15.00	0.3945	0.3750	156.0	223.0	285.0	346.0			
16.00	0.4150	0.3870	149.0	211.0	272.0	327.0			
17.00	0.4335	0.4005	139.0	197.0	254.0	308.0	353.0		
18.00	0.4660	0.4125	133.0	185.0	235.0	288.0	335.0		
19.00	0.5050	0.4310	122.0	170.0	218.0	265.0	309.0	350.0	
20.00	0.5410	0.4505	120.0	160.0	205.0	248.0	291.0	328.0	360.0
12.50	0.3625	0.3505	163.0	237.0	305.0				
13.50	0.3735	0.3625	163.0	236.0	306.0				
14.50	0.3900	0.3725	157.0	227.0	292.0	345.0			
15.50	0.4080	0.3830	153.0	216.0	276.0	331.0			
16.50	0.4310	0.3965	140.0	199.0	256.0	309.0			
17.50	0.4535	0.4070	135.0	188.0	242.0	294.0	341.0		
18.50	0.4850	0.4270	128.0	176.0	224.0	272.0	314.0	354.0	
19.50	0.5290	0.4410	125.0	164.0	211.0	256.0	297.0	337.0	

GLASS BEADS PADDLE 100 RPM

SETTINGS OF CARRIER DEMODULATOR :
SPAN = 412 ± 1
ZERO = 290 ± 1

RF,%	(NO STIR) SCALE HEIGHT M	(STIR) SCALE HEIGHT M	PRESSURE DROP, PA AT BED HEIGHT ABOVE LOWEST PRESSURE TAP, M. 0.050	0.075	0.100	0.125	0.150	0.175	0.200
12.00	0.3630	0.3515	196.0	279.0	354.0				
13.00	0.3755	0.3625	187.0	265.0	339.0				
14.00	0.3900	0.3700	180.0	254.0	327.0				
15.00	0.4135	0.3840	168.0	239.0	306.0	363.0			
16.00	0.4360	0.3950	161.0	223.0	290.0	345.0			
17.00	0.4655	0.4095	153.0	212.0	272.0	326.0	372.0		
18.00	0.5010	0.4250	145.0	199.0	255.0	306.0	353.0	387.0	
19.00	0.5430	0.4400	136.0	189.0	241.0	289.0	335.0	372.0	
20.00	0.5940	0.4540	128.0	178.0	227.0	273.0	315.0	353.0	385.0
10.00	0.3750	0.3635	214.0	307.0	399.0				
11.00	0.3905	0.3750	208.0	300.0	390.0	460.0			
12.00	0.4060	0.3850	201.0	288.0	372.0	444.0			
13.00	0.4270	0.3965	193.0	274.0	354.0	427.0			
14.00	0.4500	0.4075	187.0	260.0	337.0	408.0	472.0		
15.00	0.4730	0.4190	176.0	249.0	322.0	391.0	455.0		
16.00	0.5050	0.4330	166.0	237.0	305.0	370.0	428.0	483.0	
17.00	0.5380	0.4450	163.0	226.0	290.0	352.0	411.0	464.0	
12.00	0.3550	0.3445	183.0	260.0					
12.50	0.3595	0.3465	182.0	257.0	314.0				
13.00	0.3700	0.3505	177.0	252.0	316.0				
13.50	0.3770	0.3550	172.0	244.0	308.0				
14.00	0.3825	0.3590	169.0	243.0	307.0				
14.50	0.3885	0.3640	164.0	236.0	301.0				
15.00	0.4000	0.3680	166.0	231.0	295.0	333.0			
15.50	0.4035	0.3750	162.0	228.0	291.0	333.0			
16.00	0.4170	0.3825	158.0	222.0	285.0	330.0			
16.50	0.4290	0.3880	152.0	216.0	276.0	323.0			
17.00	0.4350	0.3925	150.0	211.0	269.0	311.0			
17.50	0.4490	0.3995	144.0	203.0	259.0	304.0	340.0		
18.00	0.4650	0.4050	135.0	194.0	250.0	293.0	333.0		
18.50	0.4820	0.4130	138.0	191.0	245.0	290.0	327.0		
19.00	0.4990	0.4210	134.0	186.0	238.0	284.0	321.0		
19.50	0.5270	0.4330	127.0	173.0	223.0	270.0	307.0	339.0	
20.00	0.5500	0.4430	117.0	167.0	216.0	260.0	296.0	328.0	
10.00	0.3250	0.3205	222.0	295.0					
10.50	0.3300	0.3255	213.0	294.0					
11.00	0.3370	0.3305	207.0	290.0					
11.50	0.3425	0.3345	201.0	280.0					
12.00	0.3475	0.3375	196.0	274.0					
12.50	0.3515	0.3410	190.0	267.0					
13.00	0.3580	0.3450	184.0	260.0					
13.50	0.3640	0.3475	180.0	253.0	312.0				
14.00	0.3685	0.3500	175.0	250.0	313.0				
14.50	0.3760	0.3530	171.0	247.0	389.0				
15.00	0.3825	0.3570	167.0	241.0	306.0				

15.50	0.3920	0.3630	164.0	235.0	299.0	
16.00	0.4000	0.3655	160.0	231.0	293.0	
16.50	0.4075	0.3710	160.0	225.0	289.0	328.0
17.00	0.4210	0.3800	152.0	218.0	279.0	323.0
17.50	0.4285	0.3850	150.0	213.0	274.0	317.0

GLASS BEADS IMPELLER BS 100 RPM

SETTINGS OF CARRIER DEMODULATOR :
SPAN = 412 ± 1
ZERO = 306 ± 1

RF.%	(NO STIR) SCALE HEIGHT M	(STIR) SCALE HEIGHT M	PRESSURE DROP, PA AT BED HEIGHT ABOVE LOWEST PRESSURE TAP, M. 0.050	0.075	0.100	0.125	0.150	0.175	0.200
12.00	0.3655	0.3625	183.0	262.0	342.0				
13.00	0.3805	0.3725	175.0	248.0	322.0				
14.00	0.3950	0.3815	163.0	231.0	305.0	373.0			
15.00	0.4130	0.4025	160.0	221.0	285.0	351.0	414.0		
16.00	0.4355	0.4185	153.0	208.0	265.0	324.0	382.0		
17.00	0.4580	0.4370	147.0	199.0	254.0	309.0	362.0	412.0	
18.00	0.4990	0.4625	142.0	182.0	234.0	283.0	330.0	376.0	418.0
19.00	0.5255	0.4830	135.0	173.0	222.0	268.0	311.0	355.0	400.0
20.00	0.5815	0.5350	125.0	157.0	200.0	244.0	284.0	321.0	361.0

GLASS BEADS IMPELLER BS 150 RPM

SETTINGS OF CARRIER DEMODULATOR :
SPAN = 412 ± 1
ZERO = 306 ± 1

PF,%	(NO STIR) SCALE HEIGHT M	(STIR) SCALE HEIGHT M	PRESSURE DROP, PA AT BED HEIGHT ABOVE LOWEST PRESSURE TAP, M. 0.050	0.075	0.100	0.125	0.150	0.175	0.200	0.250
12.00	0.3710	0.3665	205.0	275.0	356.0					
13.00	0.3825	0.3760	189.0	260.0	339.0	414.0				
14.00	0.4010	0.3870	180.0	249.0	322.0	396.0				
15.00	0.4210	0.3975	173.0	239.0	310.0	380.0	443.0			
16.00	0.4410	0.4075	172.0	233.0	301.0	365.0	431.0			
17.00	0.4750	0.4265	162.0	221.0	284.0	344.0	401.0	447.0		
18.00	0.5115	0.4485	159.0	205.0	263.0	321.0	371.0	419.0	457.0	
19.00	0.5590	0.4790	150.0	190.0	245.0	298.0	350.0	391.0	429.0	
20.00	0.6070	0.5095	144.0	184.0	234.0	285.0	331.0	371.0	410.0	452.0

GLASS BEADS IMPELLER MD 100 RPM

SETTINGS OF CARRIER DEMODULATOR :
SPAN = 412 ± 1
ZERO = 290 ± 1

RF,%	(NO STIR) SCALE HEIGHT M	(STIR) SCALE HEIGHT M	PRESSURE DROP, PA AT BED HEIGHT ABOVE LOWEST PRESSURE TAP, M 0.050	0.075	0.100	0.125	0.150	0.175	0.200	0.250
12.00	0.3775	0.3655	181.0	254.0	331.0					
13.00	0.3915	0.3795	164.0	237.0	309.0	379.0				
14.00	0.4075	0.3915	153.0	218.0	285.0	354.0				
15.00	0.4250	0.4105	143.0	199.0	264.0	325.0	380.0			
16.00	0.4455	0.4255	132.0	187.0	246.0	301.0	354.0	404.0		
17.00	0.4775	0.4455	124.0	170.0	222.0	274.0	322.0	371.0		
18.00	0.5150	0.4655	116.0	157.0	204.0	252.0	295.0	341.0	389.0	
19.00	0.5700	0.4985	101.0	141.0	187.0	230.0	271.0	312.0	357.0	416.0
20.00	0.6300	0.5360	95.0	130.0	174.0	213.0	252.0	290.0	329.0	396.0

GLASS BEADS IMPELLER MD 150 RPM

SETTINGS OF CARRIER DEMODULATOR
SPAN = 412 ± 1
ZERO = 290 ± 1

RF,%	(NO STIR) SCALE HEIGHT M	(STIR) SCALE HEIGHT M	PRESSURE DROP, PA AT BED HEIGHT ABOVE LOWEST PRESSURE TAP, M. 0.050	0.075	0.100	0.125	0 150	0 175	0.200
12.00	0.3790	0.3650	185.0	254.0	329.0				
13.00	0.3925	0.3710	169.0	243.0	316.0	389.0			
14.00	0.4080	0.3790	162.0	231.0	304.0	375.0			
15.00	0.4235	0.3915	157.0	221.0	291.0	360.0			
16.00	0.4520	0.4095	144.0	199.0	271.0	331.0	389.0		
17.00	0.4730	0.4210	137.0	186.0	255.0	311.0	369.0		
18.00	0.5120	0.4373	126.0	171.0	234.0	288.0	343.0	393.0	
19.00	0.5560	0.4485	125.0	164.0	223.0	274.0	324.0	377.0	425.0
20.00	0.6155	0.4665	116.0	156.0	210.0	259.0	304.0	353.0	402.0

ALUMINIUM 0 RPM

SETTINGS OF CARRIER DEMODULATOR :
SPAN = 412 ± 1
ZERO = 274 ± 1

RF1. RF2,%	(NO STIR) SCALE HEIGHT M	(STIR) SCALE HEIGHT M	PRESSURE DROP, PA AT BED HEIGHT ABOVE LOWEST PRESSURE TAP, M. 0.050	0.075	0.100	0.125	0.150	0.175	0.200
15.20	0.3320	------	101.0	139.0					
16.20	0.3370	------	99.0	133.0					
17.20	0.3430	------	96.0	128.0					
18.20	0.3490	------	92.0	123.0					
19.20	0.3560	------	87.0	117.0	142.0				
20.20	0.3650	------	84.0	111.0	137.0				
21.20	0.3720	------	80.0	106.0	131.0				
22.20	0.3830	------	77.0	102.0	125.0	153.0			
23.20	0.3950	------	74.0	97.0	118.0	144.0			
24.20	0.4070	------	72.0	93.0	113.0	135.0	148.0		
25.20	0.4240	------	69.0	88.0	107.0	128.0	140.0		
23.25	0.4370	------	66.0	84.0	101.0	122.0	132.0	147.0	
24.25	0.4630	------	62.0	78.0	94.0	115.0	123.0	137.0	148.0
25.25	0.4850	------	58.0	74.0	89.0	109.0	116.0	128.0	141.0

POOR

QUALITY

ORIGINAL